AD_____

AWARD NUMBER: DAMD17-02-1-0661

TITLE: Analysis of Microtubule Mediated Functions of Prostate Specific Membrane Antigen

PRINCIPAL INVESTIGATOR: Ayyappan K Rajasekaran, Ph.D

CONTRACTING ORGANIZATION: University of California, Los Angeles
Los Angeles, California 90024-1406

REPORT DATE: April 2006

TYPE OF REPORT: Final Addendum

PREPARED FOR: U.S. Army Medical Research and Materiel Command
Fort Detrick, Maryland 21702-5012

REPORT DOCUMENTATION PAGE

Form Approved
OMB No. 0704-0188

1. REPORT DATE *(DD-MM-YYYY)*	**2. REPORT TYPE**	**3. DATES COVERED** *(From - To)*
April 2006	Final Addendum	25 Mar 05 – 24 Mar 06

Analysis of Microtubule Mediated Functions of Prostate Specific Membrane Antigen

5a. CONTRACT NUMBER

5b. GRANT NUMBER
DAMD17-02-1-0661

5c. PROGRAM ELEMENT NUMBER

6. AUTHOR(S)

Ayyappan K Rajasekaran, Ph.D

E-mail: arajasekaran@mednet.ucla.edu

5d. PROJECT NUMBER

5e. TASK NUMBER

5f. WORK UNIT NUMBER

7. PERFORMING ORGANIZATION NAME(S) AND ADDRESS(ES)

University of California, Los Angeles
Los Angeles, California 90024-1406

8. PERFORMING ORGANIZATION REPORT NUMBER

9. SPONSORING / MONITORING AGENCY NAME(S) AND ADDRESS(ES)
U.S. Army Medical Research and Materiel Command
Fort Detrick, Maryland 21702-5012

10. SPONSOR/MONITOR'S ACRONYM(S)

11. SPONSOR/MONITOR'S REPORT NUMBER(S)

12. DISTRIBUTION / AVAILABILITY STATEMENT
Approved for Public Release; Distribution Unlimited

13. SUPPLEMENTARY NOTES

14. ABSTRACT

Prostate specific membrane antigen is type II membrane protein predominantly expressed in prostate epithelial and prostate cancer cells. This protein is expressed on the apical plasma membrane in prostate tissue and in cultured polarized epithelial cells. Antibodies against PSMA are being used for the diagnosis and treatment of prostate cancer. Understanding the mechanism by which PSMA is targeted to the apical plasma membrane should give novel insights into improvements in using anti-PSMA antibodies against prostate cancer. We have established a role for microtubules in the apical targeting of PSMA in cultured epithelial cells and have designed approaches to increase the efficacy of anti-PSMA antibodies for the treatment of prostate cancer. We have now generated data indicating that microtubule depolymerization disrupts the polarity of syntaxin 3 leading to non polarized expression of PMSA. Thus these new studies identified a potential mechanisms by which microtubules redirect PSMA to the basolateral plasma membrane.

15. Subject Terms (keywords previously assigned to proposal abstract or terms which apply to this award)

Prostate specific membrane antigen, endocytosis, transcytosis, microtubules

16. SECURITY CLASSIFICATION OF:			**17. LIMITATION OF ABSTRACT**	**18. NUMBER OF PAGES**	**19a. NAME OF RESPONSIBLE PERSON**
a. REPORT	**b. ABSTRACT**	**c. THIS PAGE**			USAMRMC
U	U	U	UU	79	**19b. TELEPHONE NUMBER** *(include area code)*

Table of Contents

Introduction/Body:

PSMA, a transmembrane glycoprotein of approximately 100kD, is expressed in prostate epithelial cells (Horoszewicz et al., 1987; Israeli et al., 1993). In addition to being expressed in non-neoplastic prostate epithelium, PSMA is expressed by a very high proportion of prostate cancers. Expression is further increased in higher-grade cancers and metastatic disease, and in hormone-refractory prostate cancers (Wright et al., 1995). PSMA is a type II membrane protein with a short N-terminal cytoplasmic tail and a large C-terminal extracellular domain (Israeli et al., 1993). The extracellular domain of PSMA has several potential N-glycosylation sites and shows homology (54% at nucleic acid level) to the transferrin receptor. Recently, it has been shown that PSMA is homologous to glutamate carboxypeptidase II (85% at nucleic acid level) and has been suggested to have folate hydrolase activity and N-acetylated α-linked acidic dipeptidase (NAALADase) activity. Abundance of PSMA in prostate cancer cells and the cell surface localization of this protein make PSMA an ideal candidate for immunotherapy for prostate cancer.

We have shown that PSMA is localized to the apical plasma membrane in polarized MDCK cells (Christiansen et al., 2003, see enclosed reprint). We have also shown that PSMA is localized to the recycling endosomal compartment and that association of PSMA cytoplasmic tail with filamin A is necessary for targeting PSMA to the recycling endosome (Anilkumar et al., 2003). We have also discovered a novel internalization motif MXXXL in the cytoplasmic tail of PSMA that might have a role in the internalization and targeting of PSMA to the recycling endosomal compartment (Rajasekaran et al., 2003). We now have evidence that intact microtubules are necessary for the apical localization of PSMA in MDCK cells. The goal of this proposal has been to determine the mechanism by which microtubles are involved in the apical localization of PSMA. We have accomplished the goals of this project and have published several important publications related to the goals of this project. The reprints of these publications are enclosed.

Role of microtubules in apical targeting of PSMA and its clinical implication:

PSMA is expressed on the apical plasma membrane of polarized epithelial cells

Immunofluorescence analysis of tissue sections revealed prominent PSMA localization at the apical plasma membrane of prostatic epithelial cells, with staining at the lumenal interface of the gland (Christiansen et al., 2005). Consistent with the apical localization surface immunofluorescence analysis performed on confluent monolayers of MDCK cells expressing PSMA (MDCK-PSMA) revealed a similar pattern of expression, with PSMA staining localized primarily to the apical membrane in these cells. This localization was further confirmed by a selective cell surface biotinylation assay. Results of this assay demonstrated that 70 to 79% of PSMA at the cell surface was localized to the apical plasma membrane (Christiansen et al., 2005).

PSMA is targeted directly to the apical plasma membrane

Apical proteins may be targeted directly from the TGN or may be delivered first to the basolateral plasma membrane before undergoing transcytosis to the apical surface. In order to distinguish between these pathways, an antibody internalization based targeting assay was employed. Confluent monolayers of MDCK-PSMA cells grown on transwell filters were metabolically labeled with [^{35}S]-cystine/methionine for a brief pulse and chased in the presence of mAb J591 added to either the apical or basolateral chamber. The results of this experiment revealed that majority of the newly synthesized PSMA are targeted directly to the apical plasma membrane (Christiansen et al, 2005).

The extracellular domain of PSMA contains information for apical targeting

Although signals for apical targeting may be localized throughout the length of a given transmembrane protein, such signals most commonly reside within the extracellular domain. In order to assess the significance of this domain in apical targeting, a GFP tagged form of PSMA was created in which the majority of the extracellular domain was removed (PSMA-Δ103-750). Cell surface biotinylation assays demonstrated that this protein was localized in a non-polarized fashion. Immunoblot analysis performed on the same membranes revealed that 90-95% of the α-subunit of the sodium pump (Na,K-ATPase α-sub) was localized at the basolateral surface of these cells demonstrating that the uniform plasma membrane distribution of PSMA is not merely attributable to a general loss of epithelial polarity.

In order to evaluate the targeting potential offered by the lumenal domain, a secreted form of PSMA (sPSMA) lacking the cytoplasmic and transmembrane domains was created. The sPSMA protein was secreted from MDCK cells as a ~100 kDa glycoprotein that was recognized by the mAb J591 and that migrated with a molecular mass of ~80 kDa following treatment with tunicamycin or N-glycosidase. A stable MDCK cell line expressing sPSMA (MDCK-sPSMA) was grown to confluence on transwell filters, and the conditioned media was collected from the apical and basolateral chambers. sPSMA was secreted almost exclusively from the apical plasma membrane, further implicating the existence of a targeting signal encoded within the extracellular domain of PSMA (Christiansen et al., 2005).

Apical targeting of PSMA requires N-glycosylation

The extracellular domain of PSMA is highly glycosylated, with approximately 25% of the mass of PSMA attributable to N-linked carbohydrates. We next investigated the role of N-glycosylation in trafficking of PSMA.

Confluent monolayers of MDCK-PSMA cells were metabolically labeled in the presence or absence of tunicamycin. This drug prevents N-glycosylation in the endoplasmic reticulum, and has been used extensively to assess the role of glycosylation in protein trafficking. Selective biotinylation of the apical or basolateral plasma membrane revealed that while the majority of surface PSMA is normally localized to the apical plasma membrane, inhibition of N-glycosylation abolished the polarized expression of PSMA and resulted in equivalent levels at both plasma membrane surfaces (Christiansen et al, 2005).

Inhibition of N-glycosylation also resulted in a dramatic alteration in PSMA localization within post-Golgi transport vesicles. Incubation of MDCK-PSMA cells at 20°C was used to

inhibit post-Golgi transit and accumulate proteins within the TGN. Both PSMA and a GFP tagged version of the basolaterally targeted Na,K-ATPase β-subunit (Na,K-β-GFP) were localized to the TGN following incubation at 20°C. These cells were subsequently transferred to 37°C, allowing proteins to exit from the TGN. In the absence of tunicamycin, PSMA and Na,K-ATPase localized to distinct post-Golgi vesicles in regions proximal to the TGN, with only ~8% (7/87) of red and green vesicles overlapping. However, the level of co-localization of vesicles containing these markers increased to approximately 43% (38/88) when cells are incubated with tunicamycin, indicating a role for N-glycosylation in PSMA sorting into distinct post-Golgi vesicles.

Microtubules are necessary for apical targeting of PSMA

The integrity of the microtubule cytoskeleton is essential for the targeted delivery of many apical proteins in polarized epithelial cells. To address the significance of microtubules in PSMA targeting, MDCK-PSMA cells were treated with the microtubule-depolymerizing agent, nocodazole. Nocodazole treatment resulted in a dramatic redistribution of PSMA. Surface immunofluoresence revealed increased PSMA expression at the basolateral plasma membrane relative to untreated cells. These data were also confirmed by cell surface biotinylation experiments, which demonstrated a homogeneous distribution of PSMA at both plasma membrane domains following nocodazole treatment. Polarity of the basolateral marker Na,K-ATPase was unaffected by nocodazole treatment, confirming the conservation of TJ integrity and epithelial polarity in these cells (Christiansen et al., 2005).

While tunicamycin and nocodazole treatment both resulted in a loss of PSMA polarity, the localization of PSMA within post-Golgi vesicles after treatment with these drugs was distinctly different. Following release from a 20°C block, PSMA and Na,K-β-GFP did not show an increased co-localization in the presence of nocodazole, with only ~8% (4/52) of red and green post-Golgi vesicles. These results indicate that targeting of PSMA into distinct post-Golgi vesicles was unaffected by microtubule depolymerization.

While microtubule depolymerization does not impact the sorting of PSMA into post-Golgi vesicles, the delivery of these vesicles to the plasma membrane fails to occur in a polarized manner. Confluent monolayers of MDCK-PSMA cells on transwell filters were pulsed and chased in the presence of extracellular mAb J591. In the absence of nocodazole, approximately 1.9 fold more radiolabeled PSMA was precipitated when J591 was added to the apical chamber compared to the basolateral, consistent with our earlier findings. However, in the presence of nocodazole, equivalent levels of radiolabeled PSMA were precipitated regardless of the chamber to which J591 was added, thus demonstrating that newly synthesized PSMA was delivered in a non-polarized fashion. These results suggest that microtubule integrity is necessary for proper delivery and retention of PSMA at the plasma membrane domain.

Vinca alkaloids promote mAb J591 uptake from the basolateral plasma membrane

Since nocodazole treatment reversed the polarity of PSMA, we investigated the effect of commonly used chemotherapeutic agents that inhibit microtubule assembly. The vinca alkaloids are a class of drugs applied to the treatment of a number of malignant diseases, including prostate cancer. Treatment of MDCK-PSMA cells with vinblastine, vincristine, or vinorelbine was sufficient to induce extensive depolymerization of the microtubule cytoskeleton. Confluent

monolayers of MDCK-PSMA cells were subjected to J591 internalization assays in order to determine how vinca alkaloid treatment influences PSMA localization. While polarized monolayers of untreated MDCK-PSMA cells readily internalized mAb J591 added to the apical chamber, very little antibody was internalized from the basolateral surface. Following treatment with vinca alkaloids, J591 was also taken up from the apical surface, albeit at decreased levels relative to untreated cells, however, these cells exhibited a dramatic increase in J591 internalization from the basolateral surface (Christiansen et al., 2005).

Polarized morphology of prostate tumor cells

We next investigated whether our observations using a polarized cultured cell line might have a practical significance in the context of prostate cancer cells, *in situ*. Histological assessment of a metastatic lesion from lymph node demonstrates diffused prostate tumor infiltration replacing the lymph node parenchyma. The enlarged tumor cells contain large and prominent nuclei and mitotic figures are readily observed. The prostate cancer cells form sheets with several areas of glandular differentiation. These glandular structures have clearly identifiable lumenal spaces occasionally containing pink secretions. The tumor cells surrounding the lumenal spaces show similar morphology to that seen in well-differentiated primary adenocarcinoma of the prostate with distinct plasma membrane organization. Immunohistochemical analysis revealed that these cells express PSMA, and that this antigen is restricted to the apical surface facing the lumen. This staining was clearly distinct from that of the endothelial cell marker CD 34 and CD31. Antibodies to these antigens stained small vessels but not the glandular structures, thus excluding the possibility that these PSMA expressing structures are actually blood vessels. These results indicate that prostatic carcinoma cells may retain a well-differentiated morphology, even following metastasis to distal sites.

Thus in this study we demonstrated that treatment of polarized epithelial cells with microtubule-targeting chemotherapeutic vinca alkaloids resulted in increased binding and endocytosis of PSMA specific antibodies from the basolateral surface in an *in vitro* system. To our knowledge, this is the first study to suggest that commonly used chemotherapeutic agents can be exploited to target intrinsic protein trafficking machinery as a means to reverse the apical polarity of an antigen to the basolateral plasma membrane. Although this has yet to be proven using an *in vivo* system, it appears that a combined therapeutic strategy to target both microtubules and an antigenic target, like PSMA, could have a synergistic effect on overall patient outcome.

Addendum (Additional work completed with the funds carried on):

As described above, we have conclusively demonstrated that the microtubules are necessary for the apical targeting of PSMA. In order to elucidate the role of microtubules in apical targeting, we investigated the effects of microtubule disruption on the localization of soluble N-ethylmaleimide-sensitive factor adaptor protein receptors (SNAREs) at the plasma membrane. SNAREs are a class of membrane anchored proteins that contain conserved coiled-coil domains and are essential for the docking and fusion of carrier vesicles with the target membrane. In addition to mediating the physical fusion of the membranes, SNAREs also confer specificity for protein cargo delivery. Vesicular

membrane SNAREs (v-SNAREs) interact only with their cognate target membrane SNAREs (t-SNAREs), which are assembled at specific intracellular locations. Within epithelial cells, t-SNAREs are expressed in a highly polarized fashion, with syntaxins 3 and 4 localized to the apical and basolateral plasma membrane, respectively (Low et al., 1996). Strikingly, we found that like PSMA syntaxin 3 was also present in the apical plasma membrane in both prostate tissues as well as in MDCK cells. Microtubule depolymerization using either nocodazole or vinca alkaloids also redirected syntaxin 3 to the basolateral plasma membrane. These results indicated that syntaxin 3 is the t-SNARE involved in the docking of PSMA containing cargo at the apical plasma membrane. It is also possible that microtubule disruption redirects syntaxin 3 to the basolateral plasma membrane and consequently PSMA is expressed on the basolateral plasma membrane. In collaboration with Dr. Thomas Weimbs (Uiversity of California, Santa Barbara) we are testing to identify a dominant negative form of syntaxin 3. If this dominant negative form syntaxin 3 prevents PSMA expression on the apical plasma membrane these results will demonstrate that syntaxin 3 is critical for PSMA expression on the apical plasma membrane. In addition, we are also trying whether stabilization of microtubules by Taxotere, a recently FDA approved drug for chemotherapy has any effect on PSMA and syntaxin 3 targeting. It is possible that Taxotere might not have any effect on redirecting PSMA to the basolateral plasma membrane and might not have significance in increasing the efficacy of PSMA-based immunotherapy for prostate cancer. These experiments are in progress and we expect to complete a manuscript on these studies.

We have completed all our initially stated goals on this project (see Statement of Work). The funds we carried on about $20,000 enabled us to find a novel role for syntaxin 3 in PSMA apical targeting and we hope will provide therapeutically valuable information for the immunotherapy against prostate cancer.

Statement of Work

Task 1: Expression of PSMA in normal prostate epithelial cells and testing the role of microtubules in the internalization of PSMA (1-8 months).

- ✓ **Prepare MLV retrovirus containing PSMA**
- ✓ **Transduce into normal prostate epithelial cells and standardize the time and the amount of virus required for optimal expression of PSMA in normal prostate epithelial cells**
- ✓ **Carry out mAb J591 uptake to monitor the internalization of PSMA by cell surface biotinylation and confocal microscopy assays**
- ✓ **Test the role of microtubules in the internalization of PSMA**

Task 2: Characterize the role of microtubules in the apical transport of PSMA in MDCK cells (1-36 months)

- ✓ **Standardize pulse chase experiments to monitor PSMA synthesis in MDCK cells**

- ✓ **Determine whether microtubules are necessary for the apical targeting of PSMA**
- ✓ **Standardize nocodazole wash off experiments and determine whether intact microtubules are necessary for the apical localization of PSMA by immunofluorescence approach**
- ✓ **Develop quantitative biochemical approach to monitor apical to basal and basal to apical transcytosis of PSMA**
- ✓ **Develop radioactive pulse chase labeling assays to determine whether PSMA is first targeted to the apical or basolateral plasma membrane.**

Task 3: Develop in vitro microtubule binding assays (24-36 months)

- ✓ **Purify full length and cytoplasmic tail deletion mutant of PSMA using a bacculovirus system**
- ✓ **Develop immunofluorescence assay to monitor PSMA binding to microtubules**
- ✓ **Develop quantitative sedimentation microtubule binding assay to test PSMA binding to microtubules.**

Task 4: Test alternate endocytic mechanism in LNCaP cells (1-24 months)

- ✓ **Develop cell surface biotinylation assay to monitor internalization of PSMA in K^+ free buffer to test clathrin-independent endocytosis**
- ✓ **Develop immunofluorescence assay to monitor internalization of PSMA in K^+ free buffer to test clathrin-independent endocytosis**
- ✓ **Test internalization of transferrin receptor in K^+ free buffer**
- ✓ **Test internalization of PSMA and transferrin receptor in MDCK cells in K^+ free buffer.**

Key Research Accomplishments:

- Established MDCK cells as a model to study targeting prostate restricted proteins.
- Determined PSMA is localized to the recycling endosomal compartment
- Identified filamin as a cytoplasmic tail binding protein of PSMA using yeast two hybrid analysis
- Characterized that filamin association is necessary for targeting to the recycling endosomal compartment
- Determined that filamin is a key regulator of PSMA localization and NAALADase activity.
- Identified a novel internalization motif in the cytoplasmic tail of PSMA
- Characterized that N-Glycosylation is necessary for apical targeting of PSMA.
- Defined that microtubules are involved in the stable localization of PSMA at the apical plasma membrane.
- Characterized that depolymerization of microtubules alters the polarity of PSMA
- Defined a clinical relevance to basolateral localization of PSMA.

- PSMA undergoes internalization in a clathrin independent manner in LNCap Cells.
- **Identified a potential role for Syntaxin 3 in the apical targeting of PSMA (Addendum**)

Reportable outcomes (publications):

1. Christiansen, J., S.A. Rajasekaran, P. Moy, A. Butch, L. Goodglick, N. Bander, R.Reiter, Z. Gu and A.K. Rajasekaran (2003). Polarity of Prostate specific membrane antigen, Prostate stem cell antigen, and prostate specific antigen in MDCK cells and in prostate tissue. Prostate, 2003 55: 9-19.

2. Anilkumar, G., S. A. Rajasekaran, S. Wang, O. Hankinson, N. Bander, and A. K Rajasekaran (2003). Prostate specific membrane antigen association with filamin A modulates its internalization and NAALADase activity. Cancer Res. 63:2645-8.

3. Rajasekaran, S.A., G. Anilkumar, E. Oshima., J.U. Bowie, H. Liu, W. Heston, N. Bander, and A.K Rajasekaran (2003). A novel cytoplasmic tail MXXXL motif mediates the internalization of prostate specific membrane antigen. Mol. Biol. Cell. 14:4835-4845.

4. Christiansen, J.J and A.K.Rajasekaran (2004). Biological impediments to antibody based cancer immunotherapy, invited review, Mol. Cancer Ther.11;1493-1501.

5. Rajasekaran, A.K, Anilkumar G and J. Christiansen (2005). Is Prostate specific membrane antigen a multifunctional protein? Am. J. Physiol. Cell Physiol. 288: C975-C981.

6. Christiansen, J.J., S. Rajasekaran, Chung, L., G. Anilkumar, N.Bander, and A. K. Rajasekaran (2005). N-glycosylation and microtubule dependent apical targeting of PSMA: Implications for prostate cancer immunotherapy. Mol. Cancer.Ther. 4:704-714 **(Cover Article)**.

7. **Potential Manuscript (Addendum**)

   Christiansen, J.J, N.Bander, T.Weimbs and A. K. Rajasekaran (2006). Role of syntaxin 3 in the apical targeting of PSMA.

Patent:

Ayyappan K Rajasekaran and Jason Christiansen (2004). A novel method to increase the efficiency of anti-PSMA antibodies in the treatment of prostate cancer (submitted to UC Regents).

Ph.D. Degree Awarded:

A UCLA Cellular and Molecular Pathology graduate student Jason Christiansen performed most of these studies. He was awarded Ph.D degree for his work in December 2004.

Conclusions: We have characterized MDCK cells as a potential model to study targeting of prostate specific proteins. Using this model we have now established that apical targeting of PSMA requires its N.glycosylation and its apical localization requires intact microtubules in MDCK cells. We have also identified a novel method to redirect apically targeted proteins to the basolateral plasma membrane to increase accessibility to circulating therapeutic agents.

References:

1. Horoszewicz, J.S., E. Kawinski, and G.P. Murphy. 1987. Monoclonal antibodies to a new antigenic marker in epithelial prostatic cells and serum of prostatic cancer patients. *Anticancer Res.* 7:927-35.

2. Israeli, R.S., C.T. Powell, W.R. Fair, and W.D. Heston. 1993. Molecular cloning of a complementary DNA encoding a prostate-specific membrane antigen. *Cancer Res.* 53:227-30.
3. Wright, Jr. 2001. Quantitation of serum prostate-specific membrane antigen by a novel protein biochip immunoassay discriminates benign from malignant prostate disease. *Cancer Res*. 61:6029-33.
4. Christiansen, J., S.A. Rajasekaran, P. Moy, A. Butch, L. Goodglick, N. Bander, R.Reiter, Z. Gu and A.K. Rajasekaran (2003). Polarity of Prostate specific membrane antigen, Prostate stem cell antigen, and prostate specific antigen in MDCK cells and in prostate tissue. Prostate, 2003 55: 9-19.
5. Rajasekaran, S.A., G. Anilkumar, E. Oshima., J.U. Bowie, H. Liu, W. Heston, N. Bander, and A.K Rajasekaran (2003) . A novel cytoplasmic tail MXXXL motif mediates the internalization of prostate specific membrane antigen. Mol. Biol. Cell. 14:4835-4845.
6. Anilkumar, G., S. A. Rajasekaran, S. Wang, O. Hankinson, N. Bander, and A. K Rajasekaran (2003). Prostate specific membrane antigen association with filamin A modulates its internalization and NAALADase activity. Cancer Res. 63:2645-8.
7. Christiansen, J.J., S. Rajasekaran, Chung, L., G. Anilkumar, N.Bander, and A. K. Rajasekaran (2005). N-glycosylation and microtubule dependent apical targeting of PSMA: Implications for prostate cancer immunotherapy. Mol. Cancer.Ther. 4:704-714.

Appendix: Copies of six reprints are enclosed.

Polarity of Prostate Specific Membrane Antigen, Prostate Stem Cell Antigen, and Prostate Specific Antigen in Prostate Tissue and in a Cultured Epithelial Cell Line

Jason J. Christiansen,[1] Sigrid A. Rajasekaran,[1] Peggy Moy,[3] Anthony Butch,[1] Lee Goodglick,[1] Zhennan Gu,[2] Robert E. Reiter,[2] Neil H. Bander,[3] and Ayyappan K. Rajasekaran[1]*

[1]*Department of Pathology and Laboratory Medicine, University of California, Los Angeles, Los Angeles, California*
[2]*Department of Urology, University of California, Los Angeles, Los Angeles, California*
[3]*Department of Urology, Weill Medical College, Cornell University, New York, New York*

BACKGROUND. Madin-Darby canine kidney (MDCK) cells are immortalized epithelial cells that have been used extensively as a model system to study intracellular molecular trafficking, polarized expression, and secretion of proteins in various epithelia. In order to determine if MDCK cells might serve as a model to study molecular events within prostate epithelial cells, we have evaluated the polarized distribution of three prostate restricted proteins, PSMA, PSCA, and PSA, in situ, and in MDCK cells.

METHODS. Using immunofluorescence, confocal microscopy, cell surface biotinylation, antibody internalization, and biochemical assays we evaluated surface expression and secretion of three prostate restricted proteins expressed in MDCK cells. We compared these patterns of expression to results observed within prostatic epithelium.

RESULTS. We demonstrate that PSMA is localized primarily to the apical plasma membrane in both the prostatic epithelium and transfected MDCK cells, whereas PSCA is expressed in a non-polarized fashion. We also show that PSA is secreted predominantly from the apical surface of transfected MDCK cells, consistent with in vivo observations.

CONCLUSIONS. Similar patterns of localization among MDCK and prostatic epithelial cells suggest that the mechanisms of polarized sorting within these cell types are conserved. Thus, MDCK cells offer a useful model system to study mechanisms of targeting of these proteins within the prostate. *Prostate 55: 9–19, 2003.* © 2003 Wiley-Liss, Inc.

KEY WORDS: **prostate; prostate neoplasm; prostate specific membrane antigen; prostate stem cell antigen; prostate specific antigen; protein targeting**

INTRODUCTION

External surfaces and internal cavities of the body are lined with a thin layer of epithelial tissue. These tissues are comprised of polarized epithelial cells in close apposition to one another and adherent upon a thin, non-cellular basement membrane attached to the underlying connective tissue. Epithelial tissues functionally partition biological compartments, physically separating them from one another or from the external environment. These tissues form selective permeability barriers between compartments, and allow for

Abbreviations used: PSMA, prostate specific membrane antigen; MDCK, Madin-Darby canine kidney cells; PSCA, prostate stem cell antigen; PSA, prostate specific antigen.

Grant sponsor: Department of Defense; Grant numbers: PC991140, PC970546; Grant sponsor: NRSA Award; Grant number: NIH-NCI-2T32CA09056-26.

*Correspondence to: Ayyappan K. Rajasekaran, Department of Pathology and Laboratory Medicine, Room 13-344 CHS, University of California, Los Angeles, Los Angeles, CA 90095.
E-mail: arajasekaran@mednet.ucla.edu
Received 10 June 2002; Accepted 9 October 2002
DOI 10.1002/pros.10203

vectorial transport of fluids, ions, proteins, and other solutes, thus enabling organs to perform vital physiological functions, such as secretion, absorption, ion transport, or formation of impervious fluid barriers [1].

The ability of epithelia to perform these specialized feats of vectorial transport resides in the unique cellular architecture of the polarized epithelial cell. These cells are composed of two biochemically distinct plasma membrane surfaces, each with a unique composition of lipids and proteins. The apical plasma membrane, which faces the lumenal or extracellular space, is physically separated from the basolateral membrane, which is in contact with adjacent cells or the underlying matrix, by the zonula occludens, or tight junctions. The tight junctions completely circumscribe the cell just below the apical surface, creating regions of tight membrane contact between adjacent cells [2]. The tight junctions prevent lateral diffusion of molecules between plasma membrane domains, as well as restrict the flow of fluid through intercellular spaces.

The glandular epithelium of the prostate is composed of specialized secretory epithelial cells that produce and secrete a portion of the seminal fluid. Recent efforts have led to the identification of several proteins with expression highly restricted to the prostatic epithelium, including prostate specific membrane antigen (PSMA) [3], prostate stem cell antigen (PSCA) [4], prostate specific antigen (PSA) [5], prostatic acid phosphatase (PAP) [6], and six transmembrane epithelial antigen of the prostate (STEAP) [7].

Originally identified in LNCaP cells, PSMA is a type II transmembrane glycoprotein of approximately 100 kDa [3]. Although the precise physiological role of PSMA is not known, the large extracellular domain possesses glutamate carboxypeptidase [8] and folate hydrolyase [9] activities, thus PSMA has been implicated in the generation of glutamate by hydrolyzing peptide substrates within prostatic fluid [8]. In addition to expression in the normal prostate, PSMA expression is increased in virtually all cases of prostate cancer, and is further upregulated in high grade tumors and androgen independent disease [10–12]. Recent findings also indicate that PSMA is selectively expressed in the neovasculature of nearly all types of solid tumors, but not in the vasculature of normal tissue [10,13–15]. There is currently a great deal of clinical interest in PSMA for diagnostic purposes, in vivo imaging strategies, and cancer therapies [16].

Expression of PSCA is also highly restricted to the prostatic epithelium, with limited expression observed in some extraprostatic tissues. PSCA is a homologue of the Thy-1/Ly-6 family of glycosylphosphatidylinositol (GPI)-anchored proteins [4]. PSCA is overexpressed in a high proportion of localized and metastatic prostate tumors, and levels of expression have been determined to correlate with tumor stage, grade, and androgen independence [17]. For this reason, the prospect of exploiting PSCA as a prognostic indicator and as a target for immunotherapy are being explored [18,19].

PSA has proven one of the most useful biological markers in the diagnosis and management of prostate cancer [20,21]. PSA is a kallikrein-like serine protease that is secreted at high levels from the apical surface of the prostatic epithelium into the lumen of the gland [22,23]. PSA is one of the most abundant proteases found in prostatic fluid [24], and is believed to enhance sperm motility by participating in the liquification of semen by degrading matrix proteins [25,26]. PSA is also found in the serum, with increased levels associated with prostate cancer [27]. This may suggest that while PSA is secreted predominantly from the apical surface into the glandular lumen, a lower level of PSA is secreted from the basolateral surface, where it can gain access to the vasculature.

Despite the prevalence of prostate cancer and other pathological conditions, such as benign prostatic hyperplasia (BPH) and prostatitis, there currently exists no described cell culture model system to study polarized sorting of proteins within the prostatic epithelium. The common prostate derived cell lines, such as LNCaP, PC3, and DU145 are unsuitable for this purpose, as they are highly transformed, non-polarized cells that fail to form tight junctions. The lack of an appropriate model system in which to study polarized sorting of proteins within the prostatic epithelium has led us to investigate the potential of using Madin-Darby canine kidney (MDCK) cells for this purpose. MDCK cells are a well-differentiated cell line with tight junctions that form polarized monolayers in culture that closely resemble epithelial tissue. MDCK cells have previously been used as a model system to study epithelial polarity within a variety of organs, including the liver [28,29], kidney [30], thymus [31], thyroid [32], and intestine [33,34]. We have expressed three prostate restricted proteins, PSMA, PSCA, and PSA, in MDCK cells and compared the pattern of expression to that observed within the prostate tissue. In this manuscript, we demonstrate that like in prostate tissue PSMA is localized predominantly to the apical plasma membrane in MDCK cells. Furthermore, we demonstrate that PSCA is expressed in a non-polarized fashion in both prostate tissue and in transfected MDCK cells. Additionally, we show that PSA, which is primarily secreted into the lumen of the prostate gland, is secreted predominantly from the apical side in MDCK cells. These studies for the first time provide evidence that MDCK cells can be utilized as model to study polarized sorting of prostate restricted proteins and suggest that these cells could be utilized to further understand the function/s of these proteins.

MATERIALS AND METHODS

ProstateTissue

Remnant prostate tissue specimens were obtained from the Human Tissue Research Center at UCLA with proper approval by the UCLA office for the protection of research subjects. Following surgical removal, remnant specimens were rapidly placed in OCT compound and snap frozen using dry ice and 2-methyl butane mixture. Frozen sections (5 μm) were prepared and utilized for immunofluorescence studies. Pathologists at UCLA evaluated all prostate tissues. Tumor and matched normal tissues from a total of 12 patients diagnosed with prostate cancer (five patients with Gleason scores of 6, six with scores of 7, and one with score of 9) were used for immunofluorescence studies.

Cell Culture

MDCK cells (clone II) were cultured in Dulbecco's Modified Eagle Medium (DMEM) supplemented with 10% fetal bovine serum, 2 mM L-glutamine, 25 U/ml penicillin, 25 μg/ml streptomycin, and 100 μM non-essential amino acids. Cells were grown at 37°C in a humidified incubator with 5% CO_2. MDCK cell lines expressing PSMA were treated overnight in media containing 10 mM sodium butyrate to increase PSMA expression.

DNA Constructs and Transfections

The cDNAs encoding full length PSMA (kindly provided by Dr. Warren Heston, Cleveland Clinic Foundation, OH) or PSCA were cloned into the pcDNA3 expression vector (Invitrogen, Carlsbad, CA). The pSecTag2/PSA vector containing the cDNA encoding the active form of PSA fused to a *myc* epitope and polyhistidine tag was purchased from Invitrogen.

To generate stable cell lines, MDCK cells were transfected using the calcium phosphate method described previously [35]. Clones were selected in the presence of 500 μg/ml geneticin (G418, Gibco BRL, Rockville, MD) for pcDNA3 vectors or 300 μg/ml Zeocin (Invitrogen) for the pSecTag2/PSA vector. Expression was confirmed by immunofluorescence and immunoblotting.

Transient transfection was performed using lipofectamine reagent (Gibco BRL) according to manufacturer's instructions.

Antibodies

The monoclonal antibody (mAb) J591 directed against an extracellular epitope of PSMA has previously been described [15]. The mAb 7E11 directed against PSMA was prepared from hybridoma 7E11 (ATCC, Rockville, MD). The mAb to GP-135 was generously provided by Dr. Ojakian (State University of New York, NY). Generation of the mAb 1G8 against PSCA was previously described [17]. Antibody to E-cadherin was purchased from Zymed (South San Fransisco, CA). Antibody to β-catenin and HRP conjugated goat-anti-mouse IgG were purchased from Transduction Laboratories (Lexington, KY). FITC conjugated goat-anti-mouse IgG, Texas Red conjugated goat-anti-mouse IgG, and CY3 conjugated donkey-anti-mouse IgG secondary antibodies were purchased from Jackson ImmunoResearch Laboratories (West Grove, PA).

Immunofluorescence

Tissue sections were fixed in cold methanol at −20°C for 30 min. Following fixation, specimens were placed in humidified chambers, washed with phosphate buffered saline containing 100 μM $CaCl_2$, 1 mM $MgCl_2$, and 0.5% bovine serum albumin (PBS-CM-BSA), incubated 1 hr with primary antibody, washed with PBS-CM-BSA, incubated for 30 min in secondary antibody, washed with PBS-CM-BSA, and rinsed with distilled water. Propidium iodide (1 μg/ml) was added after incubation with secondary antibody and RNaseA (5 μg/ml) and cells were washed twice with PBS-CM-BSA. Specimens were mounted in vectashield (Vector, Burlingame, CA) and the coverslips were sealed.

Two forms of fixation protocol were used for MDCK cells, cold methanol fixation, which renders the cells permeabilized, and paraformaldehyde (PFA) fixation, which does not permeabilize cells. Cold methanol fixation of MDCK cells was performed as described above for tissues. For non-permeablized fixation, MDCK cells grown on glass coverslips were incubated in the dark for 30 min in a 2% solution of PFA with 100 μM $CaCl_2$, and 1 mM $MgCl_2$. Coverslips were washed twice in PBS-CM-BSA and incubated with 50 mM NH_4Cl in PBS-CM for 10 min and further processed similar to tissues. For cell surface staining, MDCK cells expressing PSMA were grown to confluency on glass coverslips. Media was removed and replaced with chilled DMEM containing 10 μg/ml J591. Cells were incubated on ice for 1 hr, rinsed with cold PBS-CM-BSA, fixed in cold methanol, and incubated with secondary antibody as described above.

For surface staining of MDCK cells expressing PSCA, confluent monolayers were grown on polycarbonate transwell filters (Corning, New York). Cells were stained for 30 min with 10 μg/ml of 1G8 in PBS (2% FCS) added on ice to both the apical and basolateral chambers. After removal of unbound antibody, cells were fixed in cold methanol and incubated with secondary antibody as described above.

Confocal Microscopy

Confocal microscopy was performed using a Fluoview laser scanning confocal microscope (Olympus America, Melville, NY) as described previously [36]. To detect FITC-labeled antigens and propidium iodide, samples were excited at 488 nm with an argon laser and light emitted between 525 and 540 nm was recorded for FITC and above 630 nm for propidium iodide. Images were generated and analyzed using the Fluoview image analysis software (version 2.1.39).

Antibody Uptake

MDCK cells expressing PSMA were grown to confluency on glass coverslips. Media was removed and replaced with 1 ml of DMEM containing 10 μg/ml J591. Cells were incubated at 37°C for 3 hr, rinsed in PBS-CM-BSA, fixed in cold methanol, and incubated with secondary antibody as described above.

Transepithelial Electrical Resistance (TER) Measurements

The resistance of MDCK monolayers on polycarbonate transwell filters (Corning) was determined using an EVOM Epithelial Voltometer (World Precision Instruments, Sarasota, FL). Values were normalized for the area of the filter after subtracting the background resistance of a filter without cells. TER of 220–250 Ωcm^2 is indicative of the presence of functional tight junctions [37].

Cell Surface Biotinylation

MDCK cells expressing PSMA were grown on transwell filters. Tight junction formation was assessed by TER. Biotinylation of apical or basolateral surfaces was performed as previously described [35]. Briefly, the cell surface of confluent monolayers was labeled on ice from apical or basolateral surface with 0.5 μg/ml of membrane impermeable EZ-Link Sulfo-NHS-Biotin (Pierce, Rockford, IL) in TEA (150 mM NaCl, 10 mM Triethanolamide pH 9.0, 1 mM $CaCl_2$, 1 mM $MgCl_2$). After quenching (50 mM NH_4Cl in PBS-CM), the cells were lysed in 0.5 ml lysis buffer (150 mM NaCl, 20 mM Tris pH8, 5 mM EDTA, 1% Triton-X-100, 0.1% BSA, 1 mM PMSF, 5 μg/ml each of antipain, leupeptin, and pepstatin). Total protein for each lysate was used for precipitation (16 hr at 4°C) with mAb J591 bound to protein A sepharose beads. Precipitates were washed, separated on a 10% SDS polyacrylamide gel, transferred to nitrocellulose, immunoblotted with the streptavidin-HRP, and visualized by ECL as described earlier [38].

PSA Assay

MDCK cells expressing PSA were grown on transwell filters. Tight junction formation was assessed by TER. Two millilitres of fresh media was added to both the apical and basolateral chambers, cells were incubated 8–10 hr at 37°C, and media was collected from each chamber.

PSA concentrations in tissue culture media were determined using the automated Access Immunoassay Analyzer (Beckman Coulter, Fullerton, CA) using the Hybritech PSA 1-Step sandwich assay. The assay measures both free and complexed PSA on an equal molar basis. Recovery experiments were performed to verify that the assay accurately measures PSA in tissue culture medium by adding known quantities of PSA to samples of DMEM tissue culture medium. Total imprecision (coefficient of variation) for the assay at PSA concentrations of 2.7 and 21.5 ng/ml were 4.6 and 3.2%, respectively.

RESULTS

Frozen sections from regions of tumor and morphologically normal tissue from 12 patients were stained for PSMA and subject to analysis. In matched tissue samples from 10 of the 12 patients, confocal microscopy revealed a prominent PSMA staining along the lumenal surface (apical) of the prostate gland in tumor tissues (Fig. 1A). Although apically localized, the staining intensity of PSMA in normal tissues was relatively weak (data not shown). In these tissues, the basolateral marker protein E-cadherin was distinctly localized to the basolateral plasma membrane (Fig. 1B). These results indicated that PSMA is predominantly localized to the apical plasma membrane in prostate gland. Tumor tissue sections from two patients (Gleason scores 6 and 7) with high levels of PSMA expression showed a distinctly non-polarized distribution of PSMA with staining on both apical and basolateral plasma membranes (Fig. 1C, arrow). Interestingly, E-cadherin in the same gland showed polarized localization to the basolateral plasma membrane (Fig. 1D).

To study the localization of PSMA in MDCK cells, we generated a stable cell line expressing PSMA (MDCK-PSMA). These cells produced a glycoprotein that migrated through an SDS polyacrylamide gel with an apparent molecular mass of 100 kDa and was recognized by the mAb, 7E11. Following treatment with *N*-glycosidase, the core, deglycosylated protein ran with a molecular mass of approximately 84 kDa. This is in agreement with observations in LNCaP cells, which express high levels of endogenous PSMA, suggesting that the transfected MDCK cell line is expressing a full-length and glycosylated form of PSMA (Fig. 2).

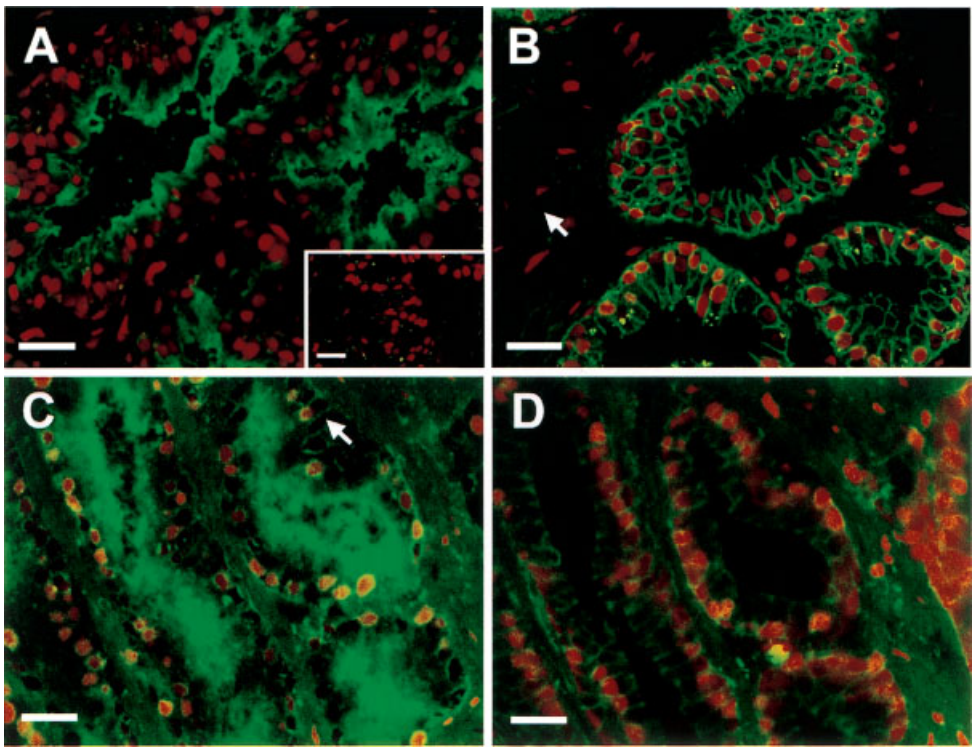

Fig. 1. Localization of PSMA and E-cadherin in prostate tissue. Tumor tissue sections stained with mAb 7E11 and FITC-conjugated secondary antibody (green) reveal an apical staining pattern for PSMA (**A**). No staining is visible after incubation with secondary antibody alone (A inset). Basolateral staining is evident when tissue sections are stained with mAb directed against E-cadherin and FITC-conjugated secondary antibody (**B**). Basolateral localization of PSMA (**C**, arrow) and E-cadherin in the same prostate gland (**D**). Propidium iodide was used to stain nuclei in all panels. Bars, 15 μm.

To determine the plasma membrane localization of PSMA in MDCK cells, confluent monolayers of MDCK-PSMA cells were grown on glass coverslips. Surface immunofluorescence and confocal microscopy analyses revealed an apical staining pattern of PSMA. The staining pattern of PSMA in horizontal (XY) and vertical (XZ) confocal microscope optical sections (Fig. 3A) was similar to that of an endogenously expressed apical marker GP-135 (Fig. 3B) in MDCK cells. The apical localization of PSMA and GP-135 can be contrasted to the typical basolateral staining pattern of β-catenin (Fig. 3C).

To further evince PSMA expression on the apical plasma membrane, we utilized an antibody internalization assay [38]. In this assay, confluent monolayers MDCK-PSMA cells were incubated with mAb J591. Tight junction prevents the mAb J591 from reaching antigens localized to the basolateral plasma membrane. Therefore, internalization of antibody will occur only from the apical plasma membrane. The vesicular endosomal staining shown in Figure 4E, demonstrates that mAb J591 was clearly internalized from the apical surface in MDCK-PSMA cells. To confirm that these monolayers contain functional tight junctions and are not permeable to antibody, we utilized an antibody against the extracellular domain of E-cadherin, a basolateral marker in MDCK cells. When cells were permeablized, E-cadherin was visualized on the basolateral plasma membrane (Fig. 4A and B). Under non-permeablized conditions, incubation of the MDCK-PSMA monolayer with E-cadherin antibody did not show staining of the basolateral plasma membrane (Fig. 4C and D).

To obtain a quantitative analysis of PSMA expression on the cell surface, we performed cell surface biotinylation experiments. Identical numbers of MDCK-PSMA cells were grown on transwell filters, and formation of tight junctions was confirmed by measuring TER. Biotinylation of either apical or basolateral surfaces was performed, cells were lysed, and the levels of biotinylated PSMA on either surface were determined (Fig. 5A). The results indicated that of the PSMA expressed on the cell surface, 70% was localized to the apical plasma membrane whereas about 30% was localized to the basolateral plasma membrane (Fig. 5B). Taken together, these results strongly suggest

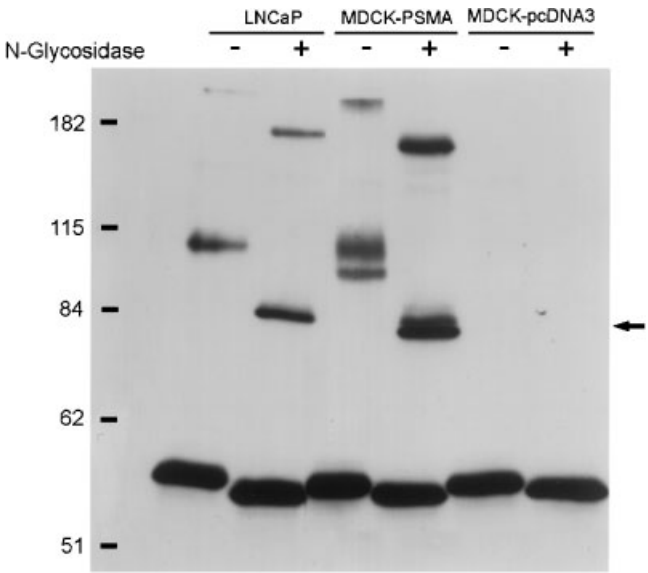

Fig. 2. PSMA expression in LNCaP and MDCK cells. PSMA was immunoprecipitated from LNCaP or MDCK cells using mAb J591. The precipitated samples were treated for 4 hr at 37°C in the presence or absence of N-glycosidase. Western blot analysis using mAb 7E11 reveals a glycoprotein of approximately 100 kDa and a core deglycosylated protein of approximately 84 kDa (arrow) in both LNCaP and MDCK-PSMA cells. No bands are recognized by 7E11 in untransfected MDCK cells. High molecular mass (200 kDa) appears to be a dimer of PSMA.

that PSMA is predominantly localized to the apical plasma membrane in both prostate tissue and polarized MDCK cells.

Tissue sections immunostained with antibody against PSCA revealed a different pattern of localization relative to PSMA. Matched tumor and morphologically normal tumor tissue sections revealed PSCA staining evident on both the apical and basolateral plasma membrane surfaces of prostatic epithelial cells (Fig. 6A). E-cadherin staining was observed at the basolateral plasma membrane in these tissues (data not shown). To investigate the expression of PSCA in MDCK cells, we generated a stable cell line expressing PSCA. Surface staining of these cells with antibody to PSCA and confocal analysis revealed PSCA to be distributed in a non-polarized manner at both the apical and basolateral plasma membrane surfaces (Fig. 6B and C).

Next, we examined polarized sorting of the secretory protein PSA in MDCK cells. PSA is secreted predominantly from the apical surface of secretory prostate epithelial cells into the lumen of the prostate gland. MDCK cells transiently transfected to express an epitope tagged version of PSA were grown on transwell filters. Following the formation of tight junctions, the PSA concentration in media from the apical and basolateral chambers was determined. The results

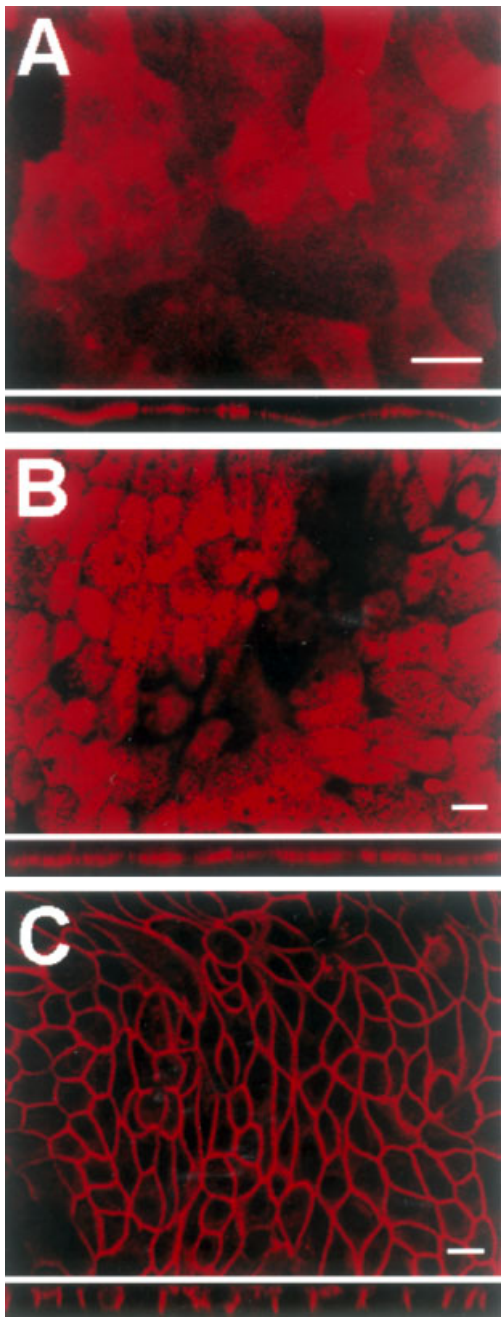

Fig. 3. Apical localization of PSMA in MDCK-PSMA cells. MDCK-PSMA cells were grown on glass coverslips and surface PSMA was labeled by incubating monolayers of cells on ice with mAb J591. Unbound J591 was removed and cells were fixed and incubated with CY3-conjugated secondary antibody. XY and XZ sections reveal PSMA to be localized to apical plasma membrane (**A**). Similar staining pattern observed for monolayers of MDCK-PSMA cells fixed in cold methanol and stained with mAb to GP-135 (an apical marker) and CY3-conjugated secondary antibody (**B**). Staining with mAb to β-catenin and CY3-conjugated secondary antibody reveals basolateral localization in XY and XZ sections (**C**). Bar, 10 μm.

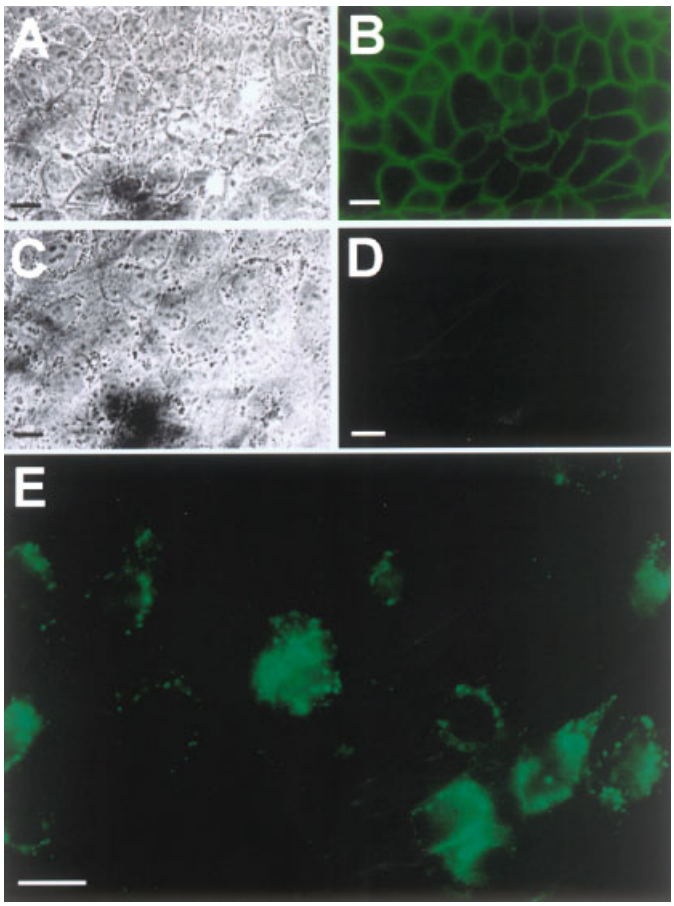

Fig. 4. Internalization of PSMA from the apical surface. Phase contrast images of confluent monolayers of MDCK-PSMA cells grown on glass coverslips are shown in **A** and **C**. In permeablized cells, mAb against E-cadherin and FITC-conjugated secondary antibody reveals a typical basolateral pattern (**B**). In non-permeablized cells, the presence of tight junctions restricts antibody from reaching E-cadherin at the basolateral surface, thus no staining is observed (**D**). Incubation of cells with mAb J591 at 37°C reveals a vesicular pat-

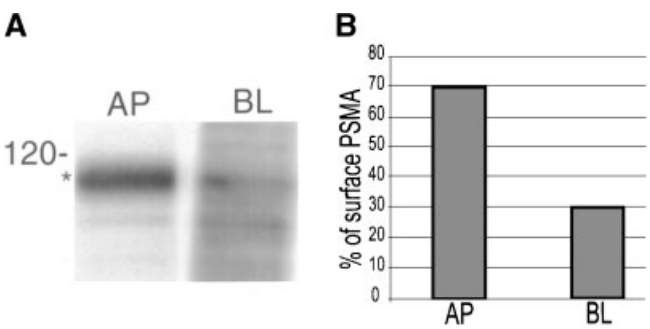

Fig. 5. Distribution of PSMA in MDCK-PSMA cells as revealed by a cell surface biotinylation assay. Monolayers of MDCK-PSMA cells were grown on transwell filters. Apical or basolateral surfaces were biotinylated and PSMA immunoprecipitated with mAb J591. SDS–PAGE and streptavidin-HRP analysis reveals surface PSMA to be localized primarily at the apical membrane (**A**). Quantification reveals 70% of cell surface PSMA to be apically localized (**B**).

presented in Figure 7A show that PSA is secreted primarily into the apical medium at an average of 2.3 times greater than into the basolateral medium.

To verify these results and demonstrate that these observations are not merely due to an artifact of transient transfection, stable MDCK cell lines expressing PSA were selected. Homogeneity of the clones was confirmed by immunofluorescence using an anti-*myc* antibody to epitope tagged PSA (data not shown). Two clones were plated on transwell filters and the formation of tight junctions was confirmed by measuring TER. Media from either chamber was analyzed for PSA concentration, and the results are shown in Figure 7B and C. Like in transiently transfected cells, two clones of MDCK-PSA cells showed 1.9–2.3 fold more secretion from the apical surface compared to the basolateral surface.

DISCUSSION

In this study, we have used laser confocal microscopy to demonstrate that PSMA is localized to the apical surface of the prostatic epithelium, lining the lumenal interface of the gland. Through cell surface staining, internalization, and biotinylation assays, we have also shown that the majority of cell surface PSMA is similarly localized to the apical plasma membrane in MDCK-PSMA cells. Since the pattern of localization in MDCK cells is consistent with the pattern of expression seen within the prostatic epithelium, it is likely that the mechanisms responsible for apical targeting of this protein are conserved between these two cell types. Immunofluorescence performed on permeablized MDCK cells reveals a vesicular intracellular staining pattern in addition to apical plasma membrane staining, with no PSMA visible on the basolateral surface in regions of cell–cell contact. However, through a highly sensitive biotinylation assay, we were able to detect a low level of PSMA on the basolateral surface. Additional experiments are currently being conducted in our laboratory to evaluate the significance of this low steady state level of basolateral PSMA and elucidate the underlying mechanisms by which PSMA is targeted to the apical plasma membrane.

In order for epithelia to perform essential tasks of vectorial transport, epithelial cells must establish and maintain an asymmetric plasma membrane composition. Proteins destined for either the apical or basolateral surface must be selectively targeted to the appropriate plasma membrane domain. Proteins destined for either the apical or basolateral surface travel together through the cisternae of the Golgi apparatus to the *trans*-Golgi Network (TGN). In polarized epithelial cells, TGN is the site at which secretory and plasma

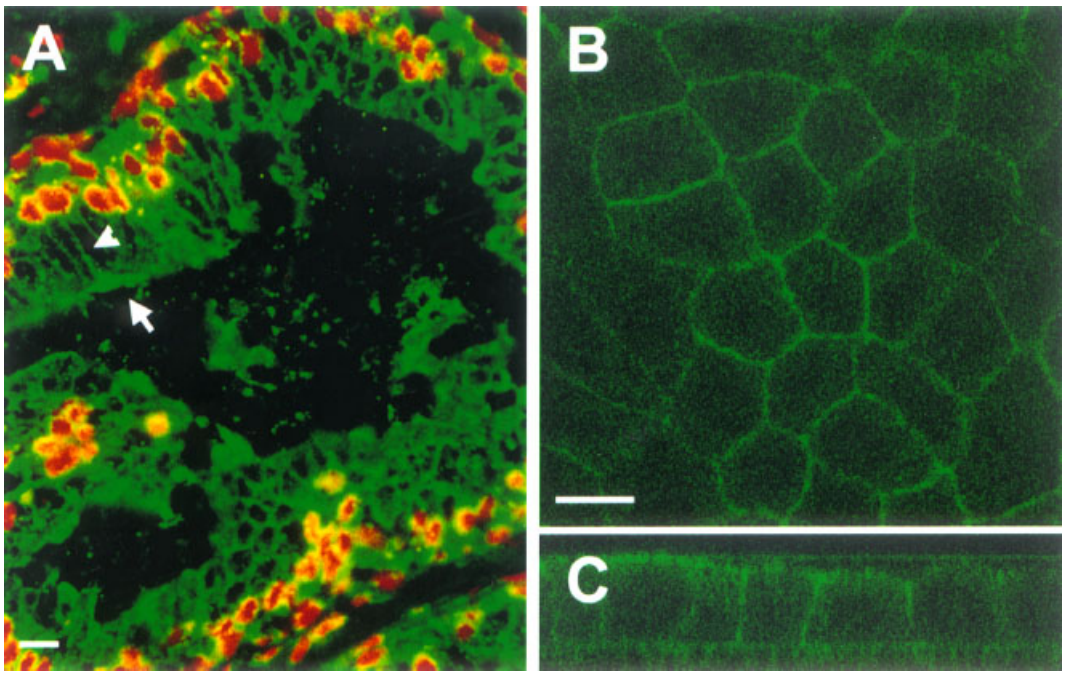

Fig. 6. Non-polarized distribution of PSCA in prostate tissue and MDCK cells. Normal tissue sections stained with propidium iodide to visualize nuclei (red), mAb 1G8, and FITC-conjugated secondary antibody (green) show PSCA to be present on both apical and basolateral plasma membrane surfaces. PSCA on the apical plasma membrane is indicated with an arrow, basolateral with an arrowhead (**A**). 1G8 was used to perform cell surface staining on confluent monolayers of MDCK-PSCA cells grown on transwell filters. Confocal microscopy reveals PSCA to be localized in a non-polarized fashion on apical and basolateral plasma membrane surfaces (**B** and **C**). Bar, 10 μm.

membrane proteins are sorted to the apical and basolateral plasma membrane domains [39]. In the TGN, sorting mechanisms interpret signals encoded within the proteins and properly direct them into discrete vesicles destined for the appropriate membrane domain [40]. Different cell types utilize different repertoires of sorting mechanisms, emphasizing the importance of choosing an appropriate model system to study protein sorting in polarized epithelia [40].

The signals responsible for the targeting of proteins to basolateral plasma membrane are thought to reside exclusively within the cytoplasmic domain. Among

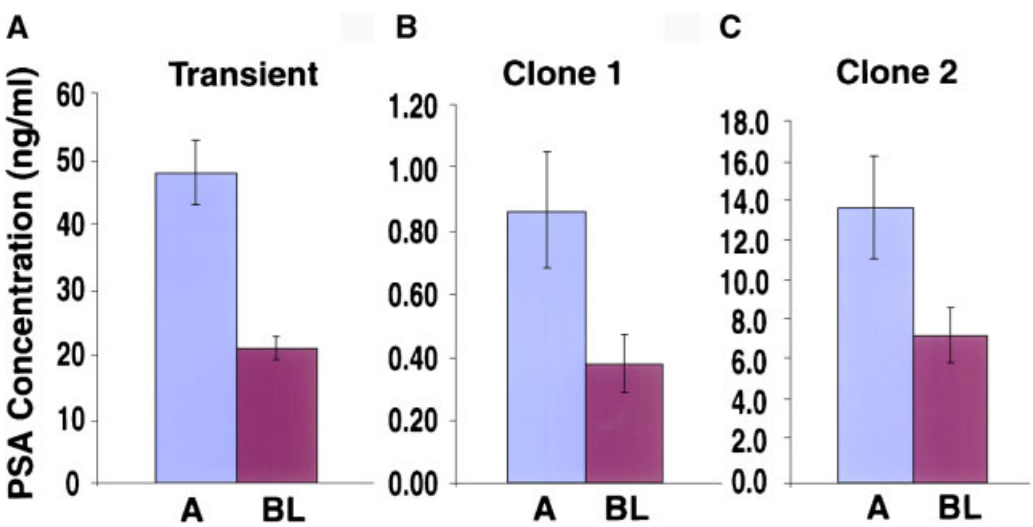

Fig. 7. Apical secretion of PSA in transfected MDCK cells. PSA is secreted predominantly form the apical surface either in transiently transfected cells (**A**) or in stable cell clones (**B** and **C**) expressing PSA. Results represent the average of 4–5 independent determinations in each case. Error bars represent standard error.

the best-characterized signals are the tyrosine- and dileucine-based motifs. These signals were originally identified through their ability to mediate internalization of proteins via clathrin coated pits, and have since been shown to interact with adaptor protein complexes. In contrast, the signals responsible for apical sorting have remained much more enigmatic. Reports have shown that a variety of molecular determinants may be involved in apical targeting, including GPI anchors, lipid rafts, N-glycosylation, O-glycosylation, and amino acid motifs encoded within the cytoplasmic or transmembrane domains. The characterization of MDCK cells as a model in which to study the sorting of PSMA should enable us to further define the mechanisms of apical targeting within epithelia. While the cytoplasmic tail of PSMA contains a dileucine-like motif the majority of cell-surface PSMA is localized to the apical plasma membrane, indicating that the transmembrane or extracellular domain of PSMA contain a dominant apical targeting signal. This possibility is currently being explored in our laboratory.

While PSMA was distinctly localized to the apical plasma membrane in most of the prostate tumor tissues examined in this study, we observed localization to the basolateral surface in tissue sections derived from two patients (Fig. 1C). Although the fluorescence intensity of the basolaterally expressed PSMA was lower than the apically localized PSMA in this sample, this result indicates that PSMA can also be targeted to the basolateral plasma membrane. The presence of PSMA on the basolateral plasma membrane may have important clinical significance. PSMA on the basolateral surface would be in closer proximity to the vasculature and thus these patients may exhibit improved response to immunotherapy. Further study will be required to evaluate this hypothesis.

The normal polarized localization of E-cadherin in the same glands that showed PSMA localized on the basolateral surface indicates that the change in polarity of PSMA is specific, and not due to a general loss of polarity or tight junction integrity. Since E-cadherin is associated with the actin cytoskeleton through its interaction with catenins [41], it is possible that the association with the actin cytoskeleton retained this protein at the basolateral plasma membrane in spite of aberrant sorting mechanisms in these tumor cells. According to this possibility, the apical localization of PSMA may be affected while the basolateral localization of E-cadherin should be maintained. Alternatively, PSMA in this tumor tissue may have a different glycosylation pattern or a mutation in the apical targeting signal, which would lead to the basolateral localization of PSMA. It is also possible that abundant levels of PSMA expressed in these tumor cells might have resulted in the saturation of the apical targeting machinery resulting in the localization of apical proteins in the basolateral plasma membrane. While additional tissue samples must be examined to further determine whether such basolateral localization of PSMA is a general phenomenon in the progression of prostate cancer, the availability of MDCK cells as a model to study polarized sorting should permit investigations into these possibilities.

We have also investigated the localization of a second membrane associated, prostate restricted antigen, PSCA. Confocal microscopy reveals that PSCA is distributed in a non-polarized manner within the prostatic epithelium. In MDCK cells, PSCA is similarly distributed to both apical and basolateral plasma membrane surfaces. The similar patterns of localization provide further evidence that MDCK cells are a useful model in which to study polarized sorting in the prostatic epithelium.

The non-polarized plasma membrane distribution of PSCA was an unexpected result for a GPI-anchored protein. In MDCK and many other epithelial cell types, the presence of such GPI-modifications has been shown to specifically target proteins to the apical plasma membrane. This targeting presumably occurs via association with membrane microdomains known as lipid rafts [42]. Exactly why PSCA is distributed in such a non-polarized manner has yet to be determined. Elucidating the targeting information encoded within PSCA and determining the ability of this GPI-anchored protein to associate with lipid rafts will be the subject of future research.

In this report, we have also studied the polarized secretion of the prostate restricted protease, PSA. Within the prostate, PSA is secreted apically from the epithelium into the lumen of the gland [23]. Low levels of PSA are also found within the blood, suggesting that a fraction of PSA may be secreted from the basolateral surface, where it can gain access to the vasculature [27]. At the levels of PSA expression observed in this study, PSA is secreted from the apical surface at levels 2–2.3 times greater than from the basolateral plasma membrane. These data are again consistent with in vivo observations suggesting that the mechanisms of apical secretion of PSA are conserved in prostate tissue and in MDCK cells.

Non-polarized secretion of proteases, such as PSA, may contribute to metastasis by degrading extracellular matrix proteins. In fact, Webber et al. demonstrated that blocking PSA activity with antibodies reduced the invasiveness of LNCaP cells, in vitro [25]. In addition, aberrantly polarized secretion of proteases may also promote cell growth by activating mitogens associated with the extracellular matrix. In this regard, PSA has been shown to activate latent growth factors, such as transforming growth factor β and insulin-like growth

factor I [43,44]. Although increased serum levels of PSA have long been known to be associated with prostate cancer, the mechanism by which this occurs is not well understood. This phenomenon could be due to saturation of the apical secretory pathway, loss epithelial polarity, a specific defect in the targeting pathway, or to the direct secretion of PSA into the serum by either invading or circulating metastatic cells. The use of MDCK cells as a model system may provide insight into the mechanism of increased PSA serum levels and help to further define role(s) for PSA in prostate cancer.

Studying the patterns and mechanisms of epithelial polarity can provide invaluable insight into normal physiology as well as the pathophysiology of disease. Understanding the extracellular environment (apical or basal) to which a protein is exposed can provide information regarding the normal physiological role of that protein. In addition, loss of polarity may provide the molecular basis for a number of pathological conditions. One of the hallmarks of cancer is the loss of normal epithelial phenotype. Very often, the progression of tumors to more aggressive phenotypes is closely associated with a concomitant loss of tight junctions and epithelial polarity [45]. Aberrant targeting of enzymes and receptors or the loss of polarity may have significant impact on disease and tumor progression. Expression of receptors within an inappropriate extracellular milieu may lead to aberrant stimulation of signaling events that could potentially provide a mitogenic stimulus. Loss of tight junctions in cancer cells may lead to aberrant surface expression of domain specific proteins, as evidenced by the non-polarized distribution of E-cadherin in transformed MDCK cells lacking tight junctions [36]. MDCK cells offer a useful system in which to study the role of tight junctions in polarized sorting of PSMA and PSA, as the permeability of these junctions can be affected by altering the extracellular calcium levels or by other mechanisms. Ultimately these studies should provide valuable insight into the function of these proteins in normal tissue and in disease.

ACKNOWLEDGMENTS

This work was supported by the Department of Defense grants PC991140 and PC970546 to AKR. JC and SAR are supported by a NRSA award NIH-NCI-2T32CA09056-26.

REFERENCES

1. Simons K, Wandinger-Ness A. Polarized sorting in epithelia. Cell 1990;62:207–210.
2. Farquhar MG, Palade GE. Junctional complexes in various epithelia. J Cell Biol 1963;17:375–412.
3. Horoszewicz JS, Kawinski E, Murphy GP. Monoclonal antibodies to a new antigenic marker in epithelial prostatic cells and serum of prostatic cancer patients. Anticancer Res 1987;7:927–935.
4. Reiter RE, Gu Z, Watabe T, Thomas G, Szigeti K, Davis E, Wahl M, Nisitani S, Yamashiro J, Le Beau MM, Loda M, Witte ON. Prostate stem cell antigen: A cell surface marker overexpressed in prostate cancer. Proc Natl Acad Sci USA 1998; 95:1735–1740.
5. Lundwall A, Lilja H. Molecular cloning of human prostate specific antigen cDNA. FEBS Lett 1987;214:317–322.
6. Vihko P, Virkkunen P, Henttu P, Roiko K, Solin T, Huhtala ML. Molecular cloning and sequence analysis of cDNA encoding human prostatic acid phosphatase. FEBS Lett 1988;236:275–281.
7. Hubert RS, Vivanco I, Chen E, Rastegar S, Leong K, Mitchell SC, Madraswala R, Zhou Y, Kuo J, Raitano AB, Jakobovits A, Saffran DC, Afar DE. STEAP: A prostate-specific cell-surface antigen highly expressed in human prostate tumors. Proc Natl Acad Sci USA 1999;96:14523–14528.
8. Carter RE, Feldman AR, Coyle JT. Prostate-specific membrane antigen is a hydrolase with substrate and pharmacologic characteristics of a neuropeptidase. Proc Natl Acad Sci USA 1996;93:749–753.
9. Pinto JT, Suffoletto BP, Berzin TM, Qiao CH, Lin S, Tong WP, May F, Mukherjee B, Heston WD. Prostate-specific membrane antigen: A novel folate hydrolase in human prostatic carcinoma cells. Clin Cancer Res 1996;2:1445–1451.
10. Silver DA, Pellicer I, Fair WR, Heston WD, Cordon-Cardo C. Prostate-specific membrane antigen expression in normal and malignant human tissues. Clin Cancer Res 1997;3:81–85.
11. Sweat SD, Pacelli A, Murphy GP, Bostwick DG. Prostate-specific membrane antigen expression is greatest in prostate adenocarcinoma and lymph node metastases. Urology 1998;52:637–640.
12. Wright GL, Jr., Grob BM, Haley C, Grossman K, Newhall K, Petrylak D, Troyer J, Konchuba A, Schellhammer PF, Moriarty R. Upregulation of prostate-specific membrane antigen after androgen-deprivation therapy. Urology 1996;48:326–334.
13. Chang SS, Reuter VE, Heston WD, Bander NH, Grauer LS, Gaudin PB. Five different anti-prostate-specific membrane antigen (PSMA) antibodies confirm PSMA expression in tumor-associated neovasculature. Cancer Res 1999;59:3192–3198.
14. Chang SS, O'Keefe DS, Bacich DJ, Reuter VE, Heston WD, Gaudin PB. Prostate-specific membrane antigen is produced in tumor-associated neovasculature. Clin Cancer Res 1999;5:2674–2681.
15. Liu H, Moy P, Kim S, Xia Y, Rajasekaran A, Navarro V, Knudsen B, Bander NH. Monoclonal antibodies to the extracellular domain of prostate-specific membrane antigen also react with tumor vascular endothelium. Cancer Res 1997;57:3629–3634.
16. Elgamal AA, Holmes EH, Su SL, Tino WT, Simmons SJ, Peterson M, Greene TG, Boynton AL, Murphy GP. Prostate-specific membrane antigen (PSMA): Current benefits and future value. Semin Surg Oncol 2000;18:10–16.
17. Gu Z, Thomas G, Yamashiro J, Shintaku IP, Dorey F, Raitano A, Witte ON, Said JW, Loda M, Reiter RE. Prostate stem cell antigen (PSCA) expression increases with high Gleason score, advanced stage, and bone metastasis in prostate cancer. Oncogene 2000;19:1288–1296.

18. Saffran DC, Raitano AB, Hubert RS, Witte ON, Reiter RE, Jakobovits A. Anti-PSCA mAbs inhibit tumor growth and metastasis formation and prolong the survival of mice bearing human prostate cancer xenografts. Proc Natl Acad Sci USA 2001; 98:2658–2663.
19. Saffran DC, Reiter RE, Jakobovits A, Witte ON. Target antigens for prostate cancer immunotherapy. Cancer Metastasis Rev 1999;18:437–449.
20. Kuriyama M, Wang MC, Lee CI, Papsidero LD, Killian CS, Inaji H, Slack NH, Nishiura T, Murphy GP, Chu TM. Use of human prostate. Cancer Res 1981;41:3874–3876.
21. Catalona WJ, Smith DS, Ratliff TL, Dodds KM, Coplen DE, Yuan JJ, Petros JA, Andriole GL. Measurement of prostate-specific antigen in serum as a screening test for prostate cancer [published erratum appears in N Engl J Med 1991 Oct 31; 325(18):1324] [see comments]. N Engl J Med 1991;324:1156–1161.
22. Ban Y, Wang MC, Watt KW, Loor R, Chu TM. The proteolytic activity of human prostate-specific antigen. Biochem Biophys Res Commun 1984;123:482–488.
23. Kumar A, Mikolajczyk SD, Goel AS, Millar LS, Saedi MS. Expression of pro form of prostate-specific antigen by mammalian cells and its conversion to mature, active form by human kallikrein 2. Cancer Res 1997;57:3111–3114.
24. Christensson A, Lilja H. Complex formation between protein C inhibitor and prostate-specific antigen in vitro and in human semen. Eur J Biochem 1994;220:45–53.
25. Webber MM, Waghray A, Bello D. Prostate-specific antigen, a serine protease, facilitates human prostate cancer cell invasion. Clin Cancer Res 1995;1:1089–1094.
26. Lilja H. A kallikrein-like serine protease in prostatic fluid cleaves the predominant seminal vesicle protein. J Clin Invest 1985;76: 1899–1903.
27. Papsidero LD, Wang MC, Valenzuela LA, Murphy GP, Chu TM. A prostate antigen in sera of prostatic cancer patients. Cancer Res 1980;40:2428–2432.
28. Tuma PL, Finnegan CM, Yi JH, Hubbard AL. Evidence for apical endocytosis in polarized hepatic cells: Phosphoinositide 3-kinase inhibitors lead to the lysosomal accumulation of resident apical plasma membrane proteins. J Cell Biol 1999;145: 1089–1102.
29. Sun AQ, Ananthanarayanan M, Soroka CJ, Thevananther S, Shneider BL, Suchy FJ. Sorting of rat liver and ileal sodium-dependent bile acid transporters in polarized epithelial cells. Am J Physiol 1998;275:G1045–1055.
30. Nussenzveig DR, Matos MD, Thaw CN. Human calcitonin receptor is directly targeted to and retained in the basolateral surface of MDCK cells. Am J Physiol 1998;275:C1264–1276.
31. Lipardi C, Nitsch L, Zurzolo C. Mechanisms of apical protein sorting in polarized thyroid epithelial cells. Biochimie 1999;81: 347–353.
32. Prabakaran D, Ahima RS, Harney JW, Berry MJ, Larsen PR, Arvan P. Polarized targeting of epithelial cell proteins in thyrocytes and MDCK cells. J Cell Sci 1999;112:1247–1256.
33. Eldering JA, Grünberg J, Hahn D, Croes HJ, Fransen JA, Sterchi EE. Polarised expression of human intestinal *N*-benzoyl-L-tyrosyl-*p*-aminobenzoic acid hydrolase (human meprin) alpha and beta subunits in Madin-Darby canine kidney cells. Eur J Biochem 1997;247:920–932.
34. Delgrossi MH, Breuza L, Mirre C, Chavrier P, Le Bivic A. Human syntaxin 3 is localized apically in human intestinal cells. J Cell Sci 1997;110:2207–2214.
35. Rajasekaran AK, Humphrey JS, Wagner M, Miesenböck G, Le Bivic A, Bonifacino JS, Rodriguez-Boulan E. TGN38 recycles basolaterally in polarized Madin-Darby canine kidney cells. Mol Biol Cell 1994;5:1093–1103.
36. Rajasekaran SA, Palmer LG, Quan K, Harper JF, Ball WJ, Jr., Bander NH, Peralta Soler A, Rajasekaran AK. Na,K-ATPase beta-subunit is required for epithelial polarization, suppression of invasion, and cell motility. Mol Biol Cell 2001;12:279–295.
37. Gonzalez-Mariscal L, Chávez de Ramírez B, Cereijido M. Tight junction formation in cultured epithelial cells (MDCK). J Membr Biol 1985;86:113–125.
38. Liu H, Rajasekaran AK, Moy P, Xia Y, Kim S, Navarro V, Rahmati R, Bander NH. Constitutive and antibody-induced internalization of prostate-specific membrane antigen. Cancer Res 1998;58:4055–4060.
39. Rodriguez-Boulan E, Powell SK. Polarity of epithelial and neuronal cells. Annu Rev Cell Biol 1992;8:395–427.
40. Matter K, Mellman I. Mechanisms of cell polarity: Sorting and transport in epithelial cells. Curr Opin Cell Biol 1994;6:545–554.
41. Ozawa M, Ringwald M, Kemler R. Uvomorulin–catenin complex formation is regulated by a specific domain in the cytoplasmic region of the cell adhesion molecule. Proc Natl Acad Sci USA 1990;87:4246–4250.
42. Simons K, Ikonen E. Functional rafts in cell membranes. Nature 1997;387:569–572.
43. Killian CS, Corral DA, Kawinski E, Constantine RI. Mitogenic response of osteoblast cells to prostate-specific antigen suggests an activation of latent TGF-beta and a proteolytic modulation of cell adhesion receptors. Biochem Biophys Res Commun 1993; 192:940–947.
44. Cohen P, Peehl DM, Graves HC, Rosenfeld RG. Biological effects of prostate specific antigen as an insulin-like growth factor binding protein-3 protease. J Endocrinol 1994;142:407–415.
45. Vessey CJ, Wilding J, Folarin N, Hirano S, Takeichi M, Soutter P, Stamp GW, Pignatelli M. Altered expression and function of E-cadherin in cervical intraepithelial neoplasia and invasive squamous cell carcinoma. J Pathol 1995;176:151–159.

[CANCER RESEARCH 63, 2645–2648, May 15, 2003]

Prostate-specific Membrane Antigen Association with Filamin A Modulates Its Internalization and NAALADase Activity[1]

Gopalakrishnapillai Anilkumar, Sigrid A. Rajasekaran, Song Wang, Oliver Hankinson, Neil H. Bander,[2] and Ayyappan K. Rajasekaran[3]

Department of Pathology and Laboratory Medicine, David Geffen School of Medicine, University of California Los Angeles, Los Angeles, California 90095 [G. A., S. A. R., S. W., O. H., A. K. R.], and Department of Urology, Weill Medical College of Cornell University, New York, New York 10021 [N. H. B.]

ABSTRACT

Prostate-specific membrane antigen (PMSA) is an integral membrane protein highly expressed by prostate cancer cells. We reported previously that PSMA undergoes internalization via clathrin-coated pits (Liu *et al.*, Cancer Res., *58:* 4055–4060, 1998). In this study we demonstrate that filamin A, an actin cross-linking protein, associates with the cytoplasmic tail of PSMA and that this association of PSMA with filamin is involved in its localization to the recycling endosomal compartment. By ectopically expressing PSMA in filamin-negative and -positive cell lines, we additionally show that filamin binding to PSMA reduces the internalization rate of PSMA and its *N*-acelylated-α linked-acidic dipeptidase activity. These results suggest that filamin might be an important regulator of PSMA function.

INTRODUCTION

PSMA[4] is a type-II integral membrane protein of M_r 100,000 with a short 19 amino acid cytoplasmic tail, predominantly localized to the epithelial cells of the prostate gland (1, 2). PSMA has been shown to have two enzymatic activities; folate hydrolase (3) and NAALADase (4). In normal prostate epithelial cells, expression of PSMA is very low, and the level increases several fold in high-grade prostate cancers, metastatic diseases, and hormone-refractory prostate carcinoma (5). mAbs raised against the extracellular domain of PSMA have been conjugated with either radioactive ligands or cytotoxins for use as immunotoxins for the specific targeting of prostate cancer cells (6). The importance of PSMA was additionally illustrated by the finding that it is also expressed in endothelial cells of the neovasculature but is absent in normal endothelial cells (7).

PSMA is constitutively internalized via clathrin-coated pits in LNCaP cells (8). In addition, antibody specific for PSMA extracellular domain increased the rate of internalization of PSMA (8). Deletion of the cytoplasmic tail of PSMA resulted in the loss of internalization of PSMA, indicating that the cytoplasmic tail is crucial for its internalization.[5] To additionally understand the mechanism of PSMA internalization we used the cytoplasmic tail of PSMA as bait in a yeast two-hybrid screening approach to identify PSMA interacting proteins. In this study we report that the cytoplasmic tail of PSMA associates with filamin A, an actin cross-linking phosphoprotein and that this association modulates the internalization rate of PSMA and its localization to the REC. Our studies also suggest that PSMA-filamin association is involved in the regulation of NAALADase activity of PSMA.

MATERIALS AND METHODS

Antibodies and Reagents. Mouse mAb, J591, against the extracellular domain of PSMA has been described (7). Mouse mAb against filamin A was from Chemicon International Inc. (Temecula, CA). FITC- and Texas Red-labeled, affinity-purified secondary antibodies were obtained from Jackson ImmunoResearch Laboratories (West Grove, PA), and horseradish peroxidase-conjugated antimouse antibody and streptavidin were from Transduction Laboratories. PC3 cells stably expressing PSMA have been described earlier (9) and were kindly provided by Dr. Warren Heston (Cleveland Clinic Foundation, Cleveland, OH). M2 and A7 melanoma cell lines were generously provided by Dr. Thomas Stossel (Harvard Medical School, Boston, MA).

Cell Culture and Transfections. PC3-PSMA cells were cultured in RPMI 1640 supplemented with 10% fetal bovine serum, MEM nonessential amino acid solution (Invitrogen, Grand Island, NY), and penicillin/streptomycin. A7 and M2 cells were grown in MEM containing 8% newborn FCS, 2% fetal bovine serum, MEM nonessential amino acid solution, and penicillin/streptomycin. The calcium phosphate method was used for all of the transfections (10).

Yeast Two-Hybrid Analysis. Two complementary oligonucleotides, representing the 19 amino acid cytoplasmic tail of PSMA, were synthesized, annealed, and cloned into the bait vector pGBKT7. This bait was used to screen a human prostate-specific cDNA library using a yeast strain AH109. Library screening and β-galactosidase assays were performed as per the guidelines of the Matchmaker Two-Hybrid System 3 of Clontech (Palo Alto, CA).

GST Pull-Down and Immunoprecipitation. A 520-bp DNA fragment corresponding to the NH_2-terminal 1–173 amino acids of PSMA was cloned in fusion with GST in the pGEX-4X vector. The GST-PSMA fusion protein overexpressed in *Escherichia coli* was purified to homogeneity according to the manufacturer's instructions (Amersham Biosciences, Piscataway, NJ). DNA representing the 23rd-24th repeats (2466–2647 amino acids) of filamin A was cloned in pET 28-b, a T7-based bacterial expression vector. This construct was used to generate ^{35}S-labeled filamin A in a coupled *in vitro* transcription and translation system obtained from Promega (Madison, WI). The GST pull-down assay was carried out in a 50 μl reaction volume [binding buffer: 50 mM Tris (pH 8.0), 150 mM NaCl, 1 mM EDTA, 12.5 mM $MgCl_2$, and 10% glycerol] containing 500 ng of affinity purified GST-PSMA, and 5 μl of *in vitro* transcription and translation reaction containing radioactive filamin A. The binding reaction was carried out at 4°C for 2 h, and the bound filamin was pulled down using GST beads. Purified GST protein incubated with radioactive filamin A was used as a control in the assay. Bound proteins were analyzed by 15% SDS-PAGE followed by autoradiography.

For immunoprecipitation, PC3-PSMA were rinsed with ice-cold PBS and lysed in 1 ml of lysis buffer [10 mM Tris (pH 7.4), 150 mM NaCl, 1% Triton-X-100, 40 mM *N*-octylglucoside, 0.2 mM sodium vanadate, 1 mM EDTA, 1 mM EGTA, 50 μg/ml DNase, 1 mM phenylmethylsulfonyl fluoride, and 5 μg/ml each of antipapain, leupeptin, and pepstatin] on ice for 30 min. The lysates were subjected to immunoprecipitation using and mAb J591 and immunoblotted with antifilamin antibody.

Immunofluorescence and Confocal Microscopy. Immunofluorescence and confocal microscopy were performed as described earlier (10). Cells were grown to 70% confluency on coverslips, washed twice using PBS, and fixed with methanol. After blocking with BSA, cells were incubated with antifilamin mAbs for 1 h at room temperature, washed, and counterstained with Cy3-conjugated rabbit antimouse secondary antibody for visualizing filamin. FITC-conjugated J591 anti-PSMA antibody was used for the PSMA staining. To detect FITC- and Cy3-labeled antigens, samples were excited at 488 nm and

Received 1/30/03; accepted 3/25/03.

The costs of publication of this article were defrayed in part by the payment of page charges. This article must therefore be hereby marked *advertisement* in accordance with 18 U.S.C. Section 1734 solely to indicate this fact.

[1] Supported by Department of Defense Grants DAMD 17-00-1-0009 DAMD 17-02-1-0661, and 2T32CA09056-26.

[2] N. H. B. is a paid consultant of BZL, Inc. (Framingham, MA), and has developed mAb J591 used in this study, which was patented by the Cornell Research Foundation and licensed to BZL.

[3] To whom requests for reprints should be addressed, at David Geffen School of Medicine, University of California Los Angeles, Department of Pathology and Laboratory Medicine, Room 13-344 CHS, Los Angeles, CA 90095. Email: arajasekaran@mednet.ucla.edu.

[4] The abbreviations used are: PSMA, prostate-specific membrane antigen; REC, recycling endosomal compartment; NAAG, *N*-acetyl-aspartyl glutamate; NAALADase, *N*-acelylated-α linked-acidic dipeptidase; mAb, monoclonal antibody; GST, glutathione *S*-transferase.

[5] S. Rajasekaran, G. Anilkumar, and A. K. Rajasekaran, unpublished observations.

550 nm, and the light emitted between 520–540 nm and 560–610 nm, respectively, was recorded. Colocalization of filamin A and PSMA was carried out using a Fluoview laser scanning confocal microscope (Olympus America Inc., Melville, NY). Images were generated using Fluoview software (version 2.1.39).

Internalization of PSMA. Internalization of PSMA was determined by a cell surface biotinylation assay as described previously (8).

NAALADase Assay. Radioenzymatic assay using [^{3}H]NAAG (NEN, Boston, MA) was performed as described previously (11). A7 and M2 melanoma cells stably expressing PSMA were incubated in 500 μl of Krebs Ringer bicarbonate medium containing 1 μCi/ml [^{3}H]NAAG at 37°C for 1 h. After the incubation, the cells were placed on ice and washed three times with ice-cold Krebs Ringer medium. The cells were lysed using 1 M NaOH, and the radioactivity was determined using a scintillation counter (Beckman LK 6500). The counts were normalized with the total amount of PSMA expressed on the cell surface determined by cell surface biotinylation.

RESULTS

Identification of PSMA Binding Partners Using Yeast Two-Hybrid Analysis. The 19 amino acid cytoplasmic NH_2 terminus of PSMA was used as a bait to screen a human prostate cDNA library in yeast strain AH 109. Several rounds of library screening (1.4×10^6 clones) identified a number of interacting clones that grew on selective media indicating the presence of interactors for the cytoplasmic domain of PSMA. Among all of the positive clones sequenced, 50% represented two distinct COOH-terminal regions, corresponding to the 22–24th and 23–24th repeats of filamin A. Filamin has three isoforms: filamin A (also called ABP 280, filamin α, Filamin), filamin B (also called ABP278, filaminβ), and filamin C (also called ABPL, filamin γ; Ref. 12). We also obtained partial cDNA clones identical to the COOH-terminal region of filamin B and filamin C (Fig. 1*B*). The amino acid sequence alignment of the regions of the three isoforms of filamin that interacted with the cytoplasmic tail of PSMA encompassed their 22–24th repeat as shown in Fig. 1*A*. There was 70% identity at the amino acid level among the different filamin isoforms in this region.

PSMA Binds to Filamin *in Vitro* and *in Vivo*. An *in vitro* GST pull-down assay was carried out to determine whether PSMA interacted directly with filamin A. As shown in Fig. 1*C* the interaction between PSMA and filamin was readily detected. Coimmunoprecipitation analysis was performed to determine whether filamin and PSMA associate *in vivo*. PC3-PSMA cells were lysed in an immunoprecipitation buffer, and PSMA was immunoprecipitated by mAb J591. Coimmunoprecipitating filamin was detected by antifilamin antibody. In agreement with the two-hybrid and bacterial fusion protein analyses, filamin was coimmunoprecipitated *in vivo* from prostate epithelial cells (Fig. 1*D*).

Colocalization of PSMA and Filamin in PC3-PSMA Cells. Confocal microscopy revealed that PSMA colocalized with filamin at the plasma membrane region (Fig. 2, *A–C*) indicating that PSMA and filamin associate at the plasma membrane. In addition to its plasma membrane localization, PSMA also exhibited a distinct spot-like staining at the perinuclear region (Fig. 2*B, arrowhead*), a staining pattern similar to that of the recycling endosome (13). Therefore, to examine whether PSMA is localized to the recycling endosome, we tested whether the PSMA codistributes with a recycling endosomal marker (internalized transferrin). The internalized transferrin clearly colocalized with PSMA in the perinuclear region (Fig. 2, *D–F*), indicating that PSMA is localized to the REC in PC3-PSMA cells.

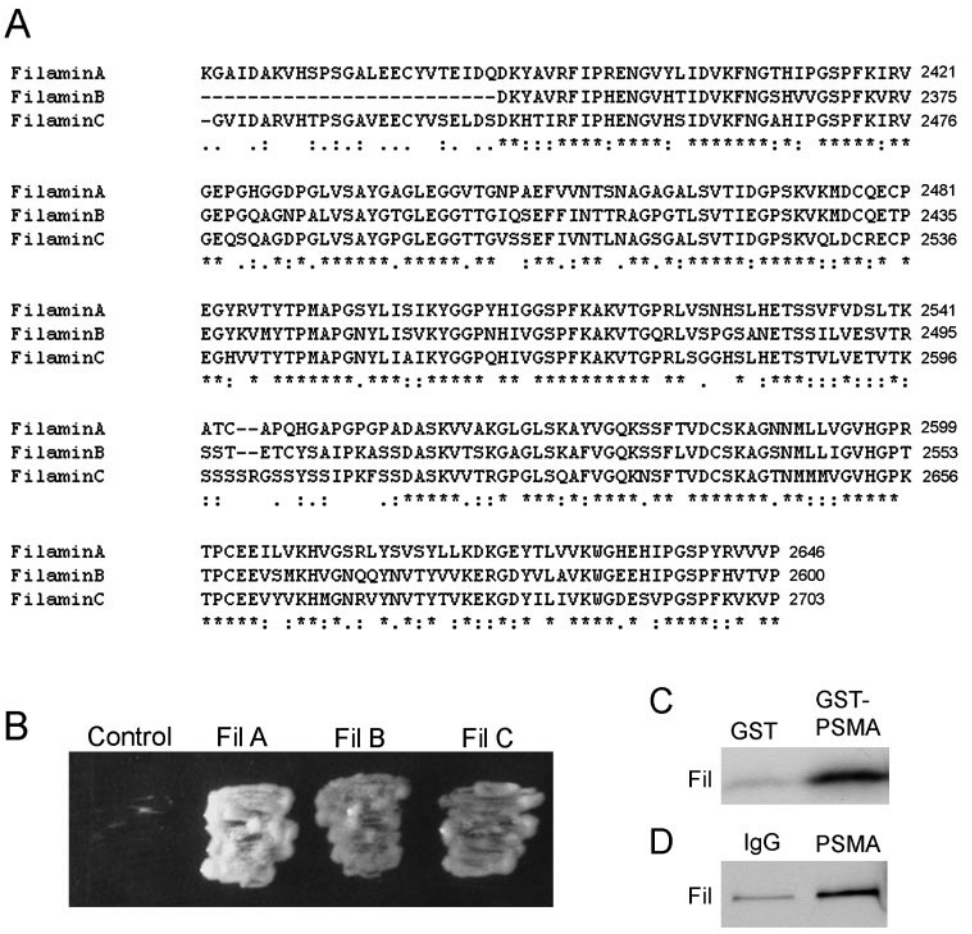

Fig. 1. Association of PSMA with filamin *in vitro* and *in vivo*. *A*, amino acid alignment of regions of filamin A, B, and C that interact with the cytoplasmic tail of PSMA in the yeast two-hybrid screening. * represents identical amino acids in all three of the filamins; *colons* represent conserved substitutions. *B*, growth of yeast expressing the bait alone (*control*) or the COOH-terminal region of filamin A, B, or C cDNA clones on medium lacking tryptophan, leucine, histidine, and adenine. *C*, filamin A and PSMA interact directly *in vitro*. An NH_2-terminal region of PSMA was expressed in *E. coli* as a GST fusion product (*GST-PSMA*) and was used to pull-down the COOH-terminal region of filamin A. Filamin A was generated as described in "Materials and Methods." GST protein alone was used as a control (*GST*). *D*, association of PSMA and filamin A *in vivo*. Protein lysate was prepared from PC3 cells expressing PSMA, and total PSMA was immunoprecipitated with mAb J591 antibody or control IgG and immunoblotted for filamin.

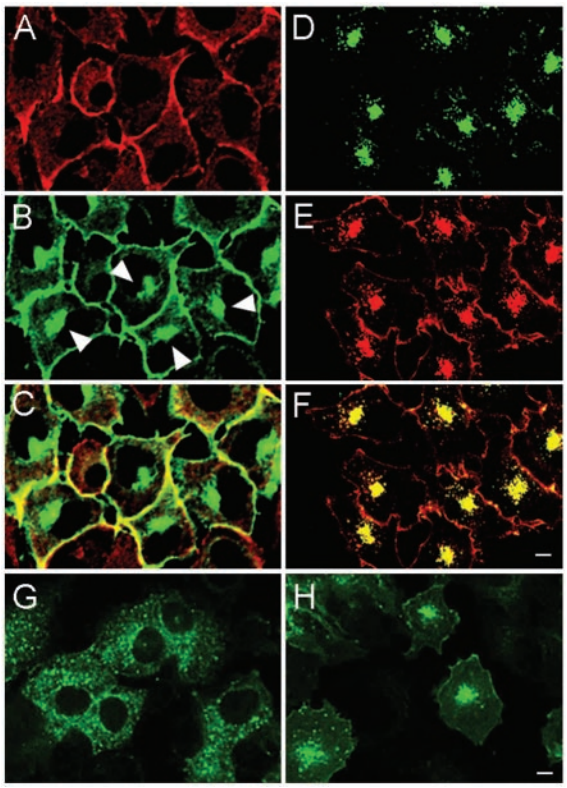

Fig. 2. Colocalization of PSMA with filamin A and localization of internalized PSMA to the REC. Confocal microscope optical sections of PC3-PSMA cells stained for filamin A (*A*) and PSMA (*B*). The merged image is shown in *C*. *Arrowheads* indicate the REC. FITC-labeled transferrin uptake (*D*), PSMA internalization as revealed by the uptake of mAb J591 (*E*), and (*F*) the merged image of *D* and *E*. Note the accumulation of transferrin and PSMA in the REC. Localization of internalized PSMA in filamin A-negative M2 (*G*) and filamin A-positive A7 cells (*H*). *Bar*, 10 μm.

Localization of PSMA in Filamin-negative and -positive Cell Lines. Next, we tested whether PSMA-filamin association is involved in the localization of PSMA to the REC. Because PC3 cells contain filamin, we used M2 cells, a cell line derived from human malignant melanoma, which is negative for filamin expression, and A7 cells, a subline generated by stable transfection of M2 with filamin cDNA. These cells do not express endogenous PSMA, and, therefore, PSMA was ectopically expressed in these cell lines. Strikingly, in filamin-negative M2 cells, PSMA showed vesicular staining throughout the cytoplasm (Fig. 2*G*), whereas in A7 cells, a distinct spot-like staining (Fig. 2*H*), as seen in PC3-PSMA cells (compare Fig. 2, *B* and *H*) was observed. These results indicate that filamin is involved in the localization of PSMA to the REC.

Decreased Internalization of PSMA in Filamin-positive Cells. Localization of PSMA to the REC in filamin-positive A7 cells indicated that PSMA filamin association might affect internalization of PSMA. Therefore, we tested the rate of internalization of PSMA in M2 and A7 cells using a cell surface biotinylation assay. M2 cells showed ~2-fold increase in the internalization of PSMA (Fig. 3, *A* and *B*). Strikingly, at 60 min, 100% of the total surface PSMA was internalized in M2 cells. In A7 cells, at 60 min there was a slight decrease in the internalized PSMA as compared with the 30-min time point, which is possibly because of degradation. These results indicate that filamin might be involved in the modulation of internalization rate of PSMA.

Increased NAALADase Activity of PSMA in Filamin-deficient Cells. We then tested whether PSMA association with filamin is involved in the regulation of its NAALADase activity using PSMA expressing M2 and A7 cells. NAALADase activity was determined using [^{3}H]NAAG as the substrate. The activity was normalized to the amount of cell surface PSMA determined by cell surface biotinylation assay. The NAALADase activity was 1.5-fold higher in M2 cells compared with A7 cells (Fig. 4) indicating that the filamin association decreases the enzymatic activity of PSMA.

DISCUSSION

In this study, we show that the first 19 NH_2-terminal amino acids of PSMA associate with the 23rd-24th repeat of filamin A. This interaction between PSMA and filamin A found in the yeast two-hybrid analysis was confirmed using *in vitro* pull-down assays using GST-PSMA, and *in vivo* coimmunoprecipitation and colocalization experiments. We confirmed that PSMA is localized to the REC in filamin-positive cells. We also provided biochemical evidence that in the absence of filamin association, PSMA is internalized faster and exhibits increased NAALADase activity.

Filamin A is a dimeric actin cross-linking phosphoprotein located in the cortical cytoplasm adjacent to the plasma membrane. Parallel filamin dimers cross-link actin and facilitate the orthogonal branching of actin filaments, and serve as a docking site for various cell surface receptors and certain intracellular proteins involved in signal trans-

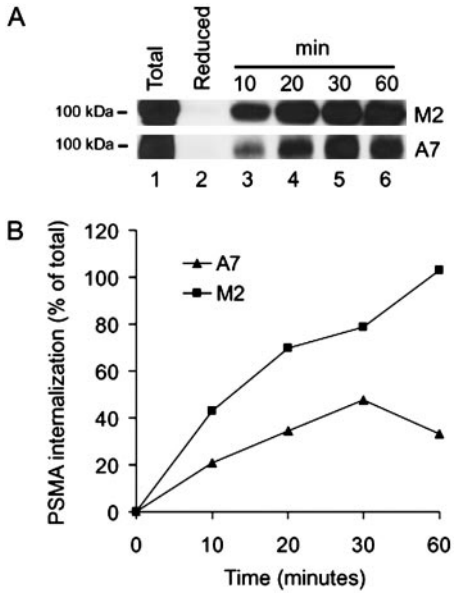

Fig. 3. Increased internalization of PSMA in a filamin-negative cell line. (*A*) The cell surface was biotinylated as described in Material and Methods. PSMA was immunoprecipitated at different time points, run on a 10% SDS-PAGE and internalized PSMA was detected with HRP-streptavidin. (*B*) Densitometric quantitation showed an approximately 50% reduction in the rate of internalization of PSMA in filamin positive cells (A7) compared with filamin negative cells (M2).

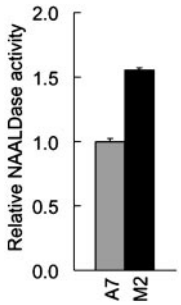

Fig. 4. Increased NAALADase activity in filamin-negative cells. A7 and M2 cells stably expressing PSMA were used for NAALADase assay. Note the 1.5-fold increase of NAALADase activity of PSMA in filamin-negative cells (*M2*); *bars*, ±SD.

duction (12). In this study, we have shown that PSMA association with filamin is necessary for its localization to the REC. In filamin-negative M2 cells, the internalized PSMA accumulated in vesicles, which were highly diffused throughout the cytoplasm. This diffused staining pattern changed into a bright spot like perinuclear staining (REC) in cells transfected with filamin A cDNA (A7 cells). REC is a collection of 50–70 nm diameter tubules containing recycling receptors and some ligands that are known to undergo recycling, and is generally found to localize near the microtubule-organizing center (14). Our results are consistent with a view that PSMA filamin association is involved in the transport of PSMA from the cell surface to the REC. However, we do not rule out the possibility that filamin might also be involved in the organization and maintenance of REC in mammalian cells. Additional experiments are necessary to unravel the role of filamin in targeting PSMA to REC and its possible involvement in the regulation of REC structure.

LNCaP cells, which express endogenous PSMA and filamin, did not show localization of PSMA to the REC, and PSMA did not coimmunoprecipitate with filamin.[6] It is possible that PSMA association with filamin is modulated by intracellular signaling mechanisms. The PSMA cytoplasmic tail has three putative phosphorylation sites. It is known that filamin A undergoes phosphorylation *in vivo*, and this regulates its interaction with the actin cytoskeleton (15). Whether the phosphorylation status of filamin or PSMA is different in LNCaP compared with PC3 cells and whether this modulates PSMA localization to the REC remains to be studied.

PSMA association with filamin A decreased its rate of internalization by ~50%. This is in agreement with an earlier observation that endocytosis of furin, an endoprotease, was reduced 42% upon binding with filamin A (16). This may occur by the stabilization of these molecules on the membrane by linking to the actin cytoskeleton via filamin A. Dissociation from filamin might facilitate the binding of adaptor proteins required for endocytosis. Liu *et al.* (16) suggested the existence of a competition between filamin A and adaptors binding to the same site of furin, thereby regulating the rate of internalization of furin. Our observations that mutation of specific cytoplasmic tail amino acid residues of PSMA resulted in the loss of its internalization[5] and that these mutants interacted more strongly with filamin A[6] support the above possibility.

In our study, we have shown that filamin binding reduced the NAALADase activity of PSMA by 64%. It is possible that the interaction between filamin A and the cytoplasmic tail of PSMA changes the conformation of the extracellular domain of PSMA, resulting in reduced substrate (NAAG) binding. The observation that the cytoplasmic tail of a protein regulates the conformation of its extracellular domain has been reported previously for calreticulin, a M_r 60,000 intracellular calcium-binding protein. The cytoplasmic tail of calreticulin interacts with a highly conserved GFFKR motif present in all of the α-subunits of integrin cytoplasmic domains, and promotes integrin to maintain a high affinity state for ligand binding (17).

The significance of the internalization of PSMA in prostate epithelial cells is not known. Antibody-induced endocytosis, high similarity at amino acid level between transferrin receptor and PSMA, and the presence of a domain similar to the transferrin receptor dimerization domain at the extracellular region of PSMA strongly suggest that PSMA could be a membrane receptor for an unknown ligand. On binding to ligand, the PSMA-ligand complex could undergo internalization. At present, there is no clue whatsoever about the nature of the ligand. If PSMA transduces a cell growth advantage signal, then its proper down-regulation by endocytosis would be important to prevent transformation of normal cells into cancerous cells. This is observed in the case of epidermal growth factor receptor. An epidermal growth factor receptor mutant unable to undergo endocytosis has been identified in human cancers (18). Endocytosis of PSMA might also be important for its role in the metastasis of prostate cancer. In this case, an increased internalization of PSMA could promote the invasive property of prostate cancer cells. It is reported that cytoplasmic tail-dependent internalization of membrane-type I matrix metalloproteinase was important for its invasion-promoting activity (19). We are currently carrying out experiments to delineate the potential importance of endocytosis of PSMA in prostate cancer.

[6] G. Anilkumar and A. K. Rajasekaran, unpublished observations.

ACKNOWLEDGMENTS

We thank Jason Christiansen for critical reading of the manuscript and members of the Rajasekaran laboratory for thoughtful comments during the progress of this work.

REFERENCES

1. Israeli, R. S., Powell, C. T., Fair, W. R., and Heston, W. D. Molecular cloning of a complementary DNA encoding a prostate-specific membrane antigen. Cancer Res., *53:* 227–230, 1993.
2. Christiansen, J. J., Rajasekaran, S. A., Moy, P., Butch, A., Goodglick, L., Gu, Z., Reiter, R., Bander, N. H., and Rajasekaran, A. K. Polarity of prostate specific membrane antigen, prostate stem cell antigen and prostate specific antigen in prostate tissue and in a cultured epithelial cells. Prostate, *55*: 9–19, 2003.
3. Pinto, J. T., Suffoletto, B. P., Berzin, T. M., Qiao, C. H., Lin, S., Tong, W. P., May, F., Mukherjee, B., and Heston, W. D. Prostate-specific membrane antigen: a novel folate hydrolase in human prostatic carcinoma cells. Clin. Cancer Res., *2:* 1445–1451, 1996.
4. Luthi-Carter, R., Barczak, A. K., Speno, H., and Coyle, J. T. Molecular characterization of human brain N-acetylated α-linked acidic dipeptidase (NAALADase). J. Pharmacol. Exp. Ther., *286:* 1020–1025, 1998.
5. Silver, D. A., Pellicer, I., Fair, W. R., Heston, W. D., and Cordon-Cardo, C. Prostate-specific membrane antigen expression in normal and malignant human tissues. Clin. Cancer Res., *3:* 81–85, 1997.
6. Tasch, J., Gong, M., Sadelain, M., and Heston, W. D. A unique folate hydrolase, prostate-specific membrane antigen (PSMA): a target for immunotherapy? Crit. Rev. Immunol., *21:* 249–261, 2001.
7. Liu, H., Moy, P., Kim, S., Xia, Y., Rajasekaran, A., Navarro, V., Knudsen, B., and Bander, N. H. Monoclonal antibodies to the extracellular domain of prostate-specific membrane antigen also react with tumor vascular endothelium. Cancer Res., *57:* 3629–3634, 1997.
8. Liu, H., Rajasekaran, A. K., Moy, P., Xia, Y., Kim, S., Navarro, V., Rahmati, R., and Bander, N. H. Constitutive and antibody-induced internalization of prostate-specific membrane antigen. Cancer Res., *58:* 4055–4060, 1998.
9. Gong, M. C., Latouche, J. B., Krause, A., Heston, W. D., Bander, N. H., and Sadelain, M. Cancer patient T cells genetically targeted to prostate-specific membrane antigen specifically lyse prostate cancer cells and release cytokines in response to prostate-specific membrane antigen. Neoplasia, *1:* 123–127, 1999.
10. Rajasekaran, S. A., Palmer, L. G., Quan, K., Harper, J. F., Ball, W. J., Jr., Bander, N. H., Peralta Soler, A., and Rajasekaran, A. K. Na. K-ATPase β-subunit is required for epithelial polarization, suppression of invasion, and cell motility. Mol. Biol. Cell, *12:* 279–295, 2001.
11. Sekiguchi, M., Okamoto, K., and Sakai, Y. Release of endogenous N-acetylaspartylglutamate (NAAG) and uptake of [3H]NAAG in guinea pig cerebellar slices. Brain Res., *482:* 78–86, 1989.
12. Stossel, T. P., Condeelis, J., Cooley, L., Hartwig, J. H., Noegel, A., Schleicher, M., and Shapiro, S. S. Filamins as integrators of cell mechanics and signalling. Nat. Rev. Mol. Cell. Biol., *2:* 138–145, 2001.
13. Lin, S. X., Grant, B., Hirsh, D., and Maxfield, F. R. Rme-1 regulates the distribution and function of the endocytic recycling compartment in mammalian cells. Nat. Cell Biol., *3:* 567–572, 2001.
14. Mukherjee, S., Ghosh, R. N., and Maxfield, F. R. Endocytosis Physiol. Rev., *77:* 759–803, 1997.
15. Ohta, Y., and Hartwig, J. H. Actin filament cross-linking by chicken gizzard filamin is regulated by phosphorylation *in vitro*. Biochemistry, *34:* 6745–6754, 1995.
16. Liu, G., Thomas, L., Warren, R. A., Enns, C. A., Cunningham, C. C., Hartwig, J. H., and Thomas, G. Cytoskeletal protein ABP-280 directs the intracellular trafficking of furin and modulates proprotein processing in the endocytic pathway. J. Cell Biol., *139:* 1719–1733, 1997.
17. Fernandez, C., Clark, K., Burrows, L., Schofield, N. R., and Humphries, M. J. Regulation of the extracellular ligand binding activity of integrins. Front Biosci., *3:* D684–D700, 1998.
18. Huang, H. S., Nagane, M., Klingbeil, C. K., Lin, H., Nishikawa, R., Ji, X. D., Huang, C. M., Gill, G. N., Wiley, H. S., and Cavenee, W. K. The enhanced tumorigenic activity of a mutant epidermal growth factor receptor common in human cancers is mediated by threshold levels of constitutive tyrosine phosphorylation and unattenuated signaling. J. Biol. Chem., *272:* 2927–2935, 1997.
19. Uekita, T., Itoh, Y., Yana, I., Ohno, H., and Seiki, M. Cytoplasmic tail-dependent internalization of membrane-type 1 matrix metalloproteinase is important for its invasion-promoting activity. J. Cell Biol., *155:* 1345–1356, 2001.

Molecular Biology of the Cell
Vol. 14, 4835–4845, December 2003

A Novel Cytoplasmic Tail MXXXL Motif Mediates the Internalization of Prostate-specific Membrane Antigen

Sigrid A. Rajasekaran,* Gopalakrishnapillai Anilkumar,* Eri Oshima,* James U. Bowie,† He Liu,‡ Warren Heston,§ Neil H. Bander,‡ and Ayyappan K. Rajasekaran*‖

*Departments of Pathology and Laboratory Medicine and †Chemistry and Biochemistry, Molecular Biology Institute, David Geffen School of Medicine, University of California, Los Angeles, Los Angeles, California 90095; ‡Department of Urology, Weill Medical College of Cornell University, New York, New York 10021; and §Department of Cancer Biology, Cleveland Clinic Foundation, Cleveland, Ohio 44195

Submitted November 13, 2002; Revised July 9, 2003; Accepted July 28, 2003
Monitoring Editor: Keith Mostov

Prostate-specific membrane antigen (PSMA) is a transmembrane protein expressed at high levels in prostate cancer and in tumor-associated neovasculature. In this study, we report that PSMA is internalized via a clathrin-dependent endocytic mechanism and that internalization of PSMA is mediated by the five N-terminal amino acids (MWNLL) present in its cytoplasmic tail. Deletion of the cytoplasmic tail abolished PSMA internalization. Mutagenesis of N-terminal amino acid residues at position 2, 3, or 4 to alanine did not affect internalization of PSMA, whereas mutation of amino acid residues 1 or 5 to alanine strongly inhibited internalization. Using a chimeric protein composed of Tac antigen, the α-chain of interleukin 2-receptor, fused to the first five amino acids of PSMA (Tac-MWNLL), we found that this sequence is sufficient for PSMA internalization. In addition, inclusion of additional alanines into the MWNLL sequence either in the Tac chimera or the full-length PSMA strongly inhibited internalization. From these results, we suggest that a novel MXXXL motif in the cytoplasmic tail mediates PSMA internalization. We also show that dominant negative μ2 of the adaptor protein (AP)-2 complex strongly inhibits the internalization of PSMA, indicating that AP-2 is involved in the internalization of PSMA mediated by the MXXXL motif.

INTRODUCTION

Prostate-specific membrane antigen (PSMA) was originally identified by the monoclonal antibody (mAb) 7E11-C5 raised against the human prostate cancer cell line LNCaP (Horoszewicz *et al*., 1987). Subsequently, the PSMA gene was cloned (Israeli *et al*., 1993) and mapped to chromosome 11q (Rinker-Schaeffer *et al*., 1995). PSMA is a type II membrane protein with a short cytoplasmic N-terminal region (19 amino acids), a transmembrane domain (24 amino acids), and a large extracellular C-terminal portion (707 amino acids) (Israeli *et al*., 1993) with several potential N-glycosylation sites. Recently, it has been shown that PSMA is homologous to glutamate carboxypeptidase II (85% at nucleic acid level) isolated from rat brain (Coyle, 1997) and has folate hydrolase activity (Pinto *et al*., 1996; Halsted *et al*., 1998), and N-acetylated α-linked acidic dipeptidase (NAALDase) activity (Carter *et al*., 1996, 1998). The extracellular domain of PSMA shows homology (26% identity at the amino acid level) to the transferrin receptor I (Israeli *et al*., 1993) and to a recently cloned transferrin receptor II (Kawabata *et al*., 1999). The functional significance of homology between PSMA and transferrin receptor is not known.

PSMA has been the subject of increasing interest in cancer research due to its potential as a diagnostic and therapeutic target for human prostate cancer (Chang *et al*., 1999a). PSMA is abundantly expressed in prostate cancer cells. Its expression is further increased in higher-grade cancers, metastatic disease, and hormone-refractory prostate carcinoma (Wright *et al*., 1996; Silver *et al*., 1997). In addition, PSMA has become the focus of even more intense interest due to the recent findings that it is selectively expressed in the neovasculature of nearly all types of solid tumors, but not in the vasculature of normal tissue (Liu *et al*., 1997; Silver *et al*., 1997; Chang *et al*., 1999b,c). The function of PSMA with respect to vascular endothelial cell biology and the direct correlation between its expression and increasing tumor aggressiveness in prostate cancer remain intriguing and unclear. Although a significant amount of research is being carried out using antibodies against PSMA for immunotherapy of prostate cancer (McDevitt *et al*., 2001; Smith-Jones *et al*., 2003), very little is known about the mechanism of internalization of this protein.

In general, the endocytic pathway includes internalization of the receptor-ligand complex via clathrin-coated pits and accumulation in the endosomes. The receptor–ligand complex then dissociates in the endosomes and the dissociated molecules are either recycled back to the cell surface or targeted to lysosomes for degradation (Pastan and Willing-

Article published online ahead of print. Mol. Biol. Cell 10.1091/mbc.E02–11–0731. Article and publication date are available at www.molbiolcell.org/cgi/doi/10.1091/mbc.E02–11–0731.

‖ Corresponding author. E-mail address: arajasekaran@mednet.ucla.edu.

Abbreviations used: NAALDase, N-acetylated α-linked acidic dipeptidase; PSMA, prostate-specific membrane antigen.

ham, 1981; Mellman, 1996). Targeting of most receptors to coated pits and their traffic through endocytic compartments are generally mediated by endocytic signals located in the cytoplasmic domain of proteins (reviewed in Trowbridge *et al*., 1993; Kirchhausen *et al*., 1997; Mukherjee *et al*., 1997; Bonifacino and Traub, 2003). These signals fall into two major categories such as tyrosine-based and di-leucine based signals.

The tyrosine-based signals are represented by NPXY and YXXΦ consensus motifs (Bonifacino and Traub, 2003) with the Y residue being critical for their function (Lazarovits and Roth, 1988). NPXY signals mediate internalization of several type-1 membrane proteins such as LDL receptor, epidermal growth factor receptor, insulin receptor, and others (Bonifacino and Traub, 2003). The YXXΦ (Φ, bulky hydrophobic side chain) signals mediate internalization and lysosomal targeting of several type I and type II membrane proteins such as transferrin receptor, mannose-6-phosphate receptor, asialoglycoprotein receptor, polymeric immunoglobulin receptor, and others (reviewed in Trowbridge *et al*., 1993; Marks *et al*., 1997; Bonifacino and Dell'Angelica, 1999; Bonifacino and Traub, 2003).

The di-leucine based signals require two consecutive leucines or a leucine-isoleucine pair for their function (Letourneur and Klausner, 1992; Sandoval and Bakke, 1994). Recent studies have identified two distinct classes of di-leucine based signals represented by [DE]XXXL[LI] and DXXLL consensus sequences. Both these signals are involved in internalization and lysosomal targeting of several membrane proteins. Proteins such as CD3-γ, LIMP-II, tyrosinase CD4, and GLUT4 have a [DE]XXXL type signal, whereas a DXXLL signal has been characterized in mannose 6-phosphate/insulin-like growth factor-II receptor, the cation-dependent mannose-6-phosphate receptor, LDL-receptor related proteins, β-secretase, and others (Bonifacino and Traub, 2003).

We have shown that PSMA undergoes internalization via clathrin-coated pits in LNCaP cells (Liu *et al*., 1998), a human prostate cancer cell line that abundantly expresses endogenous PSMA. To further understand the mechanism of PSMA internalization, we searched for possible internalization motifs in the cytoplasmic domain of PSMA. In this study we demonstrate that the cytoplasmic tail N-terminal five amino acid residues, including the start codon methionine and the fifth amino acid residue leucine form a novel MXXXL motif that mediates PSMA internalization. By transferring this MXXXL motif to a noninternalized protein, the α-chain of interleukin 2-receptor (Tac), we further show that this motif is sufficient for PSMA internalization. Furthermore, using an inducible dominant-negative μ2 subunit of the adaptor protein (AP)-2 adaptor complex, we provide evidence that internalization of this clinically important protein requires the function of AP-2.

EXPERIMENTAL PROCEDURES

Plasmid Constructs

Cloning and characterization of full-length cDNA of PSMA was described previously (Israeli *et al*., 1993). The alanine scan mutagenesis approach was used to mutate each of the cytoplasmic tail amino acids in the cytoplasmic tail of PSMA. Alanine scan mutagenesis was essentially carried out by polymerase chain reaction (PCR) by using sense primers carrying respective mutation of the cytoplasmic tail amino acid (positions 2–15) to alanine. A Kozak consensus sequence (GCCACC) and a translation start site (ATG) were incorporated at the N-terminus of the sense primers. A cytoplasmic tail deletion mutant of PSMA was created by deleting the N-terminal 15 amino acids by using PCR. An alanine and three arginine residues proximal to the transmembrane domain were retained because these three arginine residues may be necessary to maintain the type II orientation of the protein (von Heijne, 1988). Also, PSMA constructs in which the cytoplasmic tail amino acids 6–14 were

Construct	Cytoplasmic Tail Sequence																			Int
PSMA																				
Wt	M	W	N	L	L	H	E	T	D	S	A	V	A	T	A	R	R	P	R	+
Δcd	M	→													A	R	R	P	R	-
Ala 4,5	-	-	-	A	A	-	-	-	-	-	-	-	-	-	-	-	-	-	-	-
Ala 4	-	-	-	A	-	-	-	-	-	-	-	-	-	-	-	-	-	-	-	+
Ala 5	-	-	-	-	A	-	-	-	-	-	-	-	-	-	-	-	-	-	-	-
Ala 2	-	A	-	-	-	-	-	-	-	-	-	-	-	-	-	-	-	-	-	+
Ala 3	-	-	A	-	-	-	-	-	-	-	-	-	-	-	-	-	-	-	-	+
Ala 6	-	-	-	-	-	A	-	-	-	-	-	-	-	-	-	-	-	-	-	+
Ala 7	-	-	-	-	-	-	A	-	-	-	-	-	-	-	-	-	-	-	-	+
Ala 8	-	-	-	-	-	-	-	A	-	-	-	-	-	-	-	-	-	-	-	+
Ala 9	-	-	-	-	-	-	-	-	A	-	-	-	-	-	-	-	-	-	-	+
Ala 10	-	-	-	-	-	-	-	-	-	A	-	-	-	-	-	-	-	-	-	+
Val 14	-	-	-	-	-	-	-	-	-	-	-	-	-	V	-	-	-	-	-	+
Ala 8,10,14	-	-	-	-	-	-	-	A	-	A	-	-	-	A	-	-	-	-	-	+
Δ6-14	M	W	N	L	L	→									A	R	R	P	R	+
MA(5)	M	W	N	L	L	H	E	T	D	S	A	V	A	T	A	R	R	P	R	-
	A	A	A	A	A															
Tac																				
Tac Wt	R	R	Q	R	K	S	R	R	T	I										-
Tac-MWNLL	-	-	-	-	-	-	-	-	-	-	L	L	N	W	M					+
Tac-MWNAA	-	-	-	-	-	-	-	-	-	-	A	A	N	W	M					-
Tac-MWNAL	-	-	-	-	-	-	-	-	-	-	L	A	N	W	M					+
Tac-MWNLA	-	-	-	-	-	-	-	-	-	-	A	L	N	W	M					-
Tac-AWNAL	-	-	-	-	-	-	-	-	-	-	L	A	N	W	A					-
Tac-MAWNAL	-	-	-	-	-	-	-	-	-	-	L	A	N	W	A	M				-

Figure 1. Schematic representation of PSMA cytoplasmic tail mutants and Tac-PSMA chimera used in this study. Deletions are shown by horizontal arrows, and insertion of additional alanines is indicated. Amino acids converted to alanine or valine are indicated as A and V, respectively. Internalization (INT) positive (+) or negative (−) for the respective constructs is indicated.

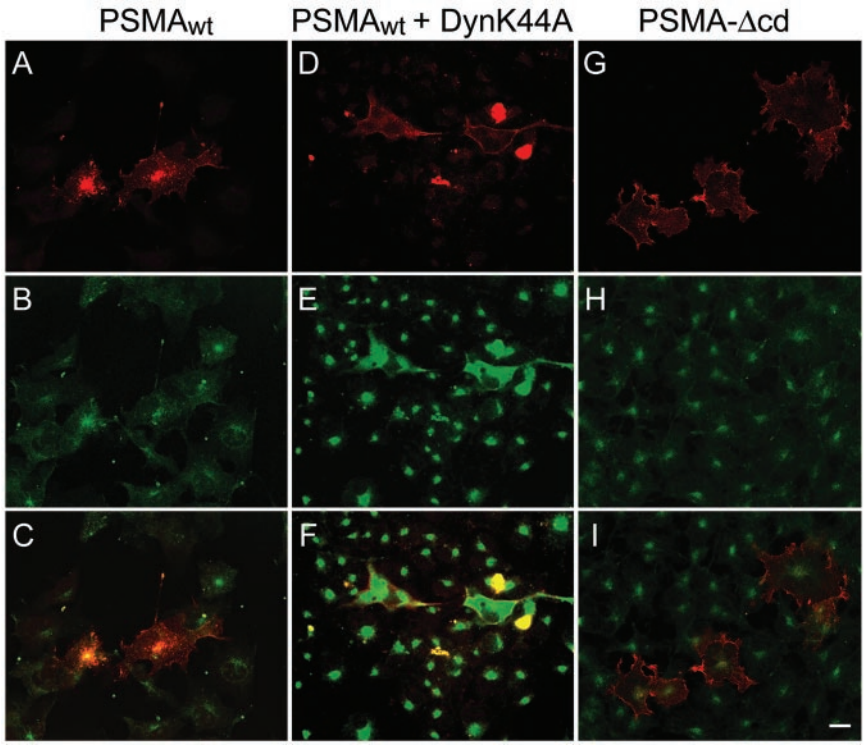

Figure 2. PSMA internalization in COS-7 cells expressing wild-type PSMA ($PSMA_{wt}$) and the cytoplasmic tail deletion mutant (PSMA-Δcd). (A–C) Internalization of $PSMA_{wt}$ and FITC-transferrin. COS cells transiently transfected with $PSMA_{wt}$ were simultaneously incubated with mAb J591 (A) and FITC-transferrin (B) for 2 h, washed, fixed in cold methanol, and stained with Texas Red-conjugated anti-mouse antibody. Representative medial optical sections are shown. (C) Merged image. The yellow color indicates the codistribution of FITC-transferrin and internalized PSMA. (D–F) COS cells expressing Dynamin K44A and $PSMA_{wt}$ cDNA were incubated with mAb J591 for 2 h, washed fixed, and stained with FITC-conjugated anti-mouse antibody to detect PSMA (D) and with polyclonal anti-dynamin antibody and Texas Red-conjugated anti-rabbit antibody to detect cells expressing the dynamin mutant (E). (F) Merged image. Note that in cells expressing DynaminK44A, PSMA was not internalized. (G–I) PSMA-Δcd–expressing cells were incubated with mAb J591 (G) and FITC-transferrin (H) as described above. PSMA-Δcd does not internalize and therefore, does not colocalize with internalized transferring (I). Bar, 5μm.

deleted or all the three putative phosphorylation sites were mutated (PSMA-T8A/S10A/T14A) and a PSMA construct containing five alanines inserted after the start codon [PSMA-MA(5)] were generated using PCR. Tac-PSMA chimera were also generated using PCR. Full-length Tac (gift from Dr. Bonifacino, National Institutes of Health, Bethesda, MD) was described previously (Leonard *et al*., 1984). Tac cytoplasmic tail chimera containing the di-leucine–like motif of PSMA (Tac-MWNLL), di-leucine motif mutated to alanine (Tac-MWNAA), leucine at position 5 mutated to alanine (Tac-MWNLA), leucine at position 4 mutated to alanine (Tac-MWNAL), methionine at first position mutated to alanine in Tac with leucine at position 4 mutated to alanine (Tac-AWNAL), and with an extraalanine (Tac-MAWNAL) were generated. Because Tac is a type I membrane protein, to have the N-terminal methionine free as in PSMA, we used primers encoding the respective amino acids in the reverse orientation. Full-length PSMA (designated as wild-type PSMA [$PSMA_{wt}$]), cytoplasmic tail mutants of PSMA, and Tac-PSMA chimeras were inserted into eukaryotic expression vector pCDNA3. The mutations were verified by DNA sequencing. Constructs used in this study are shown in Figure 1.

Cell Culture and Transfection

COS-7 cells (ATCC CRL 1651) were grown in DMEM supplemented with 10% fetal bovine serum containing streptomycin and penicillin at 5% CO_2 in a water-saturated atmosphere. Cells grown on glass coverslips were transiently transfected by the calcium phosphate method as described previously (Rajasekaran *et al*., 1994). After transfection (48 h), the cells were tested for the uptake of antibodies as described below. HeLa cells expressing hemagglutinin-tagged D176A/W421A mutant μ2 constructs under the control of a tetracycline-repressible promoter have been described previously (Nesterov *et al*., 1999). The cells were grown in DMEM supplemented with 10% fetal bovine serum containing streptomycin and penicillin, 400 μg/ml G418, 200 ng/ml puromycin, and 10 ng/ml doxycycline at 5% CO_2 in a water-saturated atmosphere. Cells plated on glass coverslips were used for transient transfection by the calcium phosphate method. Twelve hours after transfection, expression of the mutant μ2 protein was induced by replacing the culture medium with doxycyline-free medium. Eight hours before the planned experiments, sodium butyrate was added to the culture medium to ensure high expression levels of the mutant μ2 protein to replace the endogenous wild-type μ2 in AP complexes. Transfected cells were used 60 h after transfection.

Antibody Uptake and Immunofluorescence Analysis

Antibody uptake was carried out as described previously (Liu *et al*., 1998). In brief, the cells were washed with DMEM containing 0.5% fatty acid-free bovine serum albumin and incubated at 37°C for 2 h with mAb J591 (5 μg/ml). Cells were then fixed, permeabilized, and incubated with Texas Red-conjugated secondary antibody (Jackson ImmunoResearch Laboratories, West Grove, PA). To visualize PSMA localization in endosomes, cells were coincubated with fluorescein isothiocyanate (FITC)-conjugated transferrin (Jackson ImmunoResearch Laboratories) during J591 incubation. To monitor the internalization of Tac-PSMA chimera, mAb against the extracellular domain of Tac, 7G7 (Rubin *et al*., 1985) was used. For kinetic analysis of PSMA uptake the cells were incubated with J591 and FITC-conjugated transferrin for 1 h at 4°C, washed three times, and then incubated in DMEM at 37°C, 5% CO_2 to allow for uptake. The cells were fixed at the indicated time points and incubated with Texas Red-conjugated secondary antibody. Uptake of antibodies (mAbs J591 and 7G7) and transferrin were visualized and quantitated by confocal microscopy (see below). To visualize surface expression of PSMA and Tac-PSMA chimeras, COS cells transfected with the respective plasmid were fixed and stained with mAb J591 and 7G7, respectively, under nonpermeabilized conditions.

Confocal Microscopy

Codistribution of internalized mAbs J591or 7G7 and transferrin were examined using a Fluoview laser scanning confocal microscope (Olympus America, Melville, NY). To detect simultaneously FITC- and Texas Red-labeled antigens, samples were excited at 488 and 568 nm with argon and krypton lasers, respectively, and the light emitted between 525 and 540 nm was recorded for FITC and >630 nm for Texas Red. Images were generated using Fluoview software (version 2.1.39). Transfected cells (30–40) were examined for each transfection done in duplicate and the representative data are shown.

Quantification of internalization in COS cells expressing $PSMA_{wt}$ and PSMA harboring mutation of the fourth leucine (PSMA-L4A) or fourth and fifth leucine (PSMA-L4A/L5A) was done using image analysis software (Fluoview, version 2.1.39). Average pixel intensities of internalized transferrin (green), and mAb J591 (red) from optical sections of 30–40 cells were determined. Because the transferrin uptake was more or less uniform PSMA internalization was normalized to transferrin uptake. An analysis of variance was used to compare the PSMA/transferrin ratios as a function of time between $PSMA_{wt}$ and PSMA-L4A. A logarithmic transform was used to stabilize variance and for computing 95% confidence intervals for the geometric mean of PSMA-L4A mutant ratios as a percentage of $PSMA_{wt}$ ratios.

NAALDase Activity

NAALDase activity was determined as described by Sekiguchi *et al*. (1989). COS cells were transfected with $PSMA_{wt}$ on 60-mm culture dishes. After 48 h of transfection, cells were incubated with 1 μCi/ml [^{3}H]NAAG (PerkinElmer Life Sciences, Boston, MA) in Krebs-Ringer bicarbonate medium or in Dul-

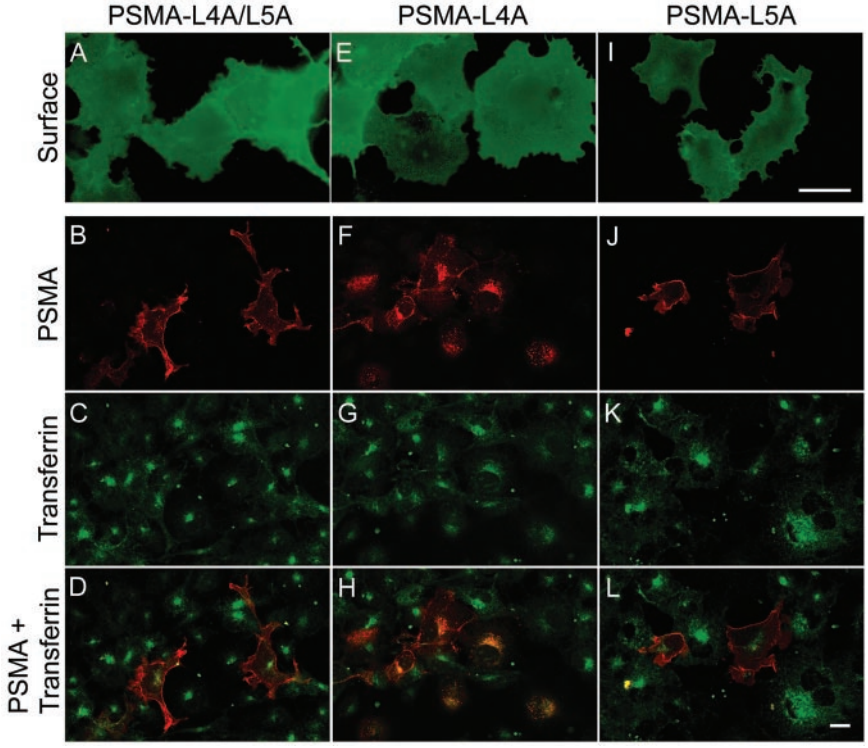

Figure 3. Internalization of the cytoplasmic tail di-leucine mutants of PSMA. (A, E, and I) Surface expression of PSMA in COS-7 cells expressing PSMA-L4A/L5A, PSMA-L4A, and PSMA-L5A mutants, respectively. Forty-eight hours after transfection, the cells were fixed in paraformaldehyde under nonpermeabilized conditions and labeled with mAb J591 followed by FITC-conjugated anti-mouse antibody and visualized by epifluorescence microscopy. (B, F, and J) Internalization of PSMA mutants. (C, G, and K) FITC-transferrin uptake. (D, H, and L) Merged images of PSMA and FITC-transferrin. Representative medial optical sections are shown. Yellow color in H indicates the codistribution of FITC-transferrin and internalized PSMA. Bars, 10 μm (A, E, and I) and 5 μm (B, C, D, F, G, H, K, and L).

becco's modified Eagle's medium for 1 h. The medium was removed and the cells were washed three times with their respective incubation medium. Cells were then lysed in 1% Triton X-100, and the radioactivity was determined using a scintillation counter (Beckman LS 6500). Counts were normalized to protein. Protein concentrations of the cell lysates were determined using the Bio-Rad DC reagent (Bio-Rad, Hercules, CA) according to manufacturer's instructions.

RESULTS

To study the internalization of PSMA, COS cells were transiently transfected with $PSMA_{wt}$ cDNA (Figure 1) and uptake of mAb J591 was monitored by immunofluorescence and confocal microscopy. The internalized antibody showed a distinct spot-like staining pattern at the perinuclear region (Figure 2A). This spot-like staining is reminiscent of the recycling endosomal compartment and internalized transferrin, a marker for this compartment, colocalized with endocytosed PSMA (Figure 2, A–C), indicating that PSMA is localized to the recycling endosome. We have shown earlier that PSMA is internalized via clathrin-coated vesicles in LNCaP cells (Liu *et al*., 1998). To further confirm that PSMA is internalized via a clathrin-dependent endocytic mechanism in COS cells, we tested whether PSMA is internalized in cells expressing a GTPase-deficient dynamin mutant (K44A), which is known to inhibit clathrin-dependent endocytosis in cultured cells (Herskovits *et al*., 1993; van der Bliek *et al*., 1993). In these cells internalization of PSMA was not detected (Figure 2, D–F) further confirming that PSMA is internalized via a clathrin-dependent endocytic pathway.

To test whether the cytoplasmic tail of PSMA contains a signal that mediates its internalization the PSMA cytoplasmic tail was deleted and the mutant (PSMA-Δcd) was expressed in COS cells. PSMA-Δcd was clearly expressed on the cell surface as revealed by immunofluorescence staining under nonpermeabilized condition (our unpublished data). Incubation of these cells with mAb J591 did not show uptake or localization to the endosomes and internalized transferrin did not reveal a codistribution with PSMA (Figure 2, G–I), indicating that the cytoplasmic tail of PSMA contains a signal that mediates its internalization.

The cytoplasmic tail of PSMA contains two consecutive leucines as reported for di-leucine-like motifs (Figure 1). To examine whether this motif functions as an internalization signal for PSMA, the di-leucine pair was converted to di-alanine (PSMA-L4A/L5A), the mutant protein was expressed in COS cells and uptake of mAb J591 was monitored. The di-alanine mutant of PSMA was clearly expressed on the cell surface as revealed by staining with mAb J591 under nonpermeabilized condition (Figure 3A). Our internalization assay revealed that mAb J591 was not internalized in cells expressing the di-alanine mutant of PSMA (Figure 3B) and did not show codistribution with the internalized FITC-transferrin (Figure 3, C and D), indicating that mutation of the di-leucine pair in the cytoplasmic tail of PSMA abrogates its internalization. We then examined whether both these leucines are essential for the internalization of PSMA. For this purpose single leucine residues at positions 4 (PSMA-L4A) and 5 (PSMA-L5A) were mutated to alanine and the uptake of mAb J591 was studied. Both these mutants were expressed on the cell surface as revealed by staining with mAb J591 under nonpermeabilized condition (Figure 3, E and I). J591 was clearly internalized in cells expressing PSMA-L4A (Figure 3F) and internalized transferrin (Figure 3G) codistributed with the internalized mAb J591 (Figure 3H). By contrast, in cells expressing PSMA-L5A, mAb J591 was not internalized (Figure 3J) and the antibody primarily stained the plasma membrane similar to cells expressing PSMA-L4/L5 (Figure 3B). In these cells, colocalization of PSMA and internalized FITC-transferrin was not

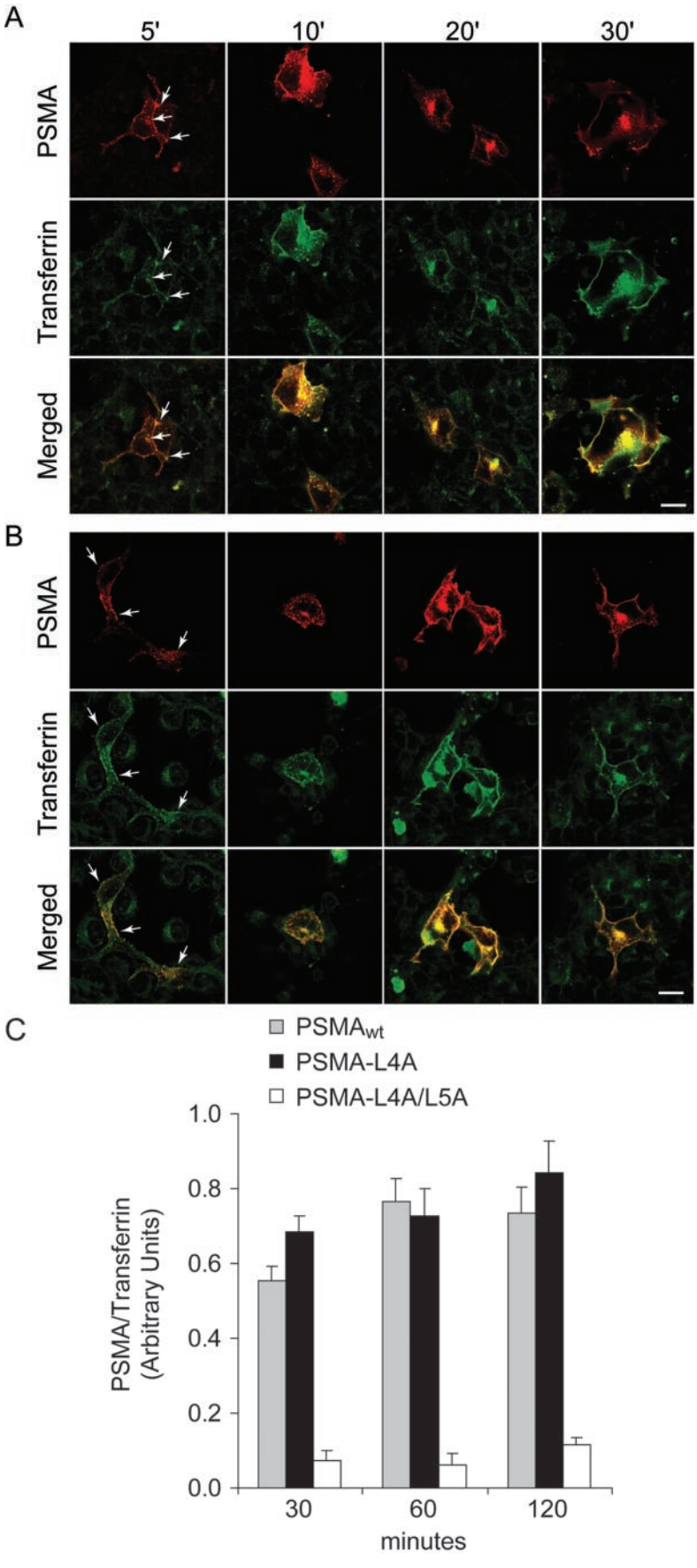

Figure 4. Kinetic analysis of internalization of PSMA$_{wt}$ and PSMA-L4A in COS cells. (A and B) Time course of PSMA$_{wt}$ (A) and PSMA-L4A (B) internalization. Transiently transfected COS cells were incubated with mAb J591 and FITC-transferrin for the indicated time points, as described under EXPERIMENTAL PROCEDURES and stained with Texas Red-conjugated anti-mouse antibody. Representative medial optical sections are shown. Arrows indicate peripheral vesicles containing PSMA and transferrin. Bar, 5 μm. (C) COS cells expressing PSMA$_{wt}$, PSMA-L4A, or PSMA-L4A/L5A were incubated with J591 and FITC-conjugated transferrin for 1 h at 4°C, washed, and incubated at 37°C to allow for uptake. The cells were fixed after 30, 60, and 120 min and incubated with Texas Red-conjugated secondary antibody. Uptake of mAbs J591 and transferrin were visualized and quantitated by confocal microscopy as described under EXPERIMENTAL PROCEDURES. PSMA internalization was normalized to transferring uptake. The bars indicate SE of 30–40 cells analyzed for each condition.

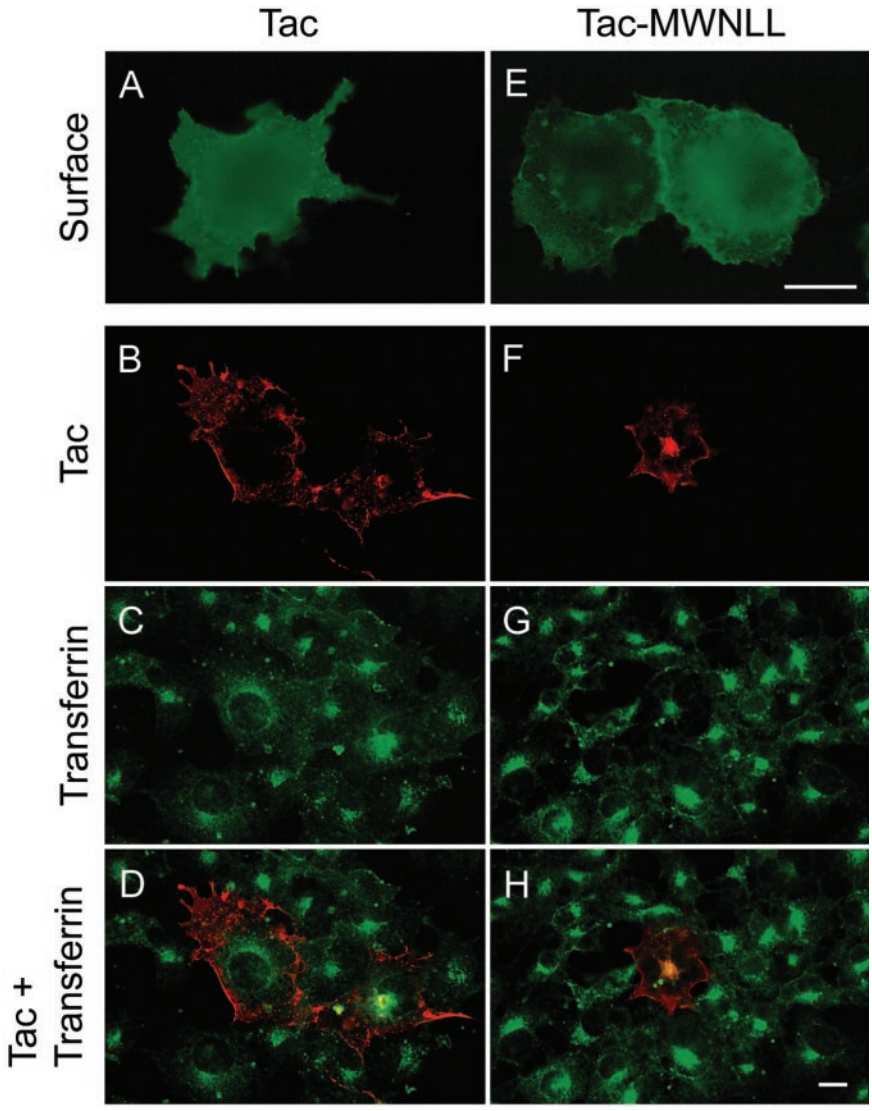

Figure 5. Internalization of Tac and Tac-PSMA chimera. (A and E) Surface expression of Tac. Forty-eight hours after transfection the cells were fixed in paraformaldehyde under nonpermeabilized condition, labeled with mAb 7G7 followed by FITC-conjugated anti-mouse antibody, and visualized by epifluorescence microscopy. (B–D, F–H) Internalization of Tac and FITC-transferrin. The cells were incubated with mAb 7G7 and FITC-transferrin for 2 h, washed, fixed in cold methanol, and stained with Texas Red-conjugated anti-mouse antibody. Representative medial optical sections are shown. (B and F) Internalization of Tac antibody. (C and G) Uptake of FITC-transferrin. (D and H) Merged images. Yellow color in H indicates the codistribution of FITC-transferrin and internalized Tac. Bars, 10 μm (A and E) and 5 μm (B, C, D, F, G, and H).

detected (Figure 3, K and L). These results indicated that the fifth leucine in the cytoplasmic tail of PSMA is crucial for its internalization.

Because PSMA-L4A was internalized similar to $PSMA_{wt}$ we determined the kinetics of PSMA uptake in cells expressing these constructs. Our efforts to obtain quantitative data by using iodinated mAb J591 were not successful because mAb J591 bound to the cell surface was not quantitatively released after acid wash procedures commonly used to release bound antibody on the cell surface. Therefore, we used immunofluorescence and confocal microscopy approaches to determine the kinetics of mAb J591 uptake in cells expressing $PSMA_{wt}$ and PSMA-L4A. As shown in Figure 4, both $PSMA_{wt}$ and PSMA-L4A expressing cells internalized PSMA rapidly. After 5-min incubation both PSMA and transferrin showed predominant plasma membrane localization with small amounts localized to peripheral vesicles (arrow). Similarly, after 10 min PSMA and transferrin codistributed in more peripheral vesicles, whereas after 20 min it accumulated in the recycling endosomal compartment. Cells expressing PSMA-L4A (Figure 4B) showed a similar internalization pattern. These results indicated that mutation of the fourth leucine in the cytoplasmic tail of PSMA has a minimal effect on the internalization of PSMA in COS cells. To obtain quantitative data we determined the average pixel intensity represented by internalized PSMA and transferrin by using image analysis software (Fluoview, version 2.1.39). Because quantification of internalized PSMA and transferrin was more reliable after 30 min, we quantified internalized PSMA in cells expressing $PSMA_{wt}$ and PSMA-L4A at 30, 60, and 120 min. We used internalized transferrin as an internal control for defining the area representing the internalized PSMA. Comparison of the internalization kinetics of $PSMA_{wt}$ and PSMA-L4A revealed that PSMA-L4A is internalized with kinetics similar to $PSMA_{wt}$ (Figure 4C). An analysis of the variance demonstrated that internalization increased with time ($p = 0.04$), but there was no statistical difference between the internalization profiles for $PSMA_{wt}$ and PSMA-L4A mutants ($p > 0.2$). The 95% confidence intervals for PSMA-L4A mutant internalization (as percentage of $PSMA_{wt}$) were 100–148% at 30 min, 72–116% at 60 min, and 89–143% at 120 min, indicating that mutation of the fourth leucine does not alter the internalization properties of PSMA.

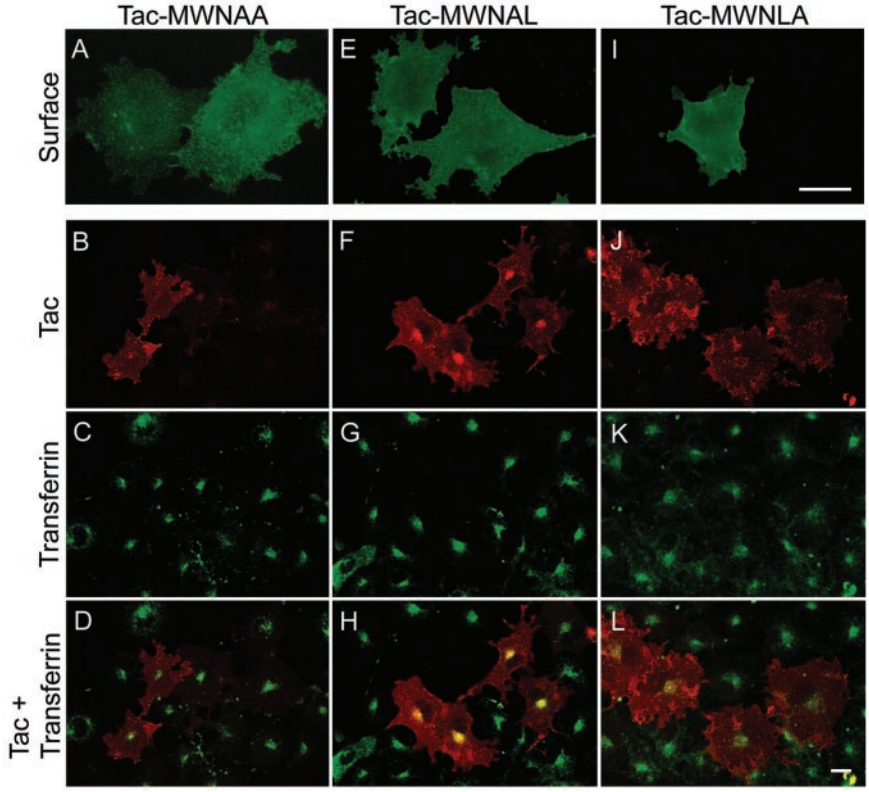

Figure 6. Internalization of Tac-PSMA chimeras harboring mutations in the di-leucine signal. Surface expression as well as internalization of PSMA was performed as described in figure legend 5. (A, E, and I) Surface expression of Tac in COS-7 cells expressing Tac-MWNAA, Tac-MWNAL, and Tac-MWNLA chimeras, respectively. (B, F, and J) Internalization of Tac chimera mutants. (C, G, and K) Uptake of FITC-transferrin. (D, H, and L) Merged images. Representative medial optical sections are shown. Yellow color in H indicates the codistribution of FITC-transferrin and internalized PSMA. Bars, 10 μm (A, E, and I) and 5 μm (B, C, D, F, G, H, J, K, and L).

To further test whether amino acid residues other than the fifth leucine are essential for the internalization of mAb J591 we systematically mutated each of the cytoplasmic tail amino acids into alanine. These point mutations did not affect the internalization of mAb J591 (our unpublished data). Moreover, the construct in which amino acids 6–14 were deleted (PSMA-Δ6–14) internalized mAb J591 when expressed in COS cells. These results demonstrated that the N-terminal first five amino acids in the cytoplasmic tail of PSMA are sufficient to mediate PSMA internalization and the fifth amino acid leucine is crucial for its internalization activity.

To further confirm that this five amino acid motif of PSMA is sufficient for internalization, we transferred the five N-terminal amino acids of PSMA to the noninternalized protein Tac, a type I membrane protein (Letourneur and Klausner, 1992). Internalization of Tac was monitored by uptake of mAb 7G7 raised against the extracellular domain of Tac (Rubin *et al*., 1985). In nonpermeabilized COS cells wild-type Tac (Tac_{wt}) showed a distinct plasma membrane localization (Figure 5A), indicating that this protein is targeted to the plasma membrane but incubation with mAb 7G7 did not result in the internalization of this antibody, confirming that Tac_{wt} is not internalized in COS cells (Figure 5B) as reported previously (Letourneur and Klausner, 1992). Codistribution of mAb 7G7 staining and internalized transferrin was not detected in these cells (Figure 5, C and D). By contrast, incorporation of the amino acids MWNLL into the Tac cytoplasmic tail (Tac-MWNLL) resulted in the internalization of mAb 7G7 (Figure 5F). The internalized antibody clearly colocalized with internalized FITC-transferrin (Figure 5, G and H) indicating that the N-terminal five amino acids in the cytoplasmic tail of PSMA are transferable and are sufficient to confer internalization properties to a noninternalized protein.

Furthermore, in cells expressing Tac-MWNAA where the two consecutive leucines are mutated to alanines, the mAb 7G7 was not internalized (Figure 6B), although this protein was clearly localized to the plasma membrane (Figure 6A). This mutant did not codistribute with internalized FITC-transferrin (Figure 6, C and D). Internalization of mAb 7G7 was maintained in cells expressing the construct where the fourth leucine is mutated to alanine (Tac-MWNAL) (Figure 6, F–H), whereas in cells expressing Tac-MWNLA, where the leucine at position 5 is mutated, the uptake of 7G7 was not detected (Figure 6, J–L). Both these mutants were clearly expressed on the plasma membrane as revealed by nonpermeablized staining by using mAb 7G7 (Figure 6, E and I). Together, these data demonstrate that the leucine at the fifth position is critical for PSMA internalization.

Although it is possible that a single leucine in the cytoplasmic tail of PSMA might play a crucial role in its internalization, it is unlikely that it can function as an internalization motif. Therefore, we decided to test for other potential amino acid residues in the five amino acid motif that might be involved in the internalization of PSMA. We have evidence that mutation of amino acids at position 2 and 3 (our unpublished data) and 4 (Figure 3) of the cytoplasmic tail of PSMA did not affect internalization, whereas mutation of leucine at position 5 abolished its internalization. The only amino acid that remained to be tested was the first amino acid methionine. Therefore, we mutated methionine in the internalizing Tac-MWNAL chimera to generate Tac-AWNAL. Although Tac-AWNAL was expressed on the cell surface (our unpublished data), a drastic reduction in the internalization of mAb 7G7 was noticed in cells expressing

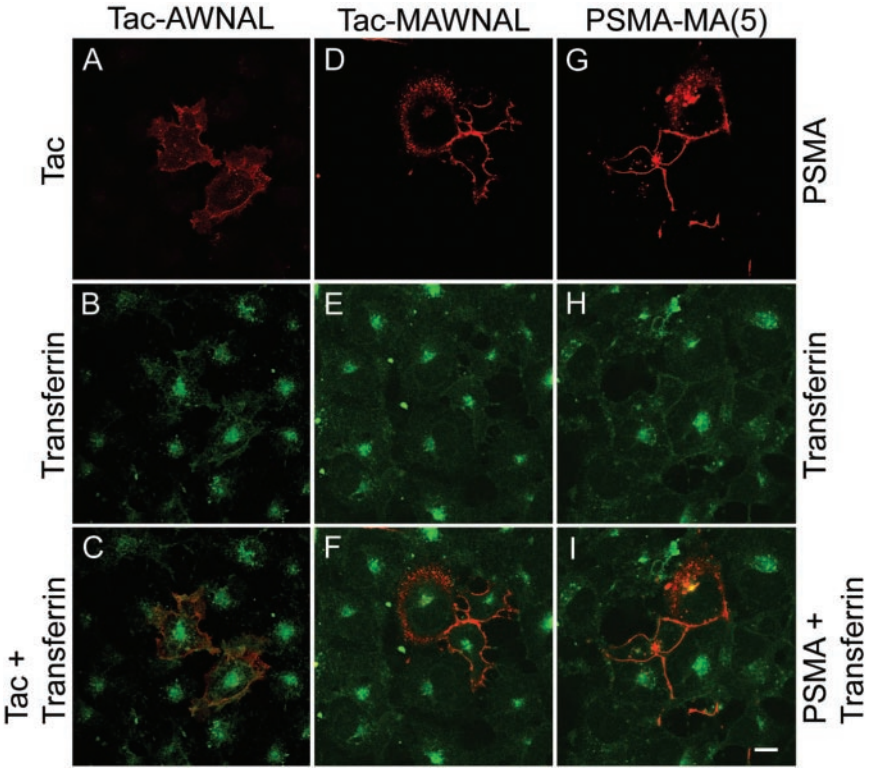

Figure 7. Internalization of Tac-PSMA chimeras Tac-AWNAL and Tac-MAWNAL, and of PSMA-MA(5). (A and D) Internalization of Tac chimera mutants and (G) mAb J591 in transiently transfected COS cells. (B, E, and H) Internalization of FITC-transferrin. (C, F, and I) Merged images. Note the lack of codistribution of Tac-chimera mutants or PSMA-MA(5) and FITC-transferrin. Bar, 5 μm.

this chimera (Figure 7A). Although in these cells FITC-transferrin was clearly internalized (Figure 7B), there was little colocalization of internalized transferrin with Tac-AWNAL (Figure 7C). Small amounts of internalized mAb J591 were seen in peripheral vesicles, in contrast to the intense fluorescence of internalized transferrin seen at the cell center. This result indicated that in addition to the fifth leucine the methionine is also required and that the N-terminal five amino acids, MWNLL, form a motif to mediate the internalization of PSMA. To test whether the length of this motif is involved in PSMA internalization, we inserted an additional alanine between tryptophan and methionine (Tac-MAWNAL) and monitored the internalization of this chimera. In COS cells, Tac-MAWNAL was clearly expressed on the cell surface as revealed by nonpermeabilized staining (our unpublished data). However, internalization of mAb7G7 was highly reduced (Figure 7D), and there was less colocalization of the chimera with internalized FITC-transferrin (Figure 7, E and F). We then tested whether incorporation of alanine into the MWNLL motif of PSMA itself affects internalization. Whereas insertion of one or two amino acids did not affect internalization, insertion of five alanines [PSMA-MA(5)] drastically reduced the internalization of PSMA (Figure 7G).

The endocytic motif of membrane receptors binds to AP complexes, which are heterotetramers and mediate the internalization of membrane receptors (Hirst and Robinson, 1998; Kirchhausen, 1999). The adaptor complex AP-2 has been shown to associate with both tyrosine (Ohno *et al*., 1995; Honing *et al*., 1996; Boll *et al*., 2002) and di-leucine–based signals (Hofmann *et al*., 1999). To obtain insights into whether AP-2 is involved in the internalization of PSMA, we monitored internalization of PSMA in a HeLa cell line that expresses a dominant negative mutant μ2 of the AP-2 complex under the control of a tetracycline-off system (Nesterov *et al*., 1999). Strikingly, mutant μ2 drastically reduced the internalization of PSMA (Figure 8A) and transferrin (Figure 8B), and transferrin showed a more diffused localization pattern that codistributed with PSMA (Figure 8C). In non-induced cells that only express wild-type μ2 PSMA as well as transferrin were clearly internalized (Figure 8, D–F), indicating that the μ2-subunit of AP-2 is involved in the internalization mediated by the MWNLL motif of PSMA.

DISCUSSION

In this study, we demonstrate that the cytoplasmic tail five N-terminal amino acids MWNLL are sufficient to mediate the internalization of PSMA. Methionine at the first position and leucine at the fifth position are essential, whereas amino acids 2, 3, and 4 are dispensable for the internalization of PSMA. Incorporation of alanine(s) into Tac-chimera (Tac-MAWNAL) and into PSMA [PSMA-MA(5)] drastically reduced the internalization, indicating that the length of this sequence is also important for its internalization function. We also present evidence that the adaptor complex AP-2 is involved in the internalization of PSMA. Based on these results, we suggest that the N-terminal five amino acid residues of PSMA form a novel autonomous methionine-leucine based internalization motif (MXXXL). To our knowledge, this is the first study describing a N-terminal amino acid (translation start site) as part of an internalization motif.

Although the presence of two consecutive leucines at position four and five suggested that the cytoplasmic tail of PSMA may contain a di-leucine–like motif, our results indicate that this might not represent a typical di-leucine motif as observed in other membrane proteins. The di-leucine–based signals of the [DE]XXXL[LI] and DXXLL types have an acidic residue at −4 from the first leucine (Pond *et al*.,

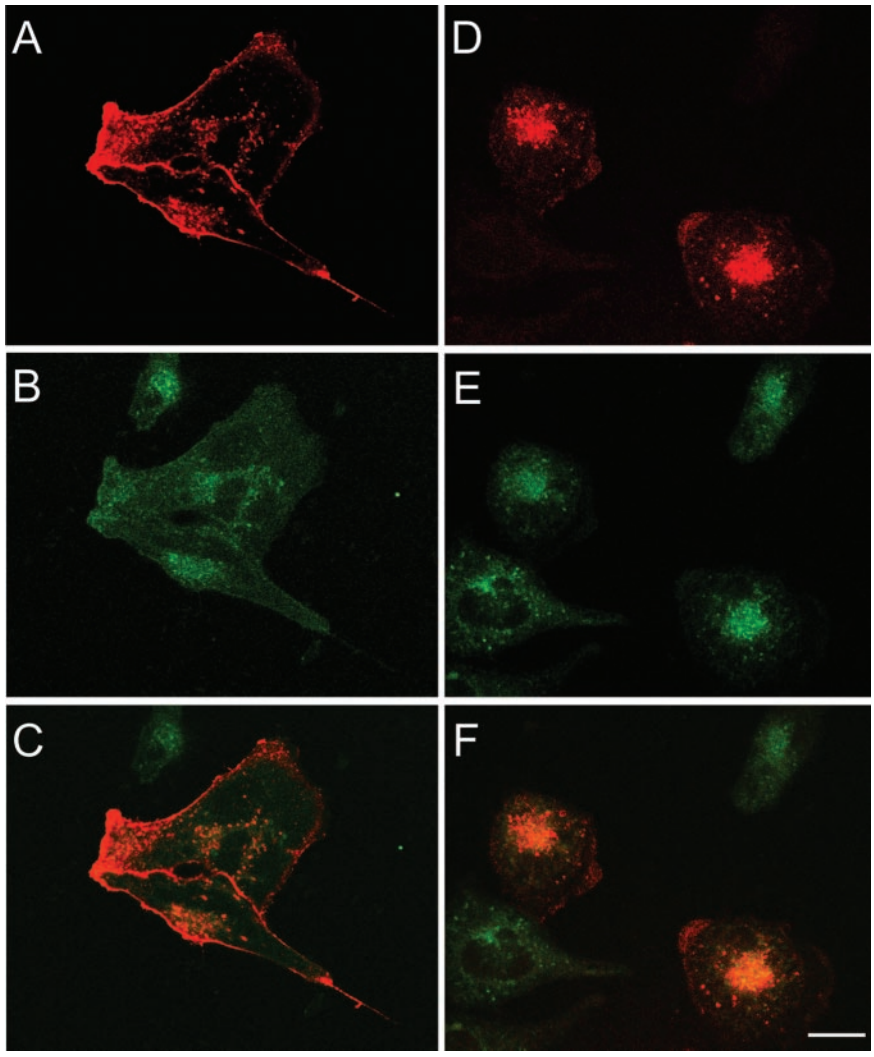

Figure 8. Internalization of $PSMA_{wt}$ in HeLa cells expressing dominant-negative AP-2 complexes. $PSMA_{wt}$ cDNA was transiently transfected into HeLa cells expressing a tetracycline-repressible dominant-negative mutant of μ2. mAb J591 internalization was monitored in mutant μ2-induced cells (A) and in noninduced cells (D). (B and E) Internalization of FITC-transferrin. (C and F) Merged images. Bar, 5 μm.

1995; Sandoval *et al*., 2000), which is absent in PSMA and is replaced by an essential methionine. In the [DE]XXXL[LI] type the first leucine is generally indispensable and substitution with other amino acids decreases the efficacy of the signal (Letourneur and Klausner, 1992), whereas in the DXXLL type both the leucines are essential and mutation of any of these residues to alanine inactivates the signal (Johnson and Kornfeld, 1992; Chen *et al*., 1997). In PSMA, mutation of the first leucine did not change significantly the internalization kinetics. Moreover, in polarized epithelial cells, proteins with di-leucine motif are targeted to the basolateral plasma membrane (Sheikh and Isacke, 1996; El Nemer *et al*., 1999; Bello *et al*., 2001). By contrast, PSMA is targeted to the apical plasma membrane in Madin-Darby canine kidney cells (Christiansen *et al*., 2003) and swapping the cytoplasmic tail of PSMA with the cytoplasmic tail of a di-leucine motif containing protein redirected PSMA to the basolateral plasma membrane (our unpublished data). The absence of tyrosine residues in the cytoplasmic tail of PSMA clearly indicates that this protein does not contain a tyrosine-based signal. Together, these results strongly indicate that the MXXXL motif of PSMA is a novel methionine-leucine–based internalization motif.

PSMA is localized to the recycling endosomal compartment as revealed by its colocalization with internalized transferrin. Colocalization of Tac-MWNLL with transferrin further indicated that the MWNLL sequence is sufficient for the localization of PSMA to the recycling endosomal compartment. We have recently shown that the cytoplasmic tail of PSMA associates with the actin cross linking protein filamin (Anilkumar *et al*., 2003) and that this association is involved in the localization of PSMA to the recycling endosomal compartment. Future studies will determine whether the MWNLL motif of PSMA associates with filamin and functions as a recycling endosome targeting signal.

We have shown that dominant negative μ2 of the AP-2 complex reduces the internalization of PSMA, indicating that the AP-2 complex is involved in the internalization mediated by the MXXXL motif of PSMA. Recent structural studies suggested that the YxxΦ endocytic determinant might associate with the μ2 adaptin as a two-pinned plug into a socket with the Y and the Φ residues (the pins) fitting into sterically and chemically complementary pockets of the μ2 surface (Owen and Evans, 1998; Owen and Luzio, 2000). Requirement of the specific length of the MXXXL motif tempts us to speculate that the first amino acid methionine

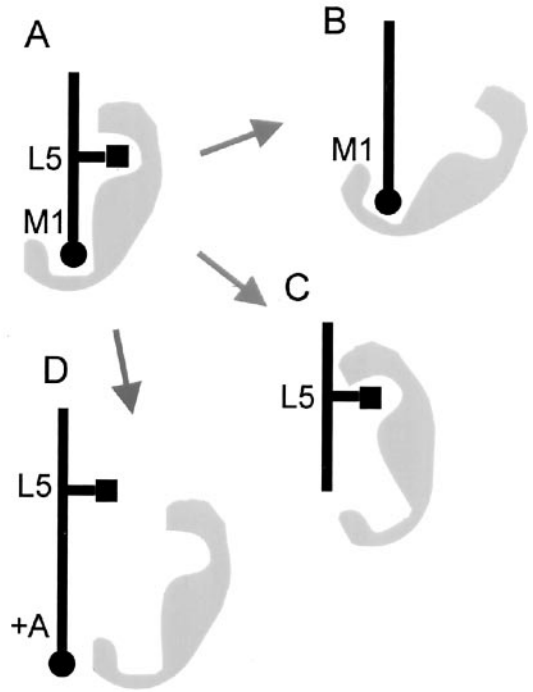

Figure 9. Schematic model of binding of the PSMA internalization motif to μ2 of the AP-2 complex. (A) The endocytic determinant of PSMA might form two pins (methionine at position 1 [black circle] and leucine at position 5 [black square]) that fit into a complementary pocket of a μ2 (gray) associating with the cytoplasmic tail of PSMA. Loss of the side chains of leucine-5 (B) or methionine-1 (C) of the internalization motif might result in an altered association of the adaptor preventing the internalization of PSMA. Similarly, extension of the length of the internalization motif with an additional alanine (D) might prevent the binding of the adaptor protein to the cytoplasmic tail of PSMA and therefore inhibit internalization of the protein.

and the fifth leucine of the PSMA endocytic determinant might function as two pins fitting into a complementary pocket of μ2 (Figure 9). Future studies will establish whether μ2 directly associates with the MXXXL motif and whether this motif can compete with the YxxΦ or [DE]XXXL[LI] motifs, which are known to associate with μ2.

The catalytic site for glutamate carboxypeptidase/NAALDase activity of PSMA resides in its extracellular domain (Speno *et al*., 1999). Millimolar concentrations of phosphate used in the culture medium almost completely inhibited the NAALDase activity in COS cells (our unpublished data; Slusher *et al*., 1999). Because our internalization assays were performed in culture medium that inhibits NAALDase activity, this enzymatic activity seems not to be necessary for the internalization of PSMA. Moreover, in LNCaP cells, incubation with the NAAG substrate for NAALDase did not increase the internalization of PSMA (our unpublished data), whereas incubation with mAb J591 or the Fab fragments of this antibody increased the internalization rate of PSMA (Liu *et al*., 1998). The antibody and the antibody fragments might mimic a putative ligand for PSMA. These results indicate that the internalization of PSMA might be an independent function from its glutamate carboxypeptidase/NAALDase activity. It is possible that PSMA might function as a receptor mediating the internalization of a putative ligand. Identification of a PSMA ligand combined with the knowledge on PSMA internalization should provide more insights into the function of this protein and, in consequence, provide valuable information for therapeutic applications of PSMA.

ACKNOWLEDGMENTS

We thank Dr. Alexander Sorkin for generously providing HeLa cells expressing a dominant negative mutant of μ2 and Dr. Joseph Coyle for the PSMA-T14V mutant plasmid construct. We thank Dr. Esteban Dell'Angelica for critical reading of the manuscript. This work was primarily supported by the Department of Defense grants DAMD17-98-1-8567 and DAMD17-02-1-0661 and in part by a CaP CURE award to A.K.R. S.A.R. was supported by U.S. Department of Health and Human Services (Institutional National Research Service Award T32CA09056. E.O. was partially supported by a Fellowship from Jonsson Comprehensive Cancer Center. N.H.B. is a paid consultant of BZL, Inc. (Framingham, MA) and has developed mAB J591 used in this study, which was patented by the Cornell Research Foundation and licensed to BZL.

REFERENCES

Anilkumar, G., Rajasekaran, S.A., Wang, S., Hankinson, O., Bander, N.H., and Rajasekaran, A.K. (2003). Prostate-specific membrane antigen association with filamin A modulates its internalization and NAALADase activity. Cancer Res. *63*, 2645–2648.

Bello, V., Goding, J.W., Greengrass, V., Sali, A., Dubljevic, V., Lenoir, C., Trugnan, G., and Maurice, M. (2001). Characterization of a di-leucine-based signal in the cytoplasmic tail of the nucleotide-pyrophosphatase NPP1 that mediates basolateral targeting but not endocytosis. Mol. Biol. Cell *12*, 3004–3015.

Boll, W., Rapoport, I., Brunner, C., Modis, Y., Prehn, S., and Kirchhausen, T. (2002). The mu2 subunit of the clathrin adaptor AP-2 binds to FDNPVY and YppO sorting signals at distinct sites. Traffic *3*, 590–600.

Bonifacino, J.S., and Dell'Angelica, E.C. (1999). Molecular bases for the recognition of tyrosine-based sorting signals. J. Cell Biol. *145*, 923–926.

Bonifacino, J.S., and Traub, L.M. (2003). Signals for sorting of transmembrane proteins to endosomes and lysosomes. Annu. Rev. Biochem. *72*, 395–447.

Carter, R.E., Feldman, A.R., and Coyle, J.T. (1996). Prostate-specific membrane antigen is a hydrolase with substrate and pharmacologic characteristics of a neuropeptidase. Proc. Natl. Acad. Sci. USA *93*, 749–753.

Chang, S.S., Bander, N.H., and Heston, W.D. (1999a). Monoclonal antibodies: will they become an integral part of the evaluation and treatment of prostate cancer–focus on prostate-specific membrane antigen? Curr. Opin. Urol. *9*, 391–395.

Chang, S.S., O'Keefe, D.S., Bacich, D.J., Reuter, V.E., Heston, W.D., and Gaudin, P.B. (1999b). Prostate-specific membrane antigen is produced in tumor-associated neovasculature. Clin. Cancer Res. *5*, 2674–2681.

Chang, S.S., Reuter, V.E., Heston, W.D., Bander, N.H., Grauer, L.S., and Gaudin, P.B. (1999c). Five different anti-prostate-specific membrane antigen (PSMA) antibodies confirm PSMA expression in tumor-associated neovasculature. Cancer Res. *59*, 3192–3198.

Chen, H.J., Yuan, J., and Lobel, P. (1997). Systematic mutational analysis of the cation-independent mannose 6-phosphate/insulin-like growth factor II receptor cytoplasmic domain. An acidic cluster containing a key aspartate is important for function in lysosomal enzyme sorting. J. Biol. Chem. *272*, 7003–7012.

Christiansen, J.J., Rajasekaran, S.A., Moy, P., Butch, A., Goodglick, L., Gu, Z., Reiter, R.E., Bander, N.H., and Rajasekaran, A.K. (2003). Polarity of prostate specific membrane antigen, prostate stem cell antigen, and prostate specific antigen in prostate tissue and in a cultured epithelial cell line. Prostate *55*, 9–19.

Coyle, J.T. (1997). The nagging question of the function of N-acetylaspartylglutamate. Neurobiol. Dis. *4*, 231–238.

El Nemer, W., Colin, Y., Bauvy, C., Codogno, P., Fraser, R.H., Cartron, J.P., and Le Van Kim, C.L. (1999). Isoforms of the Lutheran/basal cell adhesion molecule glycoprotein are differentially delivered in polarized epithelial cells. Mapping of the basolateral sorting signal to a cytoplasmic di-leucine motif. J. Biol. Chem. *274*, 31903–31908.

Halsted, C.H., Ling, E.H., Luthi-Carter, R., Villanueva, J.A., Gardner, J.M., and Coyle, J.T. (1998). Folylpoly-gamma-glutamate carboxypeptidase from pig jejunum. Molecular characterization and relation to glutamate carboxypeptidase II. J. Biol. Chem. *273*, 20417–20424.

Herskovits, J.S., Burgess, C.C., Obar, R.A., and Vallee, R.B. (1993). Effects of mutant rat dynamin on endocytosis. J. Cell Biol. *122*, 565–578.

Hirst, J., and Robinson, M.S. (1998). Clathrin and adaptors. Biochim. Biophys. Acta *1404*, 173–193.

Hofmann, M.W., Honing, S., Rodionov, D., Dobberstein, B., von Figura, K., and Bakke, O. (1999). The leucine-based sorting motifs in the cytoplasmic domain of the invariant chain are recognized by the clathrin adaptors AP1 and AP2 and their medium chains. J. Biol. Chem. *274*, 36153–36158.

Honing, S., Griffith, J., Geuze, H.J., and Hunziker, W. (1996). The tyrosine-based lysosomal targeting signal in lamp-1 mediates sorting into Golgi-derived clathrin-coated vesicles. EMBO J. *15*, 5230–5239.

Horoszewicz, J.S., Kawinski, E., and Murphy, G.P. (1987). Monoclonal antibodies to a new antigenic marker in epithelial prostatic cells and serum of prostatic cancer patients. Anticancer Res. *7*, 927–935.

Israeli, R.S., Powell, C.T., Fair, W.R., and Heston, W.D. (1993). Molecular cloning of a complementary DNA encoding a prostate-specific membrane antigen. Cancer Res. *53*, 227–230.

Johnson, K.F., and Kornfeld, S. (1992). The cytoplasmic tail of the mannose 6-phosphate/insulin-like growth factor-II receptor has two signals for lysosomal enzyme sorting in the Golgi. J. Cell Biol. *119*, 249–257.

Kawabata, H., Yang, R., Hirama, T., Vuong, P.T., Kawano, S., Gombart, A.F., and Koeffler, H.P. (1999). Molecular cloning of transferrin receptor 2. A new member of the transferrin receptor-like family. J. Biol. Chem. *274*, 20826–20832.

Kirchhausen, T. (1999). Adaptors for clathrin-mediated traffic. Annu. Rev. Cell Dev. Biol. *15*, 705–732.

Kirchhausen, T., Bonifacino, J.S., and Riezman, H. (1997). Linking cargo to vesicle formation: receptor tail interactions with coat proteins. Curr. Opin. Cell Biol. *9*, 488–495.

Lazarovits, J., and Roth, M. (1988). A single amino acid change in the cytoplasmic domain allows the influenza virus hemagglutinin to be endocytosed through coated pits. Cell *53*, 743–752.

Leonard, *et al*. (1984). Molecular cloning and expression of cDNAs for the human interleukin-2 receptor. Nature *311*, 626–631.

Letourneur, F., and Klausner, R.D. (1992). A novel di-leucine motif and a tyrosine-based motif independently mediate lysosomal targeting and endocytosis of CD3 chains. Cell *69*, 1143–1157.

Liu, H., Moy, P., Kim, S., Xia, Y., Rajasekaran, A., Navarro, V., Knudsen, B., and Bander, N.H. (1997). Monoclonal antibodies to the extracellular domain of prostate-specific membrane antigen also react with tumor vascular endothelium. Cancer Res. *57*, 3629–3634.

Liu, H., Rajasekaran, A.K., Moy, P., Xia, Y., Kim, S., Navarro, V., Rahmati, R., and Bander, N.H. (1998). Constitutive and antibody-induced internalization of prostate-specific membrane antigen. Cancer Res. *58*, 4055–4060.

Luthi-Carter, R., Barczak, A.K., Speno, H., and Coyle, J.T. (1998). Molecular characterization of human brain N-acetylated alpha-linked acidic dipeptidase (NAALADase). J. Pharmacol. Exp. Ther. *286*, 1020–1025.

Marks, M.S., Ohno, H., Kirchhausen, T., and Bonifacino, J.S. (1997). Protein sorting by tyrosine-based signals: adapting to the Ys and wherefores. Trends Cell Biol. *7*, 124–128.

McDevitt, M.R., *et al*. (2001). Tumor therapy with targeted atomic nanogenerators. Science *294*, 1537–1540.

Mellman, I. (1996). Endocytosis and molecular sorting. Annu. Rev. Cell Dev. Biol. *12*, 575–625.

Mukherjee, S., Ghosh, R.N., and Maxfield, F.R. (1997). Endocytosis. Physiol. Rev. *77*, 759–803.

Nesterov, A., Carter, R.E., Sorkina, T., Gill, G.N., and Sorkin, A. (1999). Inhibition of the receptor-binding function of clathrin adaptor protein AP-2 by dominant-negative mutant mu2 subunit and its effects on endocytosis. EMBO J. *18*, 2489–2499.

Ohno, H., Stewart, J., Fournier, M.C., Bosshart, H., Rhee, I., Miyatake, S., Saito, T., Gallusser, A., Kirchhausen, T., and Bonifacino, J.S. (1995). Interaction of tyrosine-based sorting signals with clathrin-associated proteins. Science *269*, 1872–1875.

Owen, D.J., and Evans, P.R. (1998). A structural explanation for the recognition of tyrosine-based endocytotic signals. Science *282*, 1327–1332.

Owen, D.J., and Luzio, J.P. (2000). Structural insights into clathrin-mediated endocytosis. Curr. Opin. Cell Biol. *12*, 467–474.

Pastan, I.H., and Willingham, M.C. (1981). Receptor-mediated endocytosis of hormones in cultured cells. Annu. Rev. Physiol. *43*, 239–250.

Pinto, J.T., Suffoletto, B.P., Berzin, T.M., Qiao, C.H., Lin, S., Tong, W.P., May, F., Mukherjee, B., and Heston, W.D. (1996). Prostate-specific membrane antigen: a novel folate hydrolase in human prostatic carcinoma cells. Clin. Cancer Res. *2*, 1445–1451.

Pond, L., Kuhn, L.A., Teyton, L., Schutze, M.P., Tainer, J.A., Jackson, M.R., and Peterson, P.A. (1995). A role for acidic residues in di-leucine motif-based targeting to the endocytic pathway. J. Biol. Chem. *270*, 19989–19997.

Rajasekaran, A.K., Humphrey, J.S., Wagner, M., Miesenbock, G., Le Bivic, A., Bonifacino, J.S., and Rodriguez-Boulan, E. (1994). TGN38 recycles basolaterally in polarized Madin-Darby canine kidney cells. Mol. Biol. Cell *5*, 1093–1103.

Rinker-Schaeffer, C.W., Hawkins, A.L., Su, S.L., Israeli, R.S., Griffin, C.A., Isaacs, J.T., and Heston, W.D. (1995). Localization and physical mapping of the prostate-specific membrane antigen (PSM) gene to human chromosome 11. Genomics *30*, 105–108.

Rubin, L.A., Kurman, C.C., Biddison, W.E., Goldman, N.D., and Nelson, D.L. (1985). A monoclonal antibody 7G7/B6, binds to an epitope on the human interleukin-2 (IL-2) receptor that is distinct from that recognized by IL-2 or anti-Tac. Hybridoma *4*, 91–102.

Sandoval, I.V., and Bakke, O. (1994). Targeting of membrane proteins to endosomes and lysosomes. Trends Cell Biol. *4*, 292–297.

Sandoval, I.V., Martinez-Arca, S., Valdueza, J., Palacios, S., and Holman, G.D. (2000). Distinct reading of different structural determinants modulates the dileucine-mediated transport steps of the lysosomal membrane protein LIMPII and the insulin-sensitive glucose transporter GLUT4. J. Biol. Chem. *275*, 39874–39885.

Sekiguchi, M., Okamoto, K., and Sakai, Y. (1989). Release of endogenous N-acetylaspartylglutamate (NAAG) and uptake of [3H]NAAG in guinea pig cerebellar slices. Brain Res. *482*, 78–86.

Sheikh, H., and Isacke, C.M. (1996). A di-hydrophobic Leu-Val motif regulates the basolateral localization of CD44 in polarized Madin-Darby canine kidney epithelial cells. J. Biol. Chem. *271*, 12185–12190.

Silver, D.A., Pellicer, I., Fair, W.R., Heston, W.D., and Cordon-Cardo, C. (1997). Prostate-specific membrane antigen expression in normal and malignant human tissues. Clin. Cancer Res. *3*, 81–85.

Slusher, B.S., *et al*. (1999). Selective inhibition of NAALADase, which converts NAAG to glutamate, reduces ischemic brain injury. Nat. Med. *5*, 1396–1402.

Smith-Jones, P.M., Vallabhajosula, S., Navarro, V., Bastidas, D., Goldsmith, S.J., and Bander, N.H. (2003). Radiolabeled monoclonal antibodies specific to the extracellular domain of prostate-specific membrane antigen: preclinical studies in nude mice bearing LNCaP human prostate tumor. J. Nucl. Med. *44*, 610–617.

Speno, H.S., Luthi-Carter, R., Macias, W.L., Valentine, S.L., Joshi, A.R., and Coyle, J.T. (1999). Site-directed mutagenesis of predicted active site residues in glutamate carboxypeptidase II. Mol. Pharmacol. *55*, 179–185.

Trowbridge, I.S., Collawn, J.F., and Hopkins, C.R. (1993). Signal-dependent membrane protein trafficking in the endocytic pathway. Annu. Rev. Cell Biol. *9*, 129–161.

van der Bliek, A.M., Redelmeier, T.E., Damke, H., Tisdale, E.J., Meyerowitz, E.M., and Schmid, S.L. (1993). Mutations in human dynamin block an intermediate stage in coated vesicle formation. J. Cell Biol. *122*, 553–563.

von Heijne, G. (1988). Transcending the impenetrable: how proteins come to terms with membranes. Biochim. Biophys. Acta *947*, 307–333.

Wright, G.L., Jr., Grob, B.M., Haley, C., Grossman, K., Newhall, K., Petrylak, D., Troyer, J., Konchuba, A., Schellhammer, P.F., and Moriarty, R. (1996). Upregulation of prostate-specific membrane antigen after androgen-deprivation therapy. Urology *48*, 326–334.

Minireview

Biological impediments to monoclonal antibody–based cancer immunotherapy

Jason Christiansen and Ayyappan K. Rajasekaran

Department of Pathology and Laboratory Medicine, David Geffen School of Medicine, University of California, Los Angeles, California

Abstract

The ability of antibodies to exploit antigenic differences between normal and malignant tissues and to exact a variety of antitumor responses offers significant advantages to conventional forms of therapy. Several monoclonal antibodies (mAb) have already proved to be relatively well tolerated and effective for the treatment of many different malignant diseases. However, mAbs must overcome substantial obstacles to reach antigens presented on target cells to be of therapeutic value. Intravenously administered antibodies must avoid host immune response and contend with low or heterogeneous expression of antigen on tumor cells. Antibodies must also overcome significant physical barriers en route to a solid tumor mass, including the vascular endothelium, stromal barriers, high interstitial pressure, and epithelial barriers. Here we review the application and evolution of mAbs as effective forms of treatment, with particular attention to the barriers and impediments to successful treatment and discuss strategies to overcome these barriers and improve the efficacy of mAb-based therapy. [Mol Cancer Ther 2004;3(11): 1493–501]

Introduction

Nearly a century ago, Paul Ehrlich first espoused the concept of ''magic bullets'' for the treatment of disease. By exploiting inherent differences between healthy and diseased cells, therapeutic agents could be designed to specifically target diseased cells while leaving healthy cells unperturbed. While traditional therapeutic modalities, such as chemotoxic drugs or ionizing radiation, are very effective at killing tumor cells, they often fail to adequately discriminate between normal and malignant tissues. Thus, these treatments exact a heavy toll on the patient and can severely limit the dose or duration of treatment to suboptimal levels, resulting in poor outcomes for the management of disease, quality of life, and overall survival. Clearly, elucidating novel therapeutic strategies to target cytotoxicity exclusively to malignant cells would greatly reduce deleterious side effects to normal tissues, enhance the tolerance of the patient to therapy, and result in more effective treatment.

Recent years have seen the emergence of several therapeutic strategies involving monoclonal antibodies (mAb) or related antibody fragments for the treatment of malignancy (1–4). mAbs can be developed with high specificity for antigens expressed on tumor cells and can exact a variety of antitumor responses, thus, the use of mAbs as an alternative or augmentation to therapy offers significant advantages over traditional forms of cancer treatment. While such mAb-based therapies offer a high potential to fulfill the promise of ''magic bullets'' for the treatment of malignant disease, successful application of these therapies is often hindered by several impediments. Factors inhibiting the therapeutic benefit of mAbs may include low or heterogeneous expression of target antigens by tumor cells, high background expression of antigen on normal cells, host antibody immune responses to the mAbs themselves, insufficient antitumor response after mAb binding, as well as physical obstructions preventing antibody binding, including endothelial, interstitial, and epithelial barriers. This review will focus on the successful application of mAbs as a modality of cancer treatment and will address the barriers and impediments associated with inefficient delivery of mAbs to target cells. We also examine strategies to overcome these obstacles and how the thoughtful and systematic approach to therapeutic design can improve the efficacy of mAb-based treatment of cancer. This review will also provide examples to illustrate key points, and will pay particular attention to prostate specific membrane antigen (PSMA) as a prototypical target for mAb-based therapy.

Tumor-Associated Antigens

By their very nature, antibodies are extremely selective and can exact a cytotoxic effect on target cells. The capacity of the immune system to recognize malignant cells and defend against cancer has long been appreciated. Over 50 years ago, Pressman and Korngold (5) showed that antibodies could be used to differentiate between normal and

Received 1/6/04; revised 3/29/04; accepted 5/5/04.

Grant support: Department of Defense grant DAMD17-02-1-0661 and NIH grant DK56216.

The costs of publication of this article were defrayed in part by the payment of page charges. This article must therefore be hereby marked advertisement in accordance with 18 U.S.C. Section 1734 solely to indicate this fact.

Requests for reprints: Ayyappan K. Rajasekaran, Department of Pathology and Laboratory Medicine, Room 13-344 CHS, University of California, Los Angeles, 10833 Le Conte Avenue, Los Angeles, CA 90095. Phone: 310-825-1199; Fax: 310-267-2410. E-mail: arajasekaran@mednet.ucla.edu

malignant tissues. Subsequent work by Burnet (6) in the 1960s showed that the immune system could distinguish between normal and malignant cells and that only when lymphocytes lost this capacity would neoplasms actually form. These abilities to target malignant cells and affect an antitumor response form the underlying basis for modern mAb-based cancer therapy.

While tumor cells are ultimately derived from normal progenitor cells, transformation to a malignant phenotype is often accompanied by changes in antigenicity. Expression of tumor-associated antigens (TAA) can arise due to a multiplicity of mechanisms, including alterations in glycosylation patterns (7), expression of virally encoded genes (8), chromosomal translocations (9), or overexpression of cellular oncogenes (10, 11). Hence, the first challenge confronting the development of an effective mAb-based therapeutic strategy is the identification of a suitable TAA with sufficient tumor specificity that is amenable to antibody binding on the surface of target cells.

PSMA is a transmembrane protein expressed primarily on the plasma membrane of prostatic epithelial cells (12). In addition to normal expression within the benign prostatic epithelium, PSMA levels are elevated in virtually all cases of prostatic adenocarcinoma, with highest levels of expression observed in high-grade cancers, metastatic disease, and androgen-independent tumors (12–15). The membrane-associated character and correlation between expression levels and disease grade have enabled PSMA to become an important biomarker for prostate cancer, and antibodies to PSMA are currently being developed for the diagnosis and imaging of recurrent and metastatic prostate cancer as well as for the therapeutic management of malignant disease (15–18).

Members of the epidermal growth factor (EGF) family of receptor tyrosine kinases, in particular HER-2 and epidermal growth factor receptor (EGF-R), also offer attractive targets for therapeutic mAbs. Antibodies to HER-2 are already being used within the clinic for the management of metastatic breast cancer (19, 20). The *HER-2* gene is highly overexpressed in approximately 25% to 30% of invasive breast carcinomas (10, 11), and in comparison to normal breast epithelial cells, tumor cells may have up to a 100-fold greater expression of HER-2 (10). Closely related to HER-2, EGF-R is overexpressed in many forms of cancer and, like HER-2, EGF-R is believed to play a significant role in cancer progression (21, 22). Clinical trials are currently ongoing to assess the usefulness of this protein as a target for immunotherapy (21, 23).

B- and T-cell surface antigens are also useful targets for the treatment of malignancy. Many of these antigens, such as CD20, CD22, CD25, CD33, or CD52 are expressed only on a particular lineage of hematopoietic cells (3, 4). These antigens are also expressed at high levels on the surface of various populations of malignant cells, but not on normal tissues or hematopoetic progenitor cells. Therefore, mAbs to these proteins can be used to target both benign mature cells and tumor cells for destruction, while leaving a population of progenitor cells to re-establish normal hematopoetic cell lines (3, 4).

In order for an antigen to be of value for therapy, it must be expressed at sufficiently elevated levels on tumor cells relative to indispensable, normal cells. Inadequate ratios of TAA expression on tumor cells relative to normal cells may severely increase toxicity to the patient and hamper effective treatment. One strategy used to alleviate the problem of low ratios of antigen expression on tumor cells relative to normal cells involves treatment with cytokines, such as interferon α or β. Such treatment has been used to increase expression in tumor cells, while having minimal effect on normal cells (24–26).

Avoiding Clearance of Therapeutic Antibodies

Although differences in antigenicity between normal and malignant cells have long been appreciated, the administration of exogenous antibodies for therapeutic benefit did not begin in earnest until the advent of hybridoma technology by Kohler and Milstein (27) in the 1970s. This technology enabled the large-scale preparation of clonal antibodies raised against a specific antigen to be produced in quantities sufficient to be of clinical value (Fig. 1A). Early endeavors using mouse mAbs to combat malignancy met

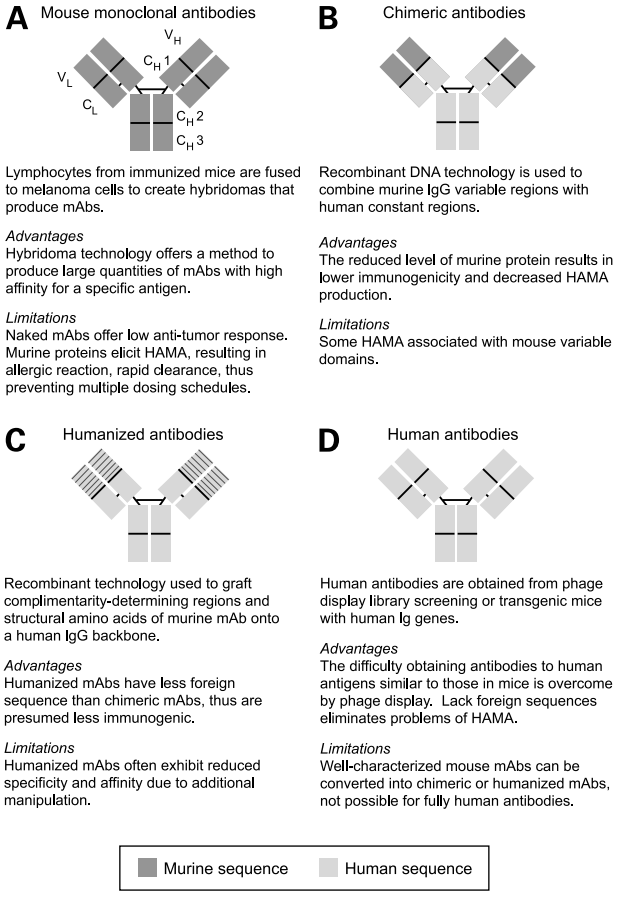

Figure 1. Diagram of the various forms of therapeutic monoclonal antibodies. Mouse monoclonal antibodies (**A**), chimeric antibodies (**B**), humanized antibodies (**C**), and human antibodies (**D**) have been developed and offer differing advantages and limitations.

with some modest degrees of success. Patients receiving doses of mAb experienced very little toxicity, with adverse effects primarily limited to mild allergic reactions. Initial trials also indicated antitumor responses experienced by a fraction of patients, including those refractory to other forms of therapy. Reports of the first full clinical remission in a B-cell lymphoma patient treated with an anti-idiotype mAb further bolstered prospect of using mAbs as an effective treatment for cancer (28).

While many viewed these initial advances as a harbinger of future success, early trials using murine mAbs were plagued by problems resulting in rapid clearance of antibody from the system (29, 30). Typically, i.v. administered murine mAbs exhibited very short half-lives within the serum, generally in the range of 18 to 48 hours (1, 31, 32). This situation was primarily ascribed to the antigenicity associated with the injection of murine antibodies, which tended to elicit the production of a human anti-mouse antibody (HAMA) immune response (30).

Fortunately, advances in molecular biology and genetic engineering have evolved to allay the problems associated with human anti-mouse antibody. Recombinant DNA technology has enabled the creation of less antigenic forms of mAbs, with the majority of the murine immunoglobulin amino acid sequences replaced with those of human proteins. Chimeric antibodies containing only the murine immunoglobulin variable regions fused to human constant domains (33, 34) and humanized mAbs, in which only the actual antigen binding regions of the mouse antibody remain (35), are far less antigenic than mouse mAbs and exhibit longer half-lives within the serum (Fig. 2B and C). The subsequent development of new technologies using phage display libraries (36) or transgenic mice expressing human immunoglobulin genes (37–39) have now enabled the creation of human antibodies (Fig. 2D).

In addition to human anti-mouse antibody, excess antigen within the circulation may also result in rapid clearance of therapeutic mAbs (40). This presence of circulating antigen may be ascribed to a high proportion of TAA expressing normal cells within the vasculature. Alternatively, excess TAA within the circulation may be due to antigen shedding from the cell surface or the presence of secreted isoforms of the TAA. The existence of excess antigen in the serum would sequester i.v. administered mAbs and result in inefficient delivery to tumor cells (40). Ideally, a TAA would be selected that does not undergo shedding or exist in a secreted form; however, administration of multiple doses of mAb can reduce the impact of high TAA within the circulation by effectively pre-clearing the antigen from the system.

Treatment of Hematological Malignancies

Following i.v. injection and distribution throughout the vascular space, therapeutic antibodies must access their target antigens on the surface of malignant cells. With few barriers present to impede mAb binding, hematologic malignancies are well suited to mAb-based therapy. In recent years, several promising mAb-based therapies for the treatment of hematologic malignancies have been developed that have received Food and Drug Administration approval or are in advanced phases of clinical testing (1, 3, 4). The chimeric antibody, rituxan (rituximab, Genentech, San Francisco, CA) was among the first mAbs awarded Food and Drug Administration approval for the treatment of non-Hodgkin's lymphoma (41). This chimeric antibody binds CD20, a cell surface antigen expressed on mature B lymphocytes and over 90% of non-Hodgkin's lymphoma cells, but not on hematopoetic progenitor or stem cells. Rituxan has proved to be well tolerated and effective in the treatment non-Hodgkin's lymphoma by itself or in combination with traditional chemotherapy, particularly in patients refractory to other types of therapy (42).

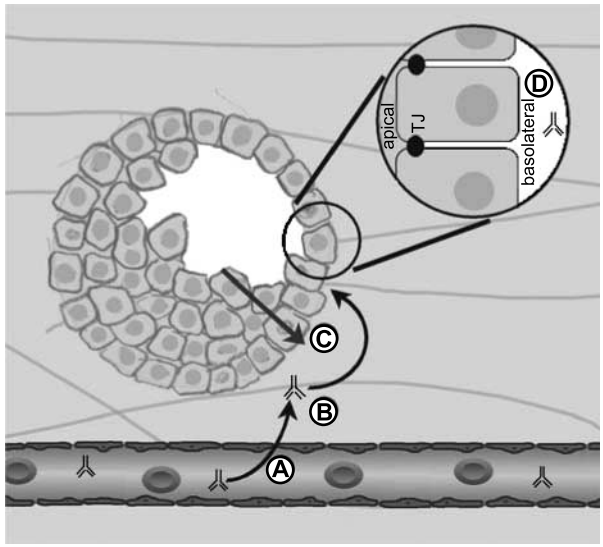

Figure 2. Schematic overview of biological barriers to effective treatment of solid tumors with mAb-based immunotherapy. To reach a target antigen at the surface of a solid tumor, i.v. injected monoclonal antibody must first traverse the microvascular endothelium (**A**), and must subsequently contend with stromal barriers (**B**), and high interstitial fluid pressure characteristic of bulky tumor masses (**C**). Monoclonal antibodies may also confront epithelial barriers (**D**), including E-cadherin and tight junctional complexes that may have a profound impact on therapy.

Campath-1 (alemtuzumab, Ilex Oncology, San Antonio, TX) has also received Food and Drug Administration approval for the treatment of patients suffering from chronic lymphocytic leukemia. This humanized mAb recognizes the CD52 antigen present on normal B and T lymphocytes, monocytes, and macrophages, as well as most B- and T-cell lymphomas (43). Campath-1 has shown significant and durable effects in the treatment in patients with previously treated, recurrent, indolent chronic lymphocytic leukemia. A 42% overall response rate was achieved among 29 patients in one phase III study (44). Other encouraging results have demonstrated the efficacy of campath-1 for patients suffering from fludarabine refractory disease (45), and a 73% response rate observed among a limited number of patients with prolymphocytic leukemia (46).

A third mAb to receive Food and Drug Administration approval for the treatment of hematologic malignancies is

the chimeric mAb, mylotarg (gemtuzumab ozogamicin, Wyeth-Ayerst Laboratories, Philadelphia, PA). This antibody targets the CD33 antigen expressed on myeloid precursors and leukemic blast cells, but like other targets for the treatment of hematologic malignancies, this antigen is absent from normal tissues and pluripotent hematopoetic stem cells (47, 48). Mylotarg has shown promise in the treatment of acute myelogenous leukemia (AML) (49, 50). In addition to rituxan, campath, and mylotarg, several other therapeutic mAbs have been developed and are in various phases of testing, including daclizumab (Zenapax, Hoffmann-LaRoche, Nutley, NJ), a humanized mAb directed against CD25, epratuzumab (LymphoCide, Immunomedics, Morris Plains, NJ), a humanized antibody to CD22.

Treatment of Solid Tumors

In comparison to the management of hematologic malignancies, successful treatment of solid tumors with mAbs has proved more elusive; however, some significant therapeutic benefits have been achieved. Herceptin (trastuzumab, Genentech) is a humanized antibody that has received Food and Drug Administration approval for the treatment of metastatic breast cancer. This mAb recognizes an extracellular epitope of the HER-2 protein. Clinical trials with herceptin have shown it to be well tolerated both as a single agent for second or third line therapy, or in combination with chemotherapeutic agents as a first line of therapy. Combination therapy resulted in a 25% improvement of overall survival in patients with HER-2–overexpressing tumors that are refractory to other forms of treatment (19, 20, 51).

The anti-epithelial cellular adhesion molecule mAb, Panorex (eclrecolomab, GlaxoSmith-Kline, United Kingdom), is another mAb-based therapy that is currently being used for the treatment of colorectal cancer. Panorex has shown tangible benefit for cancer patients and has received approval in Germany for the treatment of Dukes' stage C colorectal cancer (52, 53). Like other mAbs used for the treatment of solid tumors, Panorex has proved more efficacious in the treatment of micormetastatic lesions and minimal residual disease in comparison to bulky tumor masses (52–54).

The failure of mAbs in the treatment of bulky lesions is primarily attributable to the low level of injected mAb that actually reaches its target within a sizable solid tumor mass. Studies using radiolabeled mAbs suggested that only a very small percentage of the original injected antibody dose, approximately 0.01% to 0.1% per gram of tumor tissue, will ever reach target antigens within a solid tumor (55–57). This low level of binding is due to the series of barriers confronted by an i.v. administered mAb en route to TAAs expressed on the surface of tumor cells. These obstacles include the endothelial barrier, interstitial pressure, and stromal impediments, as well as epithelial barriers (Fig. 2). Study into the nature of these impediments has led to increased appreciation for the significance of these barriers and has led to several novel approaches designed to circumvent them.

Endothelial Barriers

The microvascular endothelium is lined with endothelial cells, the junctional contacts of which are designed to inhibit passage of macromolecules and cells. To reach antigens expressed on the surface of cells in a solid tumor mass, an i.v. administered mAb must first traverse this formidable barrier. Intratumoral injection is one strategy by which to bypass the endothelium and other physical barriers. Direct intratumoral injection results in increased levels and duration of therapeutic antibodies near the tumor mass with low levels of side effects associated with systemic i.v. injection (58, 59).

Strategies to enhance vascular permeability have been proposed as a method to mitigate the obstructive influence of the microvascular wall and have shown an ability to enhance mAb uptake into solid tumor masses. Pretreatment of patients suffering from extremity localized soft tissue sarcomas and melanomas with the pro-inflammatory cytokine, tumor necrosis factor-α, resulted in an increased perfusion of chemotherapeutic agents into tumors that was associated with improvements in overall tumor response rates (1, 60–63). Unfortunately, systemic administration of tumor necrosis factor-α or other vasoactive agents is severely limited by toxicity, as an adequate dose to increase vascular permeability around a tumor mass is typically 10 to 50 times higher than the maximum dose tolerated by a patient (63, 64). Thus, developing mechanisms to enhance vascular permeability only at sites proximal to a tumor mass would be of great benefit to circumvent this problem.

Intratumoral injection of tumor necrosis factor is capable of increasing the local vascular permeability and improving penetration of therapeutic mAbs in a mouse tumor xenograft model (65). However, such treatment would rarely be a viable clinical option for the treatment of malignancy, because intratumoral injections would be restricted to sites of known, sizable tumor masses. Therefore, mAbs have the potential to fulfill an additional role in cancer treatment to serve as carriers for the delivery of pharmacologic agents to the tumor-associated neovasculature.

Comparable strategies have shown promise to improve the efficacy of mAb therapy. Pretreatment with interleukin-2 (IL-2) conjugated to the TNT-1 mAb directed against the necrotic cells within a solid tumor xenograft resulted in a 3.5-fold enhancement in uptake of a tumor specific radiolabeled mAb without any evidence of toxicity or increase in absorbed dose to normal tissues (55, 66–68). Similar results were obtained using immunoconjugates of other vasoactive agents, including recombinant interleukin-1β (IL-1β), physalaemin, histamine, bradykinin, and leukotriene B4 (55). Furthermore, targeted delivery of tumor necrosis factor-α conjugated to the CNGRC peptide of aminopeptidase N (CD13), which targets tumor neovasculature, resulted in an 8- to 10-fold potentiation in the activity of doxyrubicin in mouse lymphoma and melanoma models without a significant increase in overall toxicity (64, 69).

In addition to the benign and malignant prostatic epithelium, PSMA is also expressed on the neovasculature associated with a variety of solid tumors, but not in the

normal endothelium (70, 71). By conjugating vasoactive agents to mAbs raised against PSMA, a localized increase in vascular permeability could be achieved exclusively at sites proximal to tumors. Using such a treatment before the administration of therapeutic agents, including antibodies, would substantially enhance the dose received by the tumor.

In addition to enhancing vascular permeability, additional approaches have attempted to exploit intracellular transport pathways as an alternative means by which to bypass the endothelial barrier. McIntosh et al. (72) have used mAbs against antigens found within caveolae of the lung microvasculature to achieve selective and efficient drug delivery to underlying lung tissue.

Stromal Barriers

After extravasation across the microvascular wall, a therapeutic mAb must still contend with substantial stromal and interstitial barriers that may result in poor and heterogeneous perfusion throughout a bulky tumor mass. Tumor shape and structure is an important factor influencing mAb uptake, because three-dimensional histocultures, tumor xenografts, and spheroids require longer to reach a steady state concerning protein-bound drug or mAb perfusion, relative to cells in monolayer cultures (73). Tissue composition may also influence mAb uptake, because skeletal muscles serve as restrictive barriers to drug distribution, causing poor perfusion into muscular organs such as the tongue or prostate. The distribution of drugs into these organs is highly heterogeneous, with perfusion limited to areas bordering fibromuscular tissue, and excluded from muscle (73).

An antibody must also contend with the excessive interstitial fluid pressure associated with the high cell density of a sizable tumor mass (74). In studies using spheroids to measure penetration of protein bound drugs, these drugs were primarily restricted to the periphery (73, 75, 76). Thus, high tumor cell density is a major barrier to distribution of maromolecular compounds within solid tumors, and restricts the use of mAb therapy to small volume disease. Reduction of cell density can significantly reduce interstitial fluid pressure, and improve uptake of mAbs and other proteinaceous drugs into the center of tumors (73). Treatment of mice implanted with tumor xenografts with several doses of tumor necrosis factor-α was shown to lower interstitial pressure and improve mAb perfusion by promoting apoptosis of tumor cells (73). Thus, pursuing a treatment regimen that combines several doses of a pro-apoptotic substance with administration of therapeutic mAbs can greatly reduce the interstitial fluid pressure within a tumor and show a synergistic effect compared with a single treatment of pro-apoptotic agents alone.

Epithelial Barriers

Epithelial cells are linked together by specialized junctional complexes that provide strong adhesive forces and between neighboring cells and restrict the diffusion of molecules through intercellular spaces. While over 90% of all cancers are carcinomas derived from epithelial tissues, the significance of these barriers is often disregarded in the treatment of malignant disease. However, these physical barriers may exert a profound impact on the efficacy of mAb therapy.

E-cadherin is one of the principal components of the adherens junctions and is of particular relevance to the mAb-based treatment of solid tumors. E-cadherin is a transmembrane protein that mediates adhesion between adjacent cells through a calcium-dependent homophilic interaction (77). These interactions are important for the aggregation of cells and can promote resistance to numerous forms of cancer therapy, including those involving mAbs (78, 79). Adhesion and aggregation among the cells of a solid tumor mass can significantly limit perfusion of therapeutic mAbs and inhibit the penetration of immune effector cells. Disruption of cell-cell adhesion using mAbs to the extracellular domain of E-cadherin can interfere with spheroid formation, and disrupt aggregation of tumor cells expressing E-cadherin (80). Furthermore, use of these anti-E-cadherin mAbs in a murine model was shown to disrupt the structure of tumor xenografts and promote overall survival (81).

Disruption of E-cadherin–mediated cellular adhesion can also be achieved through depletion of extracellular calcium. Administration of the calcium chelator, EDTA, can inhibit interactions between epithelial cells and promote the absorption and penetration of molecules through epithelial tissues (82-84). Furthermore, intratumoral injection of EDTA was showed to enhance the accumulation of the drug cisplatin within tumor xenografts and resulted in a complete cure in four of eight rats, and a substantial reduction in tumor volume for the remaining four rats. In contrast, injection of either EDTA or cisplatin alone had no substantial effect on tumor volume or overall survival (85).

Although targeted disruption of E-cadherin is a potentially valuable strategy to improve the efficacy of mAb-based therapy, it is important to note that E-cadherin is a critical component of normal epithelial tissues and is often down-regulated or absent in many forms of cancer (86, 87). Therefore, it would not be possible to systemically disrupt E-cadherin interaction through i.v. administration of blocking antibodies or other pharmacologic agents. Alternative methods may need to be devised, such that target E-cadherin functions specifically at the sites of tumor cell aggregates. Additional strategies may also include targeting other cellular adhesion molecules, such as N- or P-cadherin, which is typically up-regulated in a variety of cancers (88, 89).

In addition to the adhesive influence of homophilic E-cadherin binding, other complexes, such as the tight junctions, serve to link epithelial cells strongly together. These junctions form regions of close membrane apposition between adjacent cells and physically separate the apical plasma membrane from the basolateral and prevent both the lateral diffusion of proteins and lipids between plasma membrane domains and restrict the flow of proteins, ions, or other solutes through intercellular spaces (46). The basolateral plasma membrane is in contact with adjacent cells and the extracellular basement membrane, and is

relatively accessible to the solutes within the underlying vasculature. However, because the tight junctions restrict the flow of fluids between cells, i.v. administered agents, such as mAbs, would have very limited access to antigens on the apical plasma membrane. This situation could have a major impact on mAb-based therapy for solid tumors.

Transformation to a malignant phenotype is commonly associated with a down-regulation of E-cadherin expression and a general loss in epithelial polarity and tight junction integrity (86). Following loss of polarity, antigens normally restricted to a particular plasma membrane domain become distributed in a non-polarized fashion throughout the entire surface of the cell. Thus, while administration of mAbs directed against an antigen normally localized to the apical surface would not be readily accessible to normal epithelial cells, these mAbs may be able to preferentially target transformed cells that have lost their polarized phenotype. For instance, the carcinoembryonic antigen (CEA), which is expressed in both normal and malignant cells of the colonic epithelium, is restricted to the apical surface of normal tissues and well-differentiated tumors (90). However, following loss of tight junction integrity in poorly differentiated tumors, CEA is observed in a non-polarized fashion throughout all plasma membrane surfaces (90, 91). The appearance of CEA on the basolateral surface is associated with elevated levels of CEA within the circulation. This elevated level of circulating antigen is presumably due to the increased access of the basolateral surface to the underlying stroma and vasculature (92). This increased expression of CEA on the basolateral surface would also improve accessibility to circulating mAbs, and would explain why immunoscintigraphic studies using i.v. injected mAbs to CEA are able to specifically label primary and metastatic tumors, but not normal or well-differentiated tissues (93, 94).

It is also important to note that while many cells lose polarity as they progress to a malignant phenotype, many tumor cells may retain polarity and have well-differentiated phenotype, even after metastasis to distal sites. Furthermore, tumors are heterogeneous accumulations of cells that are in various stages of differentiation. Thus, while a therapeutic mAb directed against an apical marker may be efficient in targeting undifferentiated cells lacking E-cadherin and tight junctions, populations of well-differentiated tumor or pre-malignant cells may be considerably more resistant to this form of therapy. Such populations of cells may serve as an inoculum, providing a source of cells at various stages of malignancy to repopulate and metastasize to distal sites.

Developing a comprehensive understanding and appreciation for the expression patterns of an antigen within a tumor cell, or the degree of polarization exhibited by a particular population of tumor cells may have a strong prognostic significance and a critical impact on the effectiveness of treatment. A careful screening of tumor biopsies may help to identify those patients who are more likely to respond favorably to a particular mAb-based therapy. For example, the efficacy of treatment of prostate carcinoma with mAbs to PSMA may be highly dependent on the status of the tumor and expression of the antigen. Prostate carcinoma cells often retain high degrees of polarity and tight junction integrity, and PSMA is expressed predominantly on the apical plasma membrane in most normal and malignant tissues (95). However, *in situ* immunofluorescence revealed that PSMA was also present on the basolateral membrane, with increased accessibility to the vasculature (95). Screening for those patients with tumors that display a non-polarized distribution of PSMA or a general loss of epithelial polarity may identify those who are most likely to respond favorably to such treatment.

Eliciting a Response

After successfully negotiating the gauntlet of obstacles obstructing access to the target cells within a tumor, a therapeutic mAb must still be capable of eliciting a potent antitumor response. Although it is often ambiguous as to the exact mechanisms by which a particular mAb may mediate an antitumor response, both direct and indirect mechanisms can potentially be involved.

Antibodies of the IgG1 and IgG3 isotypes can support effector functions of both antibody dependent cell-mediated cytotoxicity and complement dependent cytotoxicity (96). Antibody dependent cell-mediated cytotoxicity is triggered by interaction between the Fc region of a cell-bound antibody and Fcγ receptors on immune effector cells such as neutrophils, macrophages, and natural killer cells. This mechanism is critical for the antitumor effects of several therapeutic mAbs, including rituxumab, because mice with normal Fcγ receptors exhibit antitumor effects following mAb treatment, while mice lacking Fcγ RI and III do not (96, 97).

Many early studies showed that murine mAbs had limited potential to elicit a potent antitumor response, because the murine Fc regions are less efficient at recruiting human effector cells than their human counterparts. This problem has been largely allayed by the use of chimeric and humanized antibodies. Genetic engineering techniques have also been used to improve the immunologic effects of therapeutic mAbs by altering antibody shape and size, increasing the valency of mAbs, and creating bifunctional antibodies with two antigenic receptors, one to a tumor antigen and another to an effector cell to increase efficiency of antibody dependent cell-mediated cytotoxicity (98, 99).

Stimulation of the immune system may also substantially improve effector functions in response to mAb therapy. Sequences of unmethylated bacterial DNA can act as a potent stimulators of immune response (96, 100, 101), and can synergistically enhance the effect of therapeutic mAbs by sensitizing malignant cells to antibody dependent cell-mediated cytotoxicity (102). Furthermore, different oligonucleotide sequences were shown to illicit different immune responses, suggesting that mAbs are capable of inducing antitumor effects by a variety of mechanisms.

In addition to immunologic effects, mAbs can induce antitumor effects by a variety of direct mechanisms, including the induction of apoptosis (103, 104), or the prevention of soluble growth factors from binding their

cognate receptors, such as EGF-R (23) and HER-2 (105, 106). Additionally, mAbs can also be engineered to deliver a cytotoxic agent directly to the tumor. This offers the potential to combine the biological effects of mAbs with the additional effect of a targeted cytotoxic response. The anti-CD33 mAb, mylotarg, is one such antibody. Combined with the cytotoxic agent, calichaemicin, mylotarg has been reported to be relatively well tolerated, and effective in the treatment of chronic lymphocytic leukemia (107). Antibodies can also be engineered to deliver ionizing radiation directly to tumor cells. mAbs to the extracellular domain of PSMA have been conjugated to both α- and β-particle emitting radionuclides, and have shown promise in the treatment of xenograft-bearing mice (16–18, 108). Clinical trials in humans also portend the promise of radiolabeled mAbs for the treatment of cancer. In a recent phase III randomized study, patients with relapsed or refractory low-grade non-Hodgkin's lymphoma were treated with a yttrium-90 and an iodine-131–labeled mAb to CD20 (ibrituximomab tiuxetan and tositumomab, respectively). Patients treated with these radiolabeled mAbs showed a statistically significant increase in overall response compared with those treated with an unlabeled version of the mAb (rituximab) (109).

Conclusion

The remarkable specificity and ability to affect an antitumor response indicate that mAbs offer great promise to fulfill the role of ''magic bullets'' in the treatment of malignancy. These agents have already become an important clinical modality in the treatment of many forms of hematologic malignancies, and some solid tumors, as well. The successes to date are a likely a mere prelude to future application of mAbs to cancer therapy. Unfortunately, the successful application of mAbs to therapy is largely inhibited by a series of formidable obstacles that prevent antibodies from reaching their target antigens on the cell surface. Hopefully, a greater appreciation of these barriers will be developed and systemic approaches to overcome these barriers will lead to improved efficacy.

Acknowledgments

We thank Dr. Neil H. Bander for his critical reading of the manuscript.

References

1. Glennie MJ, Johnson PW. Clinical trials of antibody therapy. Immunol Today 2000;21:403 – 10.

2. Von Mehren M, Adams GP, Weiner LM. Monoclonal antibody therapy for cancer. Annu Rev Med 2003;54:343 – 69.

3. Dillman RO. Monoclonal antibody therapy for lymphoma: an update. Cancer Pract 2001;9:71 – 80.

4. Countouriotis A, Moore TB, Sakamoto KM. Cell surface antigen and molecular targeting in the treatment of hematologic malignancies. Stem Cells 2002;20:215 – 29.

5. Pressman D, Korngold L. The *in vivo* localization of anti-Wagner-osteogenic-sarcoma antibodies. Cancer 1953;6:619-23.

6. Burnet FM. Immunological aspects of malignant disease. Lancet 1967; 1:1171 – 4.

7. Krzeslak A, Pomorski L, Gaj Z, Lipinska A. Differences in glycosylation of intracellular proteins between benign and malignant thyroid neoplasms. Cancer Lett 2003;196:101 – 7.

8. Mehl AM, Fischer N, Rowe M, et al. Isolation and analysis of two strongly transforming isoforms of the Epstein-Barr-Virus (EBV) – encoded latent membrane protein-1 (LMP1) from a single Hodgkin's lymphoma. Int J Cancer 1998;76:194 – 200.

9. Clark SS, McLaughlin J, Timmons M, et al. Expression of a distinctive BCR-ABL oncogene in Ph1-positive acute lymphocytic leukemia (ALL). Science 1988;239:775 – 7.

10. Slamon DJ, Godolphin W, Jones LA, et al. Studies of the HER-2/neu proto-oncogene in human breast and ovarian cancer. Science 1989;244: 707 – 12.

11. Slamon DJ, Clark GM, Wong SG, Levin WJ, Ullrich A, McGuire WL. Human breast cancer: correlation of relapse and survival with amplification of the HER-2/neu oncogene. Science 1987;235:177 – 82.

12. Silver DA, Pellicer I, Fair WR, Heston WD, Cordon-Cardo C. Prostate-specific membrane antigen expression in normal and malignant human tissues. Clin Cancer Res 1997;3:81 – 5.

13. Sweat SD, Pacelli A, Murphy GP, Bostwick DG. Prostate-specific membrane antigen expression is greatest in prostate adenocarcinoma and lymph node metastases. Urology 1998;52:637 – 40.

14. Wright GL Jr, Grob BM, Haley C, et al. Upregulation of prostate-specific membrane antigen after androgen-deprivation therapy. Urology 1996;48:326 – 34.

15. Murphy GP, Elgamal AA, Su SL, Bostwick DG, Holmes EH. Current evaluation of the tissue localization and diagnostic utility of prostate specific membrane antigen. Cancer 1998;83:2259 – 69.

16. McDevitt MR, Barendswaard E, Ma D, et al. An α-particle emitting antibody ([213Bi]J591) for radioimmunotherapy of prostate cancer. Cancer Res 2000;60:6095 – 100.

17. Bander NH, Nanus DM, Milowsky MI, Kostakoglu L, Vallabahajosula S, Goldsmith SJ. Targeted systemic therapy of prostate cancer with a monoclonal antibody to prostate-specific membrane antigen. Semin Oncol 2003; 30:667 – 76.

18. Smith-Jones PM, Vallabhajosula S, Navarro V, Bastidas D, Goldsmith SJ, Bander NH. Radiolabeled monoclonal antibodies specific to the extracellular domain of prostate-specific membrane antigen: preclinical studies in nude mice bearing LNCaP human prostate tumor. J Nucl Med 2003;44: 610 – 7.

19. Cobleigh MA, Vogel CL, Tripathy D, et al. Multinational study of the efficacy and safety of humanized anti-HER2 monoclonal antibody in women who have HER2-overexpressing metastatic breast cancer that has progressed after chemotherapy for metastatic disease. J Clin Oncol 1999;17: 2639 – 48.

20. Baselga J, Tripathy D, Mendelsohn J, et al. Phase II study of weekly intravenous recombinant humanized anti-p185HER2 monoclonal antibody in patients with HER2/neu-overexpressing metastatic breast cancer. J Clin Oncol 1996;14:737 – 44.

21. Herbst RS, Shin DM. Monoclonal antibodies to target epidermal growth factor receptor – positive tumors: a new paradigm for cancer therapy. Cancer 2002;94:1593 – 611.

22. Salomon DS, Brandt R, Ciardiello F, Normanno N. Epidermal growth factor – related peptides and their receptors in human malignancies. Crit Rev Oncol Hematol 1995;19:183 – 232.

23. Yang XD, Jia XC, Corvalan JR, Wang P, Davis CG, Jakobovits A. Eradication of established tumors by a fully human monoclonal antibody to the epidermal growth factor receptor without concomitant chemotherapy. Cancer Res 1999;59:1236 – 43.

24. Murray JL, Macey DJ, Grant EJ, et al. Enhanced TAG-72 expression and tumor uptake of radiolabeled monoclonal antibody CC49 in metastatic breast cancer patients following α-interferon treatment. Cancer Res 1995; 55:5925s – 8s.

25. Greiner JW, Guadagni F, Goldstein D, et al. Intraperitoneal administration of interferon-γ to carcinoma patients enhances expression of tumor-associated glycoprotein-72 and carcinoembryonic antigen on malignant ascites cells. J Clin Oncol 1992; 10:735 – 46.

26. Macey DJ, Grant EJ, Kasi L, et al. Effect of recombinant α-interferon on pharmacokinetics, biodistribution, toxicity, and efficacy of 131I-labeled monoclonal antibody CC49 in breast cancer: a phase II trial. Clin Cancer Res 1997;3:1547 – 55.

27. Kohler G, Milstein C. Continuous cultures of fused cells secreting antibody of predefined specificity. Nature 1975;256:495 – 7.

28. Miller RA, Maloney DG, Warnke R, Levy R. Treatment of B-cell lymphoma with monoclonal anti-idiotype antibody. N Engl J Med 1982;306: 517 – 22.

29. Sakahara H, Saga T, Onodera H, Yao Z, Nakamoto Y, Zhang M, et al. Anti-murine antibody response to mouse monoclonal antibodies in cancer patients. Jpn J Cancer Res 1997;88:895 – 9.

30. Khazaeli MB, Conry RM, LoBuglio AF. Human immune response to monoclonal antibodies. J Immunother 1994;15:42 – 52.

31. Carter P. Improving the efficacy of antibody-based cancer therapies. Nat Rev Cancer 2001;1:118 – 29.

32. Little M, Kipriyanov SM, Le Gall F, Moldenhauer G. Of mice and men: hybridoma and recombinant antibodies. Immunol Today 2000;21: 364 – 70.

33. Morrison SL, Johnson MJ, Herzenberg LA, Oi VT. Chimeric human antibody molecules: mouse antigen-binding domains with human constant region domains. Proc Natl Acad Sci USA 1984;81:6851 – 5.

34. Boulianne GL, Hozumi N, Shulman MJ. Production of functional chimaeric mouse/human antibody. Nature 1984;312:643 – 6.

35. Jones PT, Dear PH, Foote J, Neuberger MS, Winter G. Replacing the complementarity-determining regions in a human antibody with those from a mouse. Nature 1986;321:522 – 5.

36. Hoogenboom HR, Chames P. Natural and designer binding sites made by phage display technology. Immunol Today 2000;21:371 – 8.

37. Fishwild DM, O'Donnell SL, Bengoechea T, Hudson DV, Harding F, Bernhard SL, et al. High-avidity human IgGκ monoclonal antibodies from a novel strain of minilocus transgenic mice. Nat Biotechnol 1996;14:845 – 51.

38. Mendez MJ, Green LL, Corvalan JR, Jia XC, Maynard-Currie CE, Yang XD, et al. Functional transplant of megabase human immunoglobulin loci recapitulates human antibody response in mice. Nat Genet 1997;15: 146 – 56.

39. Green LL. Antibody engineering via genetic engineering of the mouse: XenoMouse strains are a vehicle for the facile generation of therapeutic human monoclonal antibodies. J Immunol Methods 1999;231:11 – 23.

40. Manshouri T, Do KA, Wang X, Giles FJ, O'Brien SM, Saffer H, et al. Circulating CD20 is detectable in the plasma of patients with chronic lymphocytic leukemia and is of prognostic significance. Blood 2003;101: 2507 – 13.

41. Leget GA, Czuczman MS. Use of rituximab, the new FDA-approved antibody. Curr Opin Oncol 1998;10:548 – 51.

42. McLaughlin P, Grillo-Lopez AJ, Link BK, Levy R, Czuczman MS, Williams ME, et al. Rituximab chimeric anti-CD20 monoclonal antibody therapy for relapsed indolent lymphoma: half of patients respond to a four-dose treatment program. J Clin Oncol 1998;16:2825 – 33.

43. Salisbury JR, Rapson NT, Codd JD, Rogers MV, Nethersell AB. Immunohistochemical analysis of CDw52 antigen expression in non-Hodgkin's lymphomas. J Clin Pathol 1994;47:313 – 7.

44. Dyer MJ. The role of CAMPATH-1 antibodies in the treatment of lymphoid malignancies. Semin Oncol 1999;26:52 – 7.

45. Keating MJ, Flinn I, Jain V, et al. Therapeutic role of alemtuzumab (Campath-1H) in patients who have failed fludarabine: results of a large international study. Blood 2002;99:3554 – 61.

46. Pawson R, Dyer MJ, Barge R, et al. Treatment of T-cell prolymphocytic leukemia with human CD52 antibody. J Clin Oncol 1997;15:2667 – 72.

47. Griffin JD, Linch D, Sabbath K, Larcom P, Schlossman SF. A monoclonal antibody reactive with normal and leukemic human myeloid progenitor cells. Leuk Res 1984;8:521 – 34.

48. Andrews RG, Singer JW, Bernstein ID. Precursors of colony-forming cells in humans can be distinguished from colony-forming cells by expression of the CD33 and CD34 antigens and light scatter properties. J Exp Med 1989;169:1721 – 31.

49. Jurcic JG, DeBlasio T, Dumont L, Yao TJ, Scheinberg DA. Molecular remission induction with retinoic acid and anti-CD33 monoclonal antibody HuM195 in acute promyelocytic leukemia. Clin Cancer Res 2000;6: 372 – 80.

50. Sievers EL, Linenberger M. Mylotarg: antibody-targeted chemotherapy comes of age. Curr Opin Oncol 2001;13:522 – 7.

51. Leyland-Jones B. Trastuzumab: hopes and realities. Lancet Oncol 2002;3:137 – 44.

52. Riethmuller G, Schneider-Gadicke E, Schlimok G, et al. Randomised trial of monoclonal antibody for adjuvant therapy of resected Dukes' C colorectal carcinoma. German Cancer Aid 17-1A Study Group. Lancet 1994;343:1177 – 83.

53. Riethmuller G, Holz E, Schlimok G, et al. Monoclonal antibody therapy for resected Dukes' C colorectal cancer: seven-year outcome of a multicenter randomized trial. J Clin Oncol 1998;16:1788 – 94.

54. Mellstedt H, Frodin JE, Masucci G, et al. The therapeutic use of monoclonal antibodies in colorectal carcinoma. Semin Oncol 1991;18: 462 – 77.

55. Khawli LA, Miller GK, Epstein AL. Effect of seven new vasoactive immunoconjugates on the enhancement of monoclonal antibody uptake in tumors. Cancer 1994;73:824 – 31.

56. Goldenberg DM. Targeting of cancer with radiolabeled antibodies. Prospects for imaging and therapy. Arch Pathol Lab Med 1988; 112:580 – 7.

57. Epenetos AA, Snook D, Durbin H, Johnson PM, Taylor-Papadimitriou J. Limitations of radiolabeled monoclonal antibodies for localization of human neoplasms. Cancer Res 1986;46:3183 – 91.

58. Cooke SP, Pedley RB, Boden R, Begent RH, Chester KA. *In vivo* tumor delivery of a recombinant single chain Fv:tumor necrosis factor-α fusion [correction of factor: a fusion] protein. Bioconjug Chem 2002;13:7 – 15.

59. Azemar M, Djahansouzi S, Jager E, et al. Regression of cutaneous tumor lesions in patients intratumorally injected with a recombinant single-chain antibody-toxin targeted to ErbB2/HER2. Breast Cancer Res Treat 2003;82:155 – 64.

60. Eggermont AM, Schraffordt Koops H, Lienard D, et al. Isolated limb perfusion with high-dose tumor necrosis factor-α in combination with interferon-γ and melphalan for nonresectable extremity soft tissue sarcomas: a multicenter trial. J Clin Oncol 1996;14:2653 – 65.

61. Fraker DL, Alexander HR, Andrich M, Rosenberg SA. Treatment of patients with melanoma of the extremity using hyperthermic isolated limb perfusion with melphalan, tumor necrosis factor, and interferon γ: results of a tumor necrosis factor dose-escalation study. J Clin Oncol 1996;14: 479 – 89.

62. Noorda EM, Vrouenraets BC, Nieweg OE, Van Coevorden F, Van Slooten GW, Kroon BB. Isolated limb perfusion with tumor necrosis factor-α and melphalan for patients with unresectable soft tissue sarcoma of the extremities. Cancer 2003;98:1483 – 90.

63. Lejeune FJ, Ruegg C, Lienard D. Clinical applications of TNF-α in cancer. Curr Opin Immunol 1998;10:573 – 80.

64. Curnis F, Sacchi A, Corti A. Improving chemotherapeutic drug penetration in tumors by vascular targeting and barrier alteration. J Clin Invest 2002;110:475 – 82.

65. Folli S, Pelegrin A, Chalandon Y, Yao X, Buchegger F, Lienard D, et al. Tumor-necrosis factor can enhance radio-antibody uptake in human colon carcinoma xenografts by increasing vascular permeability. Int J Cancer 1993;53:829 – 36.

66. LeBerthon B, Khawli LA, Alauddin M, et al. Enhanced tumor uptake of macromolecules induced by a novel vasoactive interleukin 2 immunoconjugate. Cancer Res 1991;51:2694 – 8.

67. Hennigan TW, Begent RH, Allen-Mersh TG. Histamine, leukotriene C4 and interleukin-2 increase antibody uptake into a human carcinoma xenograft model. Br J Cancer 1991;64:872 – 4.

68. Thakur ML, DeFulvio J, Tong J, John E, McDevitt MR, Damjanov I. Evaluation of biological response modifiers in the enhancement of tumor uptake of technetium-99m labeled macromolecules. A preliminary report. J Immunol Methods 1992;152:209 – 16.

69. Curnis F, Sacchi A, Borgna L, Magni F, Gasparri A, Corti A. Enhancement of tumor necrosis factor α antitumor immunotherapeutic properties by targeted delivery to aminopeptidase N (CD13). Nat Biotechnol 2000; 18:1185 – 90.

70. Chang SS, O'Keefe DS, Bacich DJ, Reuter VE, Heston WD, Gaudin PB. Prostate-specific membrane antigen is produced in tumor-associated neovasculature. Clin Cancer Res 1999;5:2674 – 81.

71. Liu H, Moy P, Kim S, et al. Monoclonal antibodies to the extracellular domain of prostate-specific membrane antigen also react with tumor vascular endothelium. Cancer Res 1997;57:3629 – 34.

72. McIntosh DP, Tan XY, Oh P, Schnitzer JE. Targeting endothelium and its dynamic caveolae for tissue-specific transcytosis *in vivo*: a pathway to overcome cell barriers to drug and gene delivery. Proc Natl Acad Sci USA 2002;99:1996 – 2001.

73. Au JL, Jang SH, Zheng J, et al. Determinants of drug delivery and transport to solid tumors. J Control Release 2001;74:31 – 46.

74. Jain RK. Vascular and interstitial barriers to delivery of therapeutic agents in tumors. Cancer Metastasis Rev 1990;9:253-66.

75. Durand RE. Distribution and activity of antineoplastic drugs in a tumor model. J Natl Cancer Inst 1989;81:146 – 52.

76. Erlanson M, Daniel-Szolgay E, Carlsson J. Relations between the penetration, binding and average concentration of cytostatic drugs in human tumour spheroids. Cancer Chemother Pharmacol 1992;29:343 – 53.

77. Damsky CH, Richa J, Solter D, Knudsen K, Buck CA. Identification and purification of a cell surface glycoprotein mediating intercellular adhesion in embryonic and adult tissue. Cell 1983;34:455 – 66.

78. Green SK, Frankel A, Kerbel RS. Adhesion-dependent multicellular drug resistance. Anticancer Drug Des 1999;14:153 – 68.

79. Damiano JS, Hazlehurst LA, Dalton WS. Cell adhesion-mediated drug resistance (CAM-DR) protects the K562 chronic myelogenous leukemia cell line from apoptosis induced by BCR/ABL inhibition, cytotoxic drugs, and γ-irradiation. Leukemia 2001;15:1232 – 9.

80. St Croix B, Sheehan C, Rak JW, Florenes VA, Slingerland JM, Kerbel RS. E-cadherin-dependent growth suppression is mediated by the cyclin-dependent kinase inhibitor p27(KIP1). J Cell Biol 1998;142:557 – 71.

81. Green SK, Karlsson MC, Ravetch JV, Kerbel RS. Disruption of cell-cell adhesion enhances antibody-dependent cellular cytotoxicity: implications for antibody-based therapeutics of cancer. Cancer Res 2002;62: 6891 – 900.

82. Sasaki H, Igarashi Y, Nagano T, Nishida K, Nakamura J. Different effects of absorption promoters on corneal and conjunctival penetration of ophthalmic β-blockers. Pharm Res 1995;12:1146 – 50.

83. Morita T, Yamamoto A, Hashida M, Sezaki H. Effects of various absorption promoters on pulmonary absorption of drugs with different molecular weights. Biol Pharm Bull 1993;16:259 – 62.

84. Murakami T, Misaki M, Kojima Y, et al. Effect of absorption promoters on subcutaneous absorption of human epidermal growth factor in rats. J Pharm Sci 1993;82:236 – 9.

85. Duvillard C, Ponelle T, Chapusot C, Piard F, Romanet P, Chauffert B. EDTA enhances the antitumor efficacy of intratumoral cisplatin in s.c. grafted rat colon tumors. Anticancer Drugs 2004;15:295 – 9.

86. Behrens J. Cadherins and catenins: role in signal transduction and tumor progression. Cancer Metastasis Rev 1999;18:15 – 30.

87. Bongiorno PF, al-Kasspooles M, Lee SW, et al. E-cadherin expression in primary and metastatic thoracic neoplasms and in Barrett's oesophagus. Br J Cancer 1995;71:166 – 72.

88. Tomita K, van Bokhoven A, van Leenders GJ, et al. Cadherin switching in human prostate cancer progression. Cancer Res 2000;60: 3650 – 4.

89. Patel IS, Madan P, Getsios S, Bertrand MA, MacCalman CD. Cadherin switching in ovarian cancer progression. Int J Cancer 2003;106:172 – 7.

90. Ahnen DJ, Nakane PK, Brown WR. Ultrastructural localization of carcinoembryonic antigen in normal intestine and colon cancer: abnormal distribution of CEA on the surfaces of colon cancer cells. Cancer 1982;49: 2077 – 90.

91. Tobioka H, Isomura H, Kokai Y, Sawada N. Polarized distribution of carcinoembryonic antigen is associated with a tight junction molecule in human colorectal adenocarcinoma. J Pathol 2002;198:207 – 12.

92. Hamada Y, Yamamura M, Hioki K, Yamamoto M, Nagura H, Watanabe K. Immunohistochemical study of carcinoembryonic antigen in patients with colorectal cancer. Correlation with plasma carcinoembryonic antigen levels. Cancer 1985;55:136 – 41.

93. Delaloye B, Bischof-Delaloye A, Buchegger F, et al. Detection of colorectal carcinoma by emission-computerized tomography after injection of 123I-labeled Fab or F(ab')2 fragments from monoclonal anti-carcinoembryonic antigen antibodies. J Clin Invest 1986;77:301 – 11.

94. Mach JP, Buchegger F, Forni M, et al. Immunoscintigraphy for the detection of human carcinoma after injection of radiolabeled monoclonal anti-carcinoembryonic antigen antibodies. Curr Top Microbiol Immunol 1983;104:49 – 55.

95. Christiansen JJ, Rajasekaran SA, Moy P, et al. Polarity of prostate specific membrane antigen, prostate stem cell antigen, and prostate specific antigen in prostate tissue and in a cultured epithelial cell line. Prostate 2003;55:9 – 19.

96. Ballas ZK, Krieg AM, Warren T, et al. Divergent therapeutic and immunologic effects of oligodeoxynucleotides with distinct CpG motifs. J Immunol 2001;167:4878-86.

97. Clynes R, Takechi Y, Moroi Y, Houghton A, Ravetch JV. Fc receptors are required in passive and active immunity to melanoma. Proc Natl Acad Sci USA 1998;95:652 – 6.

98. Zeidler R, Reisbach G, Wollenberg B, et al. Simultaneous activation of T cells and accessory cells by a new class of intact bispecific antibody results in efficient tumor cell killing. J Immunol 1999;163:1246 – 52.

99. Zeidler R, Mysliwietz J, Csanady M, et al. The Fc-region of a new class of intact bispecific antibody mediates activation of accessory cells and NK cells and induces direct phagocytosis of tumour cells. Br J Cancer 2000;83:261 – 6.

100. Krieg AM, Yi AK, Matson S, et al. CpG motifs in bacterial DNA trigger direct B-cell activation. Nature 1995;374:546 – 9.

101. Yamamoto S, Yamamoto T, Shimada S, et al. DNA from bacteria, but not from vertebrates, induces interferons, activates natural killer cells and inhibits tumor growth. Microbiol Immunol 1992;36:983 – 97.

102. Van Ojik HH, Bevaart L, Dahle CE, et al. CpG-A and B oligodeoxynucleotides enhance the efficacy of antibody therapy by activating different effector cell populations. Cancer Res 2003;63:5595 – 600.

103. Trauth BC, Klas C, Peters AM, et al. Monoclonal antibody-mediated tumor regression by induction of apoptosis. Science 1989;245:301 – 5.

104. Ishizuka H, Watanabe M, Kubota T, Matsuzaki SW, Otani Y, Kitajima M. Antitumor activity of murine monoclonal antibody NCC-ST-421 on human cancer cells by inducing apoptosis. Anticancer Res 1998; 18:2513 – 8.

105. Fitzpatrick VD, Pisacane PI, Vandlen RL, Sliwkowski MX. Formation of a high affinity heregulin binding site using the soluble extracellular domains of ErbB2 with ErbB3 or ErbB4. FEBS Lett 1998;431:102 – 6.

106. Agus DB, Akita RW, Fox WD, et al. Targeting ligand-activated ErbB2 signaling inhibits breast and prostate tumor growth. Cancer Cell 2002;2: 127 – 37.

107. Estey EH, Giles FJ, Beran M, et al. Experience with gemtuzumab ozogamycin (''mylotarg'') and all-*trans* retinoic acid in untreated acute promyelocytic leukemia. Blood 2002;99: 4222 – 4.

108. Ballangrud AM, Yang WH, Charlton DE, et al. Response of LNCaP spheroids after treatment with an α-particle emitter (213Bi) – labeled anti-prostate-specific membrane antigen antibody (J591). Cancer Res 2001; 61:2008 – 14.

109. Witzig TE, Gordon LI, Cabanillas F, et al. Randomized controlled trial of yttrium-90 – labeled ibritumomab tiuxetan radioimmunotherapy versus rituximab immunotherapy for patients with relapsed or refractory low-grade, follicular, or transformed B-cell non-Hodgkin's lymphoma. J Clin Oncol 2002;20:2453 – 63.

N-glycosylation and microtubule integrity are involved in apical targeting of prostate-specific membrane antigen: implications for immunotherapy

Jason J. Christiansen,[1] Sigrid A. Rajasekaran,[1] Landon Inge,[1] Lirong Cheng,[1] Gopalakrishnapillai Anilkumar,[1] Neil H. Bander,[2] and Ayyappan K. Rajasekaran[1]

[1]Department of Pathology and Laboratory Medicine, David Geffen School of Medicine, University of California, Los Angeles, Los Angeles, California and [2]Department of Urology, Weill Medical College, Cornell University, New York, New York

Abstract

Prostate-specific membrane antigen (PSMA) is an important biomarker expressed in prostate cancer cells with levels proportional to tumor grade. The membrane association and correlation with disease stage portend a promising role for PSMA as an antigenic target for antibody-based therapies. Successful application of such modalities necessitates a detailed knowledge of the subcellular localization and trafficking of target antigen. In this study, we show that PSMA is expressed predominantly in the apical plasma membrane in epithelial cells of the prostate gland and in well-differentiated Madin-Darby canine kidney cells. We show that PSMA is targeted directly to the apical surface and that sorting into appropriate post-Golgi vesicles is dependent upon *N*-glycosylation of the protein. Integrity of the microtubule cytoskeleton is also essential for delivery and retention of PSMA at the apical plasma membrane domain, as destabilization of microtubules with nocodazole or commonly used chemotherapeutic *Vinca* alkaloids resulted in the basolateral expression of PSMA and increased the uptake of anti-PSMA antibody from the basolateral domain. These results may have important relevance to PSMA-based immunotherapy and imaging strategies, as prostate cancer cells can maintain a well-differentiated morphology even after metastasis to distal sites. In contrast to antigens on the basolateral surface, apical antigens are separated from the circulation by tight junctions that restrict transport of molecules across the epithelium. Thus, antigens expressed on the apical plasma membrane are not exposed to i.v. given agents. The ability to reverse the polarity of PSMA from apical to the basolateral could have significant implications for the PSMA as a therapeutic target. [Mol Cancer Ther 2005;4(5):1–11]

Introduction

Prostate-specific membrane antigen (PSMA) is a 100-kDa transmembrane glycoprotein with a highly restricted profile of tissue expression. In addition to the benign prostatic epithelium, PSMA is expressed in tumor-associated neovasculature and at increased levels in most cases of prostate cancer, with the greatest levels associated with high-grade tumors, metastases, and androgen-independent disease (1–4). Overexpression of PSMA is a good prognostic indicator of disease outcome and is more highly expressed in poorly differentiated tumors than the better-known marker, prostate-specific antigen (4).

In contrast to other prostate-specific proteins, such as prostate-specific antigen or prostatic acid phosphatase, PSMA is a transmembrane protein expressed on the surface of the prostatic epithelium. As an integral membrane protein, PSMA offers a potentially valuable antigenic target for therapeutic and *in vivo* imaging strategies involving monoclonal antibodies (mAb; ref. 5). The capacity for antibodies to recognize tumor cells with high specificity and affinity has long been appreciated, and the successful clinical application of mAbs depends upon the subcellular localization and trafficking of antigen within the target cell (6).

Like all epithelial tissues, the prostatic epithelium is comprised of highly polarized cells with biochemically distinct apical and basolateral plasma membrane surfaces (7). These plasma membrane domains maintain an asymmetrical distribution of proteins and lipids, are physically separated by tight junctions that promote cell-cell contact, restrict the flow of fluid through intercellular spaces, and prevent the lateral diffusion of membrane components (8, 9). Thus, apical and basolateral plasma membrane domains are exposed to disparate extracellular environments. Whereas the basolateral plasma membrane is relatively accessible to the underlying vasculature, tight junctions prevent molecules within the circulation from reaching the apical surface (6).

The establishment of plasma membrane asymmetry requires vectorial targeting of newly synthesized proteins to either the apical or basolateral surfaces (10). Proteins targeted for a particular plasma membrane domain may arrive at their destinations via alternate routes. Whereas

Received 7/14/04; revised 1/24/05; accepted 3/1/05.

Grant support: Department of Defense grant DAMD17-02-1-0661 and NIH grant DK56216.

The costs of publication of this article were defrayed in part by the payment of page charges. This article must therefore be hereby marked advertisement in accordance with 18 U.S.C. Section 1734 solely to indicate this fact.

Requests for reprints: Ayyappan K. Rajasekaran, Department of Pathology and Laboratory Medicine, University of California, Room 13-344 CHS, Los Angeles, CA 90095. Phone: 310-825-1199; Fax: 310-267-2410. E-mail: arajasekaran@mednet.ucla.edu

many proteins are targeted directly from the trans-Golgi network to their appropriate plasma membrane domain, others are first delivered to the opposing membrane surface before undergoing transcytosis to their ultimate destination (11). The particular transport pathway by which a given protein reaches the plasma membrane is dependent upon the individual protein and governed by interactions between the cellular sorting machinery and signals encoded within that protein. Whereas the signals for basolateral targeting generally involve short amino acid–based motifs, often containing critical tyrosine or leucine residues (12, 13), targeting to the apical surface seems mediated by a far more heterogeneous array of divergent signals, including N- or O-linked oligosaccharides (14, 15), PDZ-interacting domains (16), membrane anchors (17), and amino acid sequences encoded within membrane spanning (18) or cytoplasmic domains (19). This diversity of sorting signals underscores the complexity of apical targeting and implies the existence of multiple pathways for apical targeting.

Like the plasma membrane, cytoskeletal elements also display a nonuniform distribution in polarized epithelial cells. As cells establish polarity, microtubules emanating from the microtubule organizing centers are rearranged to form longitudinal arrays with their minus ends facing the apical surface (20). This polarized arrangement of microtubules seems critical for targeting a number of apical proteins, because microtubule depolymerization or disruption of dynein function results in aberrant targeting of several apical proteins to the basolateral surface (21, 22) but does not seem to have a significant effect on targeting of basolateral proteins (21, 23).

Whereas numerous investigations have attempted to address the relevance of PSMA as a diagnostic marker and a therapeutic target, most of these studies have been done using highly transformed carcinoma cell lines such as LNCaP cells and PC3 and have largely neglected the significance of epithelial polarity. Because a well-differentiated polarized epithelial cell culture model for prostate is not available, we established the Madin-Darby canine kidney (MDCK) cell culture model for studying targeting of prostate restricted proteins. We showed that several proteins expressed in prostate gland are similarly targeted in MDCK cells, indicating that MDCK cells are a convenient and a suitable model for studying targeting of PSMA (24).

In this study, we investigated the mechanisms and cellular machinery involved in apical targeting of PSMA. We employed a series of biochemical and morphologic assays to elucidate the targeting pathway of PSMA and ascertain the role of *N*-glycosylation and microtubules in the delivery of PSMA to the apical surface. We show that *N*-glycosylation is necessary for proper targeting of PSMA into apically targeted vesicles, whereas integrity of the microtubules is necessary to deliver and retain PSMA at the apical plasma membrane domain. We exploited this intrinsic role of microtubules in the apical delivery of PSMA for the clinical benefit by using *Vinca* alkaloids to destabilize microtubules and show that these alkaloids redirect PSMA to the basolateral plasma membrane, which is accessible to the circulating therapeutic antibodies.

Materials and Methods

Cell Culture

MDCK cells (clone II) were obtained from the American Type Culture Collection (Manassas, VA) and cultured in DMEM (Life Technologies, Rockville, MD) supplemented with 10% fetal bovine serum, 2 mmol/L L-glutamine, 25 units/mL penicillin, 25 μg/mL streptomycin, and 100 μmol/L nonessential amino acids. Cells were grown at 37°C in a humidified incubator with 5% CO_2. Cells were treated for 10 hours with 10 mmol/L sodium butyrate to enhance PSMA expression. For experiments involving inhibition of *N*-glycosylation or microtubule depolymerization, cells were treated for 3 hours with 5 μg/mL tunicamycin (Sigma, St. Louis, MO) or 4 μg/mL nocodazole (Sigma), or 2 μmol/L vinblastine, vincristine, or vinorelbine (Sigma) in DMEM at 37°C before the indicated experiment unless otherwise noted.

DNA Constructs and Transfection

The cDNA encoding full-length PSMA (provided by Dr. Warren Heston) was cloned into the pcDNA3 expression vector from Invitrogen (Carlsbad, CA). The sPSMA construct was generated by PCR amplification of codons 53 to 751 using PSMA cDNA as a template. The 5′ and 3′ primers were used to introduce *Sfi*I and *Apa*I restriction sites, respectively. This cDNA was cloned into the pSecTag2A vector (Invitrogen) in fusion with an NH_2-terminal sequence encoding the cleavable murine immunoglobulin chain leader sequence for protein secretion. To create the green fluorescent protein (GFP)–tagged PSMA-Δ103-750 construct, a 309-bp DNA fragment encoding the cytoplasmic, transmembrane, and a 60-amino-acid region of the extracellular domain of PSMA was generated by reverse transcription-PCR using total RNA isolated from LNCaP cells. The PCR product was digested with *Xho*I and *Bam*HI and cloned into the pEGFP-N3 expression vector (Clontech, Palo Alto, CA). The cDNA encoding the β-subunit of the canine sodium pump (Na,K-ATPase; provided by Dr. Robert Farley) was PCR amplified and inserted into pEGFP-N3 to create a GFP fusion at the COOH terminus (Na,K-β-GFP).

MDCK cells were transfected using calcium phosphate, as previously described (25). Stable clones were selected in 500 μg/mL geneticin (G418, Life Technologies) for pcDNA3 vectors or 300 μg/mL Zeocin (Invitrogen) for pSecTag2 vector and expression verified by immunofluorescence and immunoblot.

Antibodies

The mAb J591 against an extracellular epitope of PSMA has been described (26). The mAb 7E11 against an intracellular epitope of PSMA was prepared from hybridoma 7E11 (American Type Culture Collection, Rockville, MD). Mouse mAbs raised against Na,K-ATPase α1 (M7-PB-E9) and β1-subunit (M17-P5-F11) have been described

(27, 28). Rabbit anti-mouse and mAb against α-tubulin were purchased from Sigma. Horseradish peroxidase–conjugated goat anti-mouse immunoglobulin G was purchased from Transduction Laboratories (Lexington, KY). FITC and CY3 conjugated secondary antibodies were purchased from Jackson ImmunoResearch (West Grove, PA).

Immunofluoresence and Confocal Microscopy

Tissue sections and MDCK cells were fixed in cold methanol at −20°C for 30 minutes. Following fixation, specimens were placed in humidified chambers, washed with PBS containing 0.1 mmol/L $CaCl_2$ and 1 mmol/L $MgCl_2$ and 0.5% bovine serum albumin (PBS-CM-BSA), incubated 1 hour with primary antibody, washed with PBS-CM-BSA, incubated 30 minutes in secondary antibody, washed with PBS-CM-BSA, rinsed with distilled water, and mounted in Vectashield (Vector, Burlingame, CA).

For cell surface staining, MDCK cells were grown on transwell filters and the transepithelial electrical resistance was determined using an EVOM Epithelial Voltohmeter (World Precision Instruments, Sarasota, FL). Values were normalized for filter area after subtracting the background resistance of a filter without cells. transepithelial electrical resistance values of >200 Ω/cm^2 were indicative of tight junction formation in MDCK cells (29). Medium was removed and replaced with chilled DMEM containing 10 μg/mL J591. Cells were incubated on ice for 30 minutes, rinsed with cold PBS-CM-BSA, fixed in cold methanol, and incubated with secondary antibody as described above.

Confocal microscopy was done using a Fluoview laser scanning confocal microscope (Olympus America, Melville, NY) as described (25). To detect FITC and propidium iodide, samples were excited with krypton and argon lasers and light emitted between 525 and 540 nm was recorded for FITC and above 630 nm for propidium iodide. Images were generated and analyzed using the Fluoview image analysis software, version 2.1.39 (Olympus America).

Cell Surface Biotinylation

MDCK cells were grown to confluence on transwell filters, as determined by transepithelial electrical resistance, and biotinylation of the apical or basolateral surface was done as described (25). Briefly, 0.5 μg/mL of membrane impermeable EZ-Link Sulfo-NHS-Biotin (Pierce, Rockford, IL) in TEA [150 mmol/L NaCl, 10 mmol/L Triethanolamide (pH 9.0), 1 mmol/L $CaCl_2$, and 1 mmol/L $MgCl_2$] was added to either the apical or basolateral chamber. After quenching with 50 mmol/L NH_4Cl in PBS-CM, cells were lysed in 0.5 mL of lysis buffer [150 mmol/L NaCl; 20 mmol/L Tris (pH 8); 5 mmol/L EDTA; 1% Triton X-100; 0.1% BSA; 1 mmol/L phenylmethylsulfonyl fluoride; and 5 μg/mL each of antipain, leupeptin, and pepstatin]. Total protein from each lysate was used for precipitation (16 hours at 4°C) with immobilized streptavidin gel (Pierce). Precipitates were washed and prepared for SDS-PAGE and immunoblot analysis as described (30).

SDS-PAGE and Immunoblot Analysis

Samples were separated on 10% SDS polyacrylamide gels and transferred to nitrocellulose. Membranes were incubated in 5% nonfat milk for 1 hour and immunoblotted with primary antibodies (1:1,000) for 2 hours in milk. Membranes were washed thrice with PBS with 0.3% Tween 20 (PBST), incubated with horseradish peroxidase–conjugated secondary antibody (1:4,000) in milk. After washing thrice in PBST and once in PBS, bound antibody was detected by peroxidase-catalyzed Enhanced Chemiluminescence-Plus (Amersham, Buckinghamshire, United Kingdom). Densitometric analysis and quantification of bands was done using ImageQuant software (Molecular Dynamics, Sunnyvale, CA).

Metabolic Labeling

Confluent monolayers of MDCK-PSMA cells on transwell filters were rinsed twice and incubated for 30 minutes in starving media (cystine/methionine-free DMEM; CellGro, Herndon, VA) supplemented with 0.2% BSA. Cells were either pulsed for 20 minutes in labeling medium (starving medium containing 250 μCi/mL Trans[^{35}S]-label; ICN, Costa Mesa, CA) or labeled for 4 hours in the presence or absence of 10 μg/mL of tunicamycin (Sigma). Chase was done by rinsing filters thrice with starving medium and incubating in DMEM (10% fetal bovine serum) containing 50 μg/mL of cyclohexamide (Sigma).

Targeting Assays

For the antibody internalization targeting assay, MDCK cells were metabolically labeled and chased in DMEM containing 5 μg/mL of mAb J591 added to either the apical or basolateral chamber. Following incubation, cells were rinsed thoroughly with cold PBS-CM. Filters were excised and incubated for >4 hours in lysis buffer at 4°C. Immunocomplexes were precipitated using rabbit anti-mouse–coated protein A agarose beads. Beads were rinsed and subject to SDS-PAGE. Gels were fixed in a solution of 20% methanol and 10% acetic acid, dried, enhanced with salicylic acid, and exposed to film. The relative amount of PSMA for each was calculated as a percentage of the total amount of labeled PSMA precipitated throughout the course of the experiment, as quantified by densitometry.

The biotinylation targeting assay has been previously described (31). Cells were metabolically labeled and chased. Following the indicated time intervals, cells were placed on ice and rinsed thrice with cold PBS-CM. Biotinylation of the apical or basolateral surfaces was done as described above. Filters were excised and incubated for 4 hours in lysis buffer at 4°C. PSMA was immunoprecipitated from cell lysates by incubating with protein A agarose beads coated with rabbit anti-mouse and 7E11 for 16 hours at 4°C. Beads were washed and eluted by boiling in 20 μL of 5% SDS. Eluates were removed and resuspended in 1.5 mL lysis buffer. Samples were subsequently incubated with immobilized streptavidin for 16 hours at 4°C. Beads were washed and subjected to SDS-PAGE, autoradiography, and densitometry as described above.

Polarized Secretion Assay

MDCK cells expressing sPSMA (MDCK-sPSMA) were grown on transwell filters. Following the establishment of tight junctions, as assessed by transepithelial electrical resistance, cells were rinsed thrice with fresh DMEM and

2.0 mL of fresh medium were added to both the apical and basolateral chambers. Cells were incubated for 8 to 10 hours at 37°C, at which point the conditioned medium was collected and sPSMA immunoprecipitated using immobilized J591 bound to protein A coated agarose beads. Samples were washed and subjected to SDS-PAGE, immunoblot analysis, and densitometry as described above.

Post-Golgi Analysis Assays

MDCK-PSMA cells transiently transfected to express Na,K-β-GFP were grown on glass coverslips and treated with nocodazole or tunicamycin. Cells were incubated for 6 hours at 20°C to accumulate newly synthesized protein in the Golgi and trans-Golgi network, subsequently transferred to 37°C for 30 minutes, and subjected to immunofluorescence analysis as described above. Laser scanning confocal microscopy was done using a Zeiss Axiovert 200 inverted microscope (Carl Zeiss, Inc., Thornwood, NY). Samples were excited with Argon and Helium/Neon lasers and single channel images were generated and analyzed using the Zeiss LSM 510 Meta imaging system (Carl Zeiss) by recording light emitted between 505 and 543 nm for GFP and above 560 nm for CY3.

Domain-Specific Internalization Assay

MDCK-PSMA cells were grown on 0.04-μm pore size polycarbonate transwell filters (Corning, Corning, NY) and grown to confluence as measured by transepithelial electrical resistance using an EVOM Epithelial Voltohmeter (World Precision Instruments). Values were normalized for the area of the filter after subtracting the background resistance of a filter without cells. Transepithelial electrical resistance of 220 to 250 $\Omega\ cm^2$ is indicative of the presence of functional tight junctions (24). Cells were treated with 2 μmol/L of vinblastine, vincristine, or vinorelbine at 37°C for 3 hours and subsequently incubated at 37°C for 30 minutes in the presence of the indicated drug and 5 μg/mL of J591 added to either the apical or basolateral chamber. Cells were rinsed in PBS-CM, fixed, and subjected to immunofluorescence analysis with FITC-conjugated secondary antibody. Single-channel digital microscopic images were collected with an Olympus AX70 upright microscope using identical exposure variables and analyzed with SPOT imaging software, version 4.0.4 (Diagnostic Instruments, Inc., Sterling Heights, MI).

Immunohistochemical Studies

Formalin-fixed, paraffin-embedded tissue samples from patients with metastatic prostate cancer were obtained from the tissue procurement core laboratory at the University of California at Los Angeles. Metastatic prostate–derived specimens included four lesions isolated from lymph nodes and two isolated from bone marrow. Serial 5-μm sections were deparaffinized to water and subjected to antigen retrieval for 10 minutes at room temperature in 0.05% trypsin or microwaved in citrate buffer. Following antigen retrieval, specimens were incubated in 1% hydrogen peroxide for 10 minutes, blocked with 4% fetal bovine serum in PBS for 1 hour, and incubated with mAb 7E11 (1:50) overnight at 4°C. Samples were subsequently washed and incubated at room temperature with biotinylated goat anti-mouse secondary antibody (Vector) for 1 hour. Samples were rinsed and subjected to A and B reagent. Immunoreactivity was visualized by incubation with diaminobenzidine in the presence of hydrogen peroxide. Sections were counterstained with hematoxylin and mounted for microscopic analysis. Control experiments were also done by incubating tissues with an irrelevant mouse monoclonal immunoglobulin G.

Results

PSMA Is Expressed on the Apical Plasma Membrane of Polarized Epithelial Cells

We have previously shown that the MDCK cell line is a suitable model system to study polarized sorting of prostate-restricted transmembrane and secretory proteins (24). Immunofluorescence analysis of tissue sections revealed prominent PSMA localization at the apical plasma membrane of prostatic epithelial cells, with staining at the lumenal interface of the gland (Fig. 1A), recapitulating *in situ* observations (24). Surface immunofluorescence analysis done on confluent monolayers of MDCK cells expressing PSMA (MDCK-PSMA) revealed a similar pattern of expression, with PSMA staining localized primarily to the apical membrane in these cells (Fig. 1B). A selective cell surface biotinylation assay was done to provide a quantitative analysis of relative surface PSMA levels. Results of this assay showed that 70% to 79% of PSMA at the cell surface was localized to the apical plasma membrane (Fig. 1C) thus confirming previous results (24).

PSMA Is Targeted Directly to the Apical Plasma Membrane

Apical proteins may be targeted directly from the trans-Golgi network or may be delivered first to the basolateral plasma membrane before undergoing transcytosis to the apical surface. To distinguish between these pathways, an antibody internalization-based targeting assay was employed. Confluent monolayers of MDCK-PSMA cells grown on transwell filters were metabolically labeled with [^{35}S]-cystine/methionine for a brief pulse and chased in the presence of mAb J591 added to either the apical or basolateral chamber. The J591 mAb recognizes an extracellular epitope on PSMA and is readily internalized by cells expressing PSMA (26). During the period of antibody incubation, PSMA at a particular plasma membrane surface will bind extracellular antibody, even if this localization is transient. Immunocomplexes are then precipitated from cell lysates and subjected to SDS-PAGE and autoradiography. If PSMA were to undergo direct targeting to the apical plasma membrane, a greater amount of metabolically labeled PSMA would be recovered when antibody is added to the apical chamber relative to the basolateral. At each time point subsequent to release, the level of metabolically labeled PSMA immunoprecipitated was between 1.7- and 2.0-fold greater when antibody was added to the apical rather than the basolateral chamber (Fig. 2A and B) thus indicating that whereas some PSMA may initially be delivered to the basolateral surface, the majority is targeted directly to the apical plasma membrane.

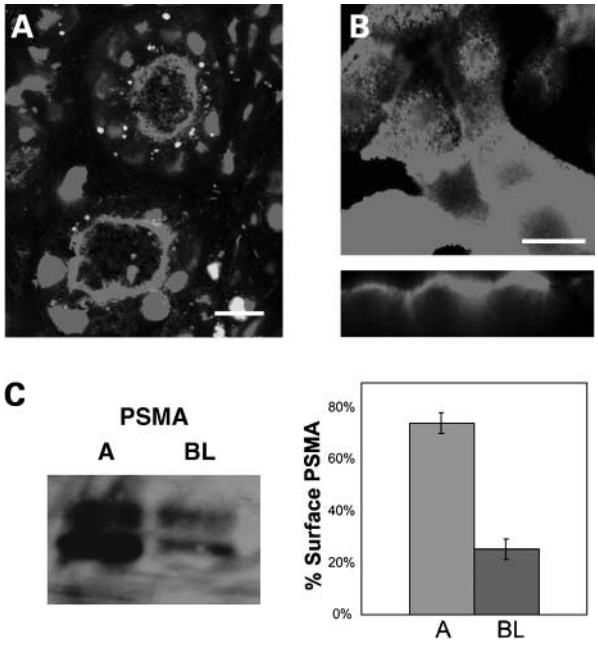

Figure 1. PSMA is expressed on the apical surface of polarized epithelial cells. **A,** immunofluorescence analysis of prostate tissue sections reveals that PSMA (*green*) is predominantly localized to the apical plasma membrane surface of the prostatic epithelium, lining the lumen of the gland. Nuclei stained with propidium iodide are in red. **B,** XY and XZ confocal sections of surface staining of MDCK-PSMA cells reveal PSMA (*green*) localized to the apical plasma membrane. **C,** results from three independent cell surface biotinylation assays confirm predominant apical localization and demonstrate that 70% to 79% of surface PSMA is localized to the apical plasma membrane; *bars,* SD. Apical (*A*), basolateral (*BL*). Bar, 10 μm (**A** and **B**).

These results were supported by a selective cell surface biotinylation-based targeting assay. Confluent monolayers of MDCK-PSMA cells were metabolically pulsed and chased in normal culture medium before opposing membrane surfaces were labeled with biotin. Autoradiography showed that PSMA is seen predominantly on the apical plasma membrane with a smaller fraction localized to the basolateral surface throughout the course of the experiment (Fig. 2C). The fact that PSMA is primarily observed at the apical plasma membrane even at the initial time point of 30 minutes further suggests that the majority of newly synthesized PSMA is targeted to the apical surface.

Extracellular Domain of PSMA Contains Information for Apical Targeting

Although signals for apical targeting may be localized throughout the length of a given transmembrane protein, such signals most commonly reside within the extracellular domain. To assess the significance of this domain in apical targeting, a GFP-tagged form of PSMA was created in which the majority of the extracellular domain was removed (PSMA-Δ103-750). Cell surface biotinylation assays showed that this protein was localized in a nonpolarized fashion (Fig. 3A). Immunoblot analysis done on the same membranes revealed that 90% to 95% of the α-subunit of the sodium pump (Na,K-ATPase α-sub) was localized at the basolateral surface of these cells (Fig. 3B), demonstrating that the uniform plasma membrane distribution of PSMA is not merely attributable to a general loss of epithelial polarity.

To evaluate the targeting potential offered by the lumenal domain, a secreted form of PSMA (sPSMA) lacking the cytoplasmic and transmembrane domains was created. The sPSMA protein was secreted from MDCK cells as a ~100-kDa glycoprotein that was recognized by the mAb J591 and that migrated with a molecular mass of ~80 kDa following treatment with tunicamycin or *N*-glycosidase (data not shown). A stable MDCK cell line expressing sPSMA

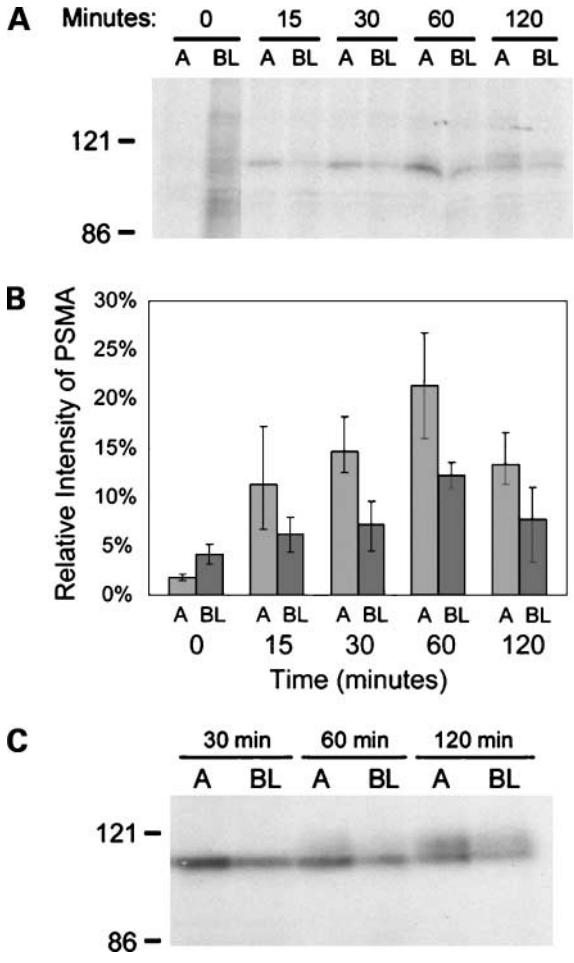

Figure 2. PSMA is targeted directly to the apical plasma membrane. MDCK-PSMA cells on transwell filters were briefly pulsed with [^{35}S]-cystine/methionine and chased in the presence of mAb J591 added to either the apical or basolateral chamber. **A,** the amount of newly synthesized PSMA precipitated was significantly greater when antibody is added to the apical chamber (*A*) compared with the basolateral (*BL*). Densitometric analysis of three independent antibody internalization targeting assays reveals increased apical targeting at each time point. **B,** data indicate that 1.7 to 2.0 times more PSMA is precipitated when J591 is added to the apical chamber (*A*) compared with the basolateral (*BL*); *bars,* SD. **C,** representative data from two independent biotinylation based targeting assays also show greater levels of newly synthesized PSMA at the apical plasma membrane relative to the basolateral throughout the course of the experiment.

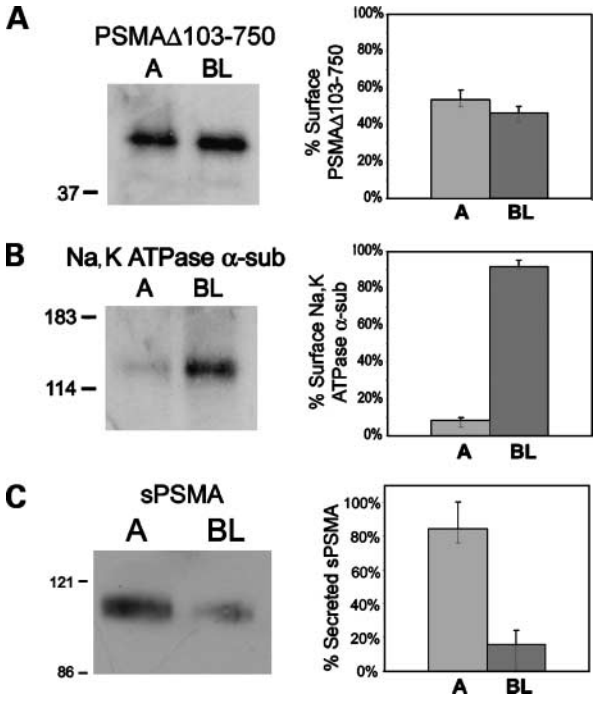

Figure 3. The extracellular domain of PSMA contains the apical targeting signal. A mutant form of PSMA lacking the extracellular domain is expressed in a nonpolarized fashion on the surface of MDCK cells. **A,** cell surface biotinylation and densitometric analysis using three different stable clones reveals that 48% to 55% of this mutant localized to the apical (*A*) plasma membrane. **B,** in contrast, 90% to 95% of the Na,K-ATPase α-subunit is found at the basolateral (*BL*) plasma membrane, indicating that the nonpolarized distribution of PSMA is not due to a general loss of polarity in these cells. **C,** a secreted form of PSMA (sPSMA) lacking the cytoplasmic and transmembrane domains is released predominantly from the apical surface of MDCK cells (78-99%). *Bars,* SD of three independent experiments.

(MDCK-sPSMA) was grown to confluence on transwell filters, and the conditioned medium was collected from the apical and basolateral chambers. As shown in Fig. 3C, sPSMA was secreted almost exclusively from the apical plasma membrane, further implicating the existence of a targeting signal encoded within the extracellular domain of PSMA.

Apical Targeting of PSMA Requires *N*-Glycosylation

The extracellular domain of PSMA is highly glycosylated, with ~25% of the mass of PSMA attributable to N-linked carbohydrates (32). Given the significance of oligosaccharide moieties in apical targeting, we investigated the role of *N*-glycosylation in trafficking of PSMA (14, 33).

Confluent monolayers of MDCK-PSMA cells were metabolically labeled in the presence or absence of tunicamycin. This drug prevents *N*-glycosylation in the endoplasmic reticulum and has been used extensively to assess the role of glycosylation in protein trafficking (34, 35). Selective biotinylation of the apical or basolateral plasma membrane revealed that whereas the majority of surface PSMA is normally localized to the apical plasma membrane, inhibition of *N*-glycosylation abolished the polarized expression of PSMA and resulted in equivalent levels at both plasma membrane surfaces (Fig. 4A).

Inhibition of *N*-glycosylation also resulted in a dramatic alteration in PSMA localization within post-Golgi transport vesicles. Incubation of MDCK-PSMA cells at 20°C was used to inhibit post-Golgi transit and accumulate proteins within the trans-Golgi network (36). As seen in Fig. 4B, both PSMA and a GFP-tagged version of the basolaterally targeted Na,K-ATPase β-subunit (Na,K-β-GFP) were localized to the trans-Golgi network following incubation at 20°C. These cells were subsequently transferred to 37°C, allowing proteins to exit from the trans-Golgi network. In the absence of tunicamycin, PSMA and Na,K-ATPase localized to distinct post-Golgi vesicles in regions proximal to the trans-Golgi network, with only ~8% (7 of 87) of red and green vesicles overlapping. However, the level of colocalization of vesicles containing these markers increased to ~43% (38 of 88) when cells are incubated with tunicamycin (Fig. 4C), indicating a role for *N*-glycosylation PSMA sorting into distinct post-Golgi vesicles.

Microtubules Are Necessary for Apical Targeting of PSMA

The integrity of the microtubule cytoskeleton is essential for the targeted delivery of many apical proteins in polarized epithelial cells (37, 38). To address the significance of microtubules in PSMA targeting, MDCK-PSMA cells were treated with the microtubule-depolymerizing agent, nocodazole. As shown in Fig. 5, nocodazole treatment resulted in a dramatic redistribution of PSMA. Surface immunofluoresence revealed increased PSMA expression at the basolateral plasma membrane relative to untreated cells (Fig. 5A). These data were also confirmed by cell surface biotinylation experiments, which show a homogeneous distribution of PSMA at both plasma membrane domains following nocodazole treatment (Fig. 5B). Polarity of the basolateral marker Na,K-ATPase was unaffected by nocodazole treatment, confirming the conservation of tight junction integrity and epithelial polarity in these cells (Fig. 5C).

Whereas tunicamycin and nocodazole treatment both resulted in a loss of PSMA polarity, the localization of PSMA within post-Golgi vesicles after treatment with these drugs was distinctly different. Following release from a 20°C block, PSMA and Na,K-β-GFP did not show an increased colocalization in the presence of nocodazole, with only ~8% (4 of 52) of red and green post-Golgi vesicles (Fig. 5D). These results indicate that targeting of PSMA into distinct post-Golgi vesicles was unaffected by microtubule depolymerization.

Whereas microtubule depolymerization does not affect the sorting of PSMA into post-Golgi vesicles, the delivery of these vesicles to the plasma membrane fails to occur in a polarized manner. Confluent monolayers of MDCK-PSMA cells on transwell filters were pulsed and chased in the presence of extracellular mAb J591. In the absence of nocodazole, ~1.9-fold more radiolabeled PSMA was precipitated when J591 was added to the apical chamber compared with the basolateral, consistent with our earlier findings (Fig. 5E). However, in the presence of nocodazole, equivalent levels of radiolabeled PSMA were precipitated regardless of the chamber to which J591 was added, thus

showing that newly synthesized PSMA was delivered in a nonpolarized fashion (Fig. 5E). These results suggest that microtubule integrity is necessary for proper delivery and retention of PSMA at the plasma membrane domain.

Vinca Alkaloids Promote mAb J591 Uptake from the Basolateral Plasma Membrane

Because nocodazole treatment reversed the polarity of PSMA, we investigated the effect of commonly used chemotherapeutic agents that inhibit microtubule assembly. The *Vinca* alkaloids are a class of drugs applied to the treatment of a number of malignant diseases, including prostate cancer. Treatment of MDCK-PSMA cells with vinblastine, vincristine, or vinorelbine was sufficient to induce extensive depolymerization of the microtubule cytoskeleton (Fig. 6A-D). Confluent monolayers of MDCK-PSMA cells were subjected to J591 internalization assays to determine how *Vinca* alkaloid treatment influences PSMA localization. Whereas polarized monolayers of untreated MDCK-PSMA cells readily internalized mAb J591 added to the apical chamber (Fig. 6E), very little antibody was internalized from the basolateral surface (Fig. 6I). Following treatment with *Vinca* alkaloids, J591 was also taken up from the apical surface, albeit at decreased levels relative to untreated cells (Fig. 6F-H); however, these cells exhibited a dramatic increase in J591 internalization from the basolateral surface (Fig. 6J-L).

Polarized Morphology of Prostate Tumor Cells

We next investigated whether our observations using a polarized cultured cell line might have a practical significance in the context of prostate cancer cells, *in situ*. Histologic assessment of a metastatic lesion from lymph node shows diffused prostate tumor infiltration replacing the lymph node parenchyma (Fig. 7A). The enlarged tumor cells contain large and prominent nuclei and mitotic figures are readily observed. The prostate cancer cells form sheets with several areas of glandular differentiation. These glandular structures have clearly identifiable lumenal spaces occasionally containing pink secretions. The tumor cells surrounding the lumenal spaces show similar morphology to that seen in well-differentiated primary adenocarcinoma of the prostate with distinct plasma membrane organization (Fig. 7A and B). Immunohistochemical analysis revealed that these cells express PSMA and that this antigen is restricted to the apical surface facing the lumen (Fig. 7C and D). This staining was clearly distinct from that of the endothelial cell marker CD34 and CD31. Antibodies to these antigens stained small vessels but not the glandular structures thus excluding the possibility that these PSMA expressing structures are actually blood vessels (Fig. 7E and F; data not shown). These results indicate that prostatic cancer in some patients retains a well-differentiated morphology, even following metastasis to distal sites.

Discussion

With expression largely restricted to the cells of the prostatic epithelium and protein levels proportional to tumor grade, PSMA has emerged as a potentially important

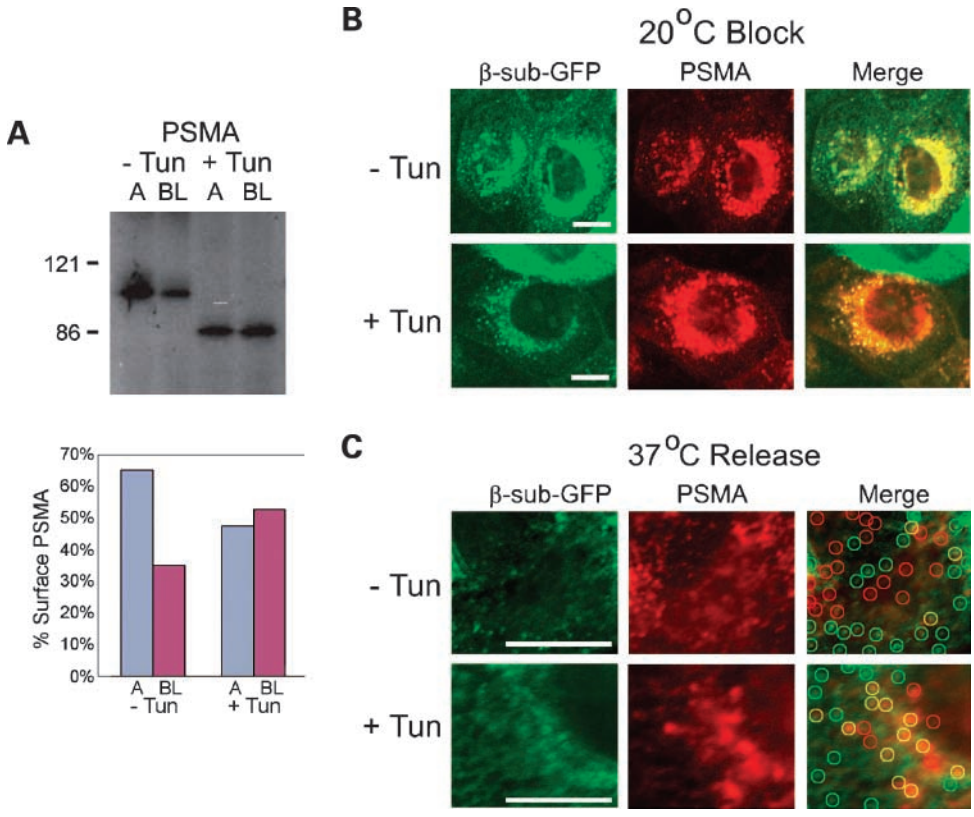

Figure 4. *N*-glycosylation is required for targeting PSMA into the proper post-Golgi vesicles. Cell surface biotinylation reveals that PSMA is distributed in a nonpolarized fashion following treatment with tunicamycin. Apical (*A*), basolateral (*BL*). **A,** following incubation at 20°C, PSMA (*red*) and Na,K-β-GFP (*green*) are accumulated in the trans-Golgi network. **B,** after release from the 20°C block, PSMA (*red*) and Na,K-β-GFP (*green*) localize to distinct post-Golgi vesicles, with limited colocalization. In the presence of tunicamycin, a significant increase in colocalization is observed. **C,** the circles in the merged image were artificially added using Photoshop to highlight the location of individual post-Golgi vesicles containing Na,K-ATPase (*green*), PSMA (*red*), or both (*yellow*). Bar, 5 μm (**B** and **C**).

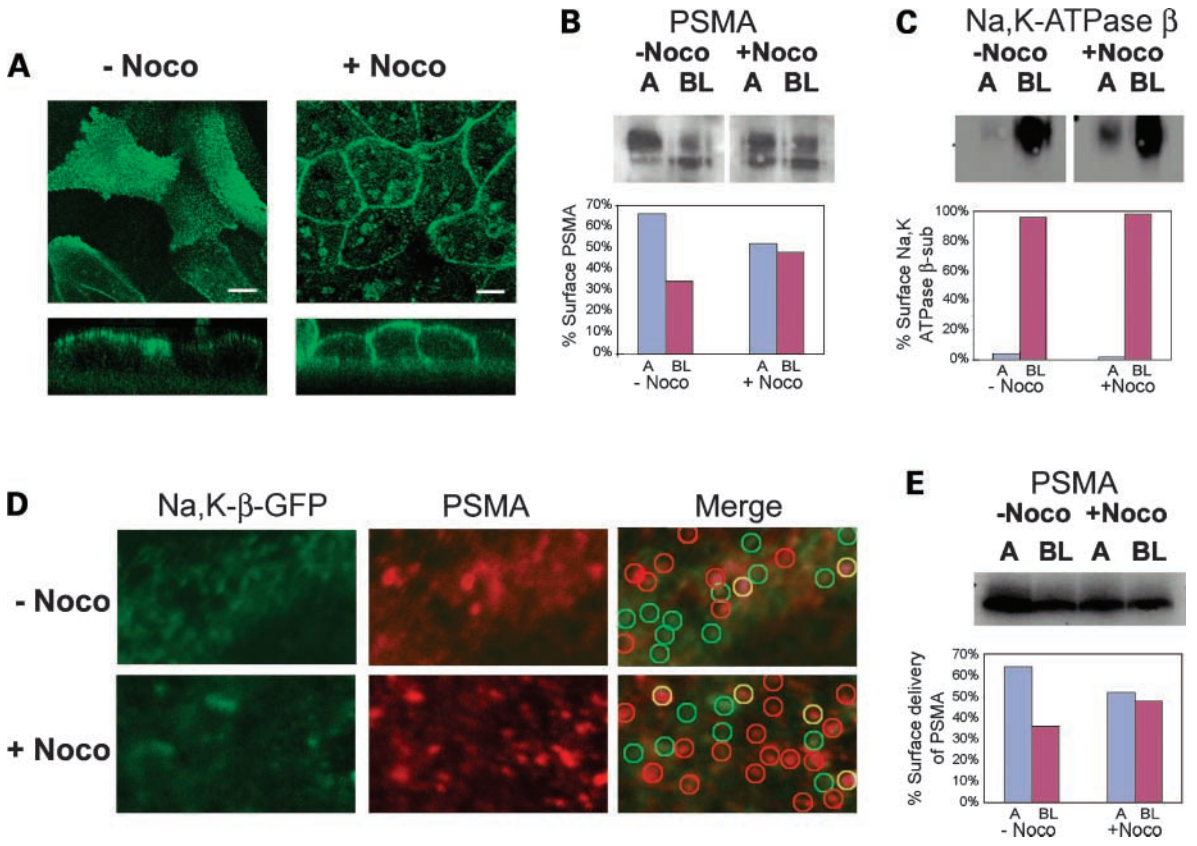

Figure 5. Intact microtubules are required for proper delivery of PSMA-containing vesicles to the apical plasma membrane. Immunofluorescence analysis of MDCK-PSMA cells (-Noco) reveals that PSMA is expressed on the apical membrane. **A,** following microtubule depolymerization (+Noco), XY and XZ confocal sections reveal PSMA staining throughout the plasma membrane and at cell borders. **B,** cell surface biotinylation assays confirm that PSMA is distributed throughout the plasma membrane. **C,** Na,K-ATPase-β subunit is still restricted to the basolateral plasma membrane following nocodazole treatment, indicating that such treatment does not result in a general loss of polarity. **D,** following release from a 20°C block, Na,K-ATPase (*green*) and PSMA (*red*) are localized to distinct post-Golgi vesicles, regardless of nocodazole treatment. The circles in the merged image were artificially added using Photoshop to highlight the location of individual post-Golgi vesicles containing Na,K-ATPase (*green*), PSMA (*red*), or both (*yellow*). **E,** representative data from two independent antibody internalization targeting assays reveal that polarized delivery of PSMA is abolished following 3 hours of nocodazole treatment. Bar, 5 μm (**A** and **D**).

biomarker for the management and therapy of prostate cancer. In this report, we have investigated the trafficking of PSMA in polarized epithelial cells and showed *N*-glycosylation and microtubule requirements for apical targeting.

Currently, no well-differentiated cell lines of prostatic origin exist that maintain epithelial polarity under culture conditions. The commonly used prostate-derived cell lines, such as LNCaP, DU145, and PC3, are all highly transformed cells that lack epithelial junctions. Therefore, we have used polarized MDCK cells to investigate PSMA trafficking. Previous efforts have shown similar patterns of localization for several prostatic antigens, including PSMA, prostate-specific antigen, and PSCA, indicating that the components of the protein trafficking machinery are conserved between cell types (24). Thus, information about protein targeting in MDCK cells can effectively be applied to prostatic epithelial cells, *in situ*.

Our results indicate that the PSMA is targeted directly from the trans-Golgi network to the apical plasma membrane and that the signal for apical sorting resides in the lumenal domain of PSMA. This apical sorting signal is dependent upon the presence of N-linked oligosaccharides, which are essential for proper targeting of PSMA into post-Golgi vesicles devoid of basolateral cargo. Unfortunately, attempts to express mutant forms of PSMA in which the various *N*-glycosylation sites had been mutated were largely unsuccessful at generating cell lines with sufficient expression at the plasma membrane. Thus, we were unable to define the specific *N*-glycosylation sites required for apical targeting.

Like *N*-glycosylation, intact microtubules are also required for proper targeting of PSMA to the apical plasma membrane. Whereas treatment with either tunicamycin or nocodazole both resulted in nonpolarized delivery of PSMA in MDCK cells, only tunicamycin treatment was associated with aberrant localization of PSMA to post-Golgi vesicles containing markers of the basolateral surface, indicating that microtubules are involved in a subsequent step in the apical delivery of PSMA.

The subcellular trafficking of PSMA may have important clinical implications, and an increased awareness of the mechanisms involved in PSMA targeting may yield practical benefits for PSMA-based prostate cancer immunotherapy. PSMA-specific mAbs conjugated to radionuclides or cytotoxic drugs have already proven effective at reducing the size of spheroids in cell culture and tumor xenografts in mouse models (39–41). However, these studies have used highly transformed cells lacking plasma membrane polarity and may not accurately reflect the more complex situation that exists *in vivo*.

To gain access to antigens on the surface of malignant cells *in vivo*, therapeutic mAbs must traverse a gamut of formidable obstacles. With few barriers to impede mAb binding, hematologic malignancies are well suited to this form of therapy (42). In comparison, successful treatment of solid tumors with mAbs has proven considerably more elusive. Studies using radiolabled mAbs show that only 0.01% to 0.1% of the original injected dose will ever reach the antigen within a solid tumor mass, per gram of tissue (43, 44). Following i.v. injection and diffusion throughout the vascular space, therapeutic antibodies must traverse the microvascular endothelium and contend with stromal and interstitial barriers associated with a sizeable tumor mass (45, 46). After navigating these formidable impediments, a mAb may still be confronted by an additional set of epithelial barriers that may severely restrict accessibility of antigens to circulating antibodies. Whereas over 90% of all cancers are carcinomas derived from epithelial tissues, the significance of these epithelial barriers is often disregarded in the treatment of malignant disease.

Although often overlooked, epithelial barriers may exert a profound effect on the efficacy of mAb therapy. The tight junctions would severely restrict the accessibility of antibodies to antigens at the apical plasma membrane. For example, the carcinoembryonic antigen, which is expressed at similar levels in both benign and malignant cells of the colonic epithelium, is restricted to the apical surface of normal tissues and well-differentiated tumors (47). However, loss of tight junction integrity in poorly differentiated tumors results in nonpolarized expression of carcinoembryonic antigen throughout the plasma membrane (47, 48). The altered localization of carcinoembryonic antigen allows accessibility of this antigen to the underlying vasculature and would explain why immunoscintigraphic studies using i.v. injected mAbs to carcinoembryonic antigen are able to specifically label primary and metastatic tumors but not normal or well-differentiated tissues (49, 50).

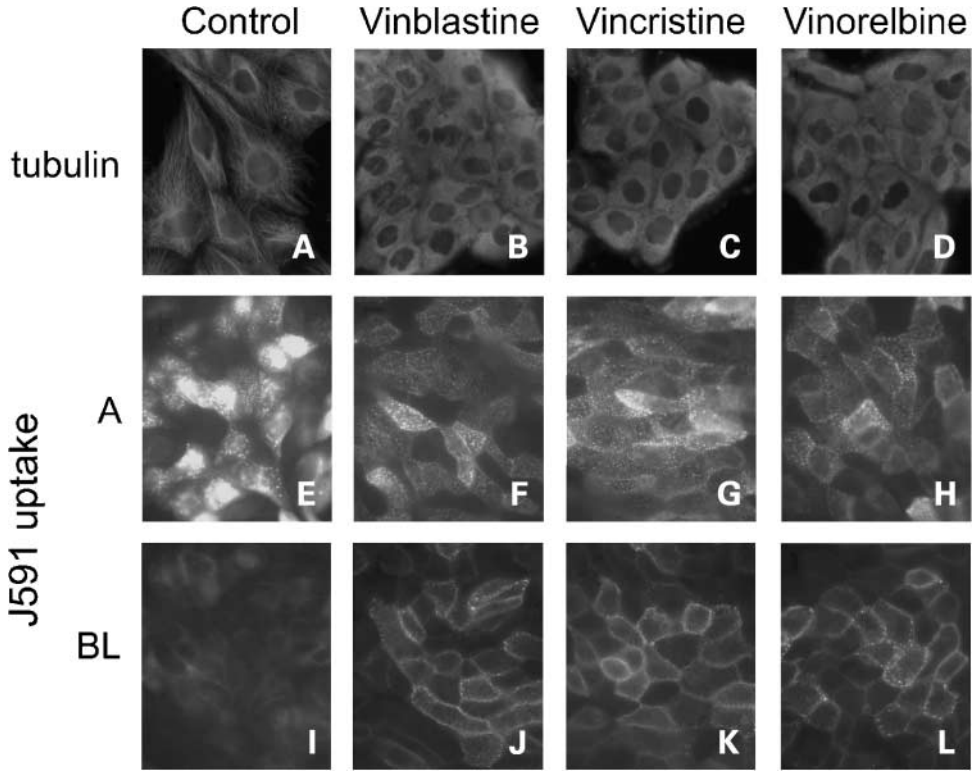

Figure 6. *Vinca* alkaloid treatment enhances J591 uptake from the basolateral surface. **A,** immunofluorescence analysis of α-tubulin reveals intact microtubules in untreated control cells. Extensive microtubules depolymerization is observed following treatment with the *Vinca* alkaloids, vinblastine (**B**), vincristine (**C**), and vinorelbine (**D**). **E,** immunofluorescence analysis following a 30-minute incubation with mAb J591 (5 μg/mL) added to the apical (*A*) chamber reveals intense staining for untreated control cells. **F-H,** although staining is relatively less intense than in control cells, immunofluorescence staining is also observed following treatment with *Vinca* alkaloids when J591 was added to the apical chamber. **I,** very minimal immunofluorescence staining is observed in control cells following incubation with J591 added to the basolateral (*BL*) chamber. **J-L,** treatment with *Vinca* alkaloids results in a dramatic increase in J591 internalized from the basolateral chamber. Bar, 10 μm.

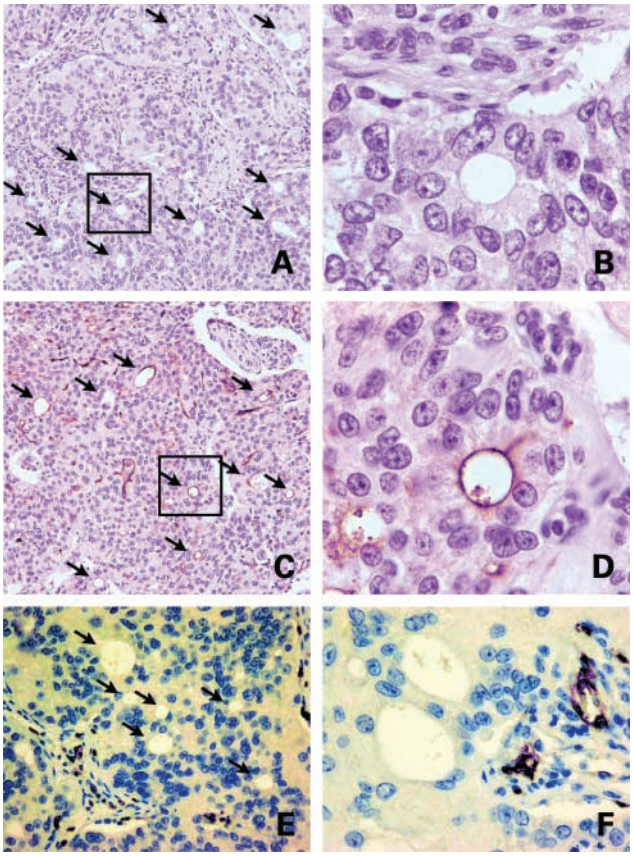

Figure 7. Metastatic prostate cancer cells within the lymph node maintain a well-differentiated epithelial morphology. **A,** histologic examination of a pelvic lymph node replaced by metastatic prostate adenocarcinoma reveals high tumor cell density and extensive tumor infiltration. Small areas where tumor cells are foaming acinar/glandular-appearing structures (*arrows*). **B,** on the high-magnification microscopic picture, the boxed region reveals a structure reminiscent of well-differentiated epithelial tissue, with a distinct lumenal space. **C** and **D,** immunohistochemical analysis of this area with antibodies to PSMA reveals polarized expression of PSMA on the apical plasma membrane at the lumenal surface of these glandular structures. In addition, some PSMA staining was visible in endothelial cells surrounding small lymphovascular lumens (**C**, *arrowhead*). **E** and **F,** immunohistochemical analysis shows that endothelial cells surrounding lymphovascular lumens stain positively for CD34. Immunohistochemical analysis of CD31 shows identical staining to CD34 (data not shown).

Because PSMA is normally targeted directly to the apical plasma membrane, therapeutic antibodies to PSMA would only bind to highly transformed and poorly differentiated tumor cells. Interestingly, we have previously observed that E-cadherin maintained a polarized expression pattern at the basolateral surface in primary prostatic tumors, even with Gleason scores up to 9 (24). Furthermore, our data show that PSMA is distributed in a highly asymmetrical fashion on the plasma membrane of some metastatic prostate cancer cells. Whereas metastatic cells are generally considered highly transformed and nonpolarized, our novel finding suggests that even within occult metastatic lesions, populations of prostatic carcinoma cells maintain a well-differentiated epithelial morphology. These results indicate that cells within high-grade primary and metastatic prostate tumors are capable of maintaining a well-differentiated morphology.

Therefore, whereas PSMA-based immunotherapy would be most effective at combating highly transformed prostate cancer cells, such an approach would offer little tangible benefit for treatment of well-differentiated tumor cells. Thus, therapeutic strategies designed to reduce the obstructive influence of epithelial barriers could substantially improve the efficacy of mAb based immunotherapy. Analogous strategies to mitigate endothelial barriers by enhancing vascular permeability or intraepithelial transport have improved mAb uptake into tumor tissues (43, 51, 52). Whereas such an approach to increase the permeability of epithelial junctions may not always be feasible, those designed to alter the polarized protein trafficking may hold significant promise for the treatment of disease. Therefore, the microtubule requirement for proper PSMA localization to the apical plasma membrane could have important implications for therapy.

We have shown that treatment of polarized epithelial cells with microtubule-targeting chemotherapeutic *Vinca* alkaloids resulted in increased binding and endocytosis of PSMA-specific antibodies from the basolateral surface in an *in vitro* system. To our knowledge, this is the first study to suggest that commonly used chemotherapeutic agents can be exploited to target intrinsic protein trafficking machinery as a means to reverse the apical polarity of an antigen to the basolateral plasma membrane. Although this has yet to be proven using an *in vivo* system, it seems that a combined therapeutic strategy to target both microtubules and an antigenic target, like PSMA, could have a synergistic effect on overall patient outcome.

Acknowledgments

We thank Dr. Jean De Vellis for use of the Zeiss Axiovert 200 confocal microscope and Dr. Warren Heston for providing the cDNA encoding PSMA.

References

1. Silver DA, Pellicer I, Fair WR, Heston WD, Cordon-Cardo C. Prostate-specific membrane antigen expression in normal and malignant human tissues. Clin Cancer Res 1997;3:81 – 5.

2. Sweat SD, Pacelli A, Murphy GP, Bostwick DG. Prostate-specific membrane antigen expression is greatest in prostate adenocarcinoma and lymph node metastases. Urology 1998;52:637 – 40.

3. Wright GL Jr, Grob BM, Haley C, et al. Upregulation of prostate-specific membrane antigen after androgen-deprivation therapy. Urology 1996;48: 326 – 34.

4. Ross JS, Sheehan CE, Fisher HA, et al. Correlation of primary tumor prostate-specific membrane antigen expression with disease recurrence in prostate cancer. Clin Cancer Res 2003;9:6357 – 62.

5. Chang SS, Heston WD. The clinical role of prostate-specific membrane antigen (PSMA). Urol Oncol 2002;7:7 – 12.

6. Christiansen JJ, Rajasekaran AK. Biological impediments to monoclonal antibody based immunotherapy. Mol Cancer Ther 2004;3:1493 – 506.

7. Rodriguez-Boulan E, Salas PJ, Sargiacomo M, et al. Methods to estimate the polarized distribution of surface antigens in cultured epithelial cells. Methods Cell Biol 1989;32:37 – 56.

8. Anderson JM, Van Itallie CM. Tight junctions and the molecular basis for regulation of paracellular permeability. Am J Physiol 1995;269: G467 – 75.

9. van Meer G, Simons K. The function of tight junctions in maintaining differences in lipid composition between the apical and the basolateral cell surface domains of MDCK cells. EMBO J 1986;5:1455 – 64.

10. Simons K, Wandinger-Ness A. Polarized sorting in epithelia. Cell 1990;62:207 – 10.

11. Apodaca G, Bomsel M, Arden J, Breitfeld PP, Tang K, Mostov KE. The polymeric immunoglobulin receptor. A model protein to study transcytosis. J Clin Invest 1991;87:1877 – 82.

12. Hunziker W, Fumey C. A di-leucine motif mediates endocytosis and basolateral sorting of macrophage IgG Fc receptors in MDCK cells. EMBO J 1994;13:2963 – 7.

13. Honing S, Hunziker W. Cytoplasmic determinants involved in direct lysosomal sorting, endocytosis, and basolateral targeting of rat lgp120 (lamp-I) in MDCK cells. J Cell Biol 1995;128:321 – 32.

14. Scheiffele P, Peranen J, Simons K. *N*-glycans as apical sorting signals in epithelial cells. Nature 1995;378:96 – 8.

15. Yeaman C, Le Gall AH, Baldwin AN, Monlauzeur L, Le Bivic A, Rodriguez-Boulan E. The *O*-glycosylated stalk domain is required for apical sorting of neurotrophin receptors in polarized MDCK cells. J Cell Biol 1997;139:929 – 40.

16. Moyer BD, Denton J, Karlson KH, et al. A PDZ-interacting domain in CFTR is an apical membrane polarization signal. J Clin Invest 1999; 104:1353 – 61.

17. Brown DA, Rose JK. Sorting of GPI-anchored proteins to glycolipid-enriched membrane subdomains during transport to the apical cell surface. Cell 1992;68:533 – 44.

18. Barman S, Nayak DP. Analysis of the transmembrane domain of influenza virus neuraminidase, a type II transmembrane glycoprotein, for apical sorting and raft association. J Virol 2000;74:6538 – 45.

19. Chuang JZ, Sung CH. The cytoplasmic tail of rhodopsin acts as a novel apical sorting signal in polarized MDCK cells. J Cell Biol 1998; 142:1245 – 56.

20. Bacallao R, Antony C, Dotti C, Karsenti E, Stelzer EH, Simons K. The subcellular organization of Madin-Darby canine kidney cells during the formation of a polarized epithelium. J Cell Biol 1989;109:2817 – 32.

21. Zegers MM, Zaal KJ, van Ijzendoorn SC, Klappe K, Hoekstra D. Actin filaments and microtubules are involved in different membrane traffic pathways that transport sphingolipids to the apical surface of polarized HepG2 cells. Mol Biol Cell 1998;9:1939 – 49.

22. Tai AW, Chuang JZ, Sung CH. Cytoplasmic dynein regulation by subunit heterogeneity and its role in apical transport. J Cell Biol 2001; 153:1499 – 509.

23. Breitfeld PP, McKinnon WC, Mostov KE. Effect of nocodazole on vesicular traffic to the apical and basolateral surfaces of polarized MDCK cells. J Cell Biol 1990;111:2365 – 73.

24. Christiansen JJ, Rajasekaran SA, Moy P, et al. Polarity of prostate specific membrane antigen, prostate stem cell antigen, and prostate specific antigen in prostate tissue and in a cultured epithelial cell line. Prostate 2003;55:9 – 19.

25. Rajasekaran SA, Palmer LG, Quan K, et al. Na,K-ATPase β-subunit is required for epithelial polarization, suppression of invasion, and cell motility. Mol Biol Cell 2001;12:279 – 95.

26. Liu H, Rajasekaran AK, Moy P, et al. Constitutive and antibody-induced internalization of prostate-specific membrane antigen. Cancer Res 1998;58:4055 – 60.

27. Sun Y, Ball WJ Jr. Identification of antigenic sites on the Na+/K(+)-ATPase β-subunit: their sequences and the effects of thiol reduction upon their structure. Biochim Biophys Acta 1994;1207:236 – 48.

28. Abbott A, Ball WJ Jr. The epitope for the inhibitory antibody M7-PB-E9 contains Ser-646 and Asp-652 of the sheep Na+,K(+)-ATPase α-subunit. Biochemistry 1993;32:3511 – 8.

29. Gonzalez-Mariscal L, Chavez de Ramirez B, Cereijido M. Tight junction formation in cultured epithelial cells (MDCK). J Membr Biol 1985;86:113 – 25.

30. Rajasekaran AK, Hojo M, Huima T, Rodriguez-Boulan E. Catenins and zonula occludens-1 form a complex during early stages in the assembly of tight junctions. J Cell Biol 1996;132:451 – 63.

31. Le Bivic A, Real FX, Rodriguez-Boulan E. Vectorial targeting of apical and basolateral plasma membrane proteins in a human adenocarcinoma epithelial cell line. Proc Natl Acad Sci U S A 1989; 86:9313 – 7.

32. Holmes EH, Greene TG, Tino WT, et al. Analysis of glycosylation of prostate-specific membrane antigen derived from LNCaP cells, prostatic carcinoma tumors, and serum from prostate cancer patients. Prostate Suppl 1996;7:25 – 9.

33. Su T, Cariappa R, Stanley K. *N*-glycans are not a universal signal for apical sorting of secretory proteins. FEBS Lett 1999;453:391 – 4.

34. Gut A, Kappeler F, Hyka N, Balda MS, Hauri HP, Matter K. Carbohydrate-mediated Golgi to cell surface transport and apical targeting of membrane proteins. EMBO J 1998;17:1919 – 29.

35. Marmorstein AD, Csaky KG, Baffi J, Lam L, Rahaal F, Rodriguez-Boulan E. Saturation of, and competition for entry into, the apical secretory pathway. Proc Natl Acad Sci U S A 2000;97:3248 – 53.

36. Griffiths G, Fuller SD, Back R, Hollinshead M, Pfeiffer S, Simons K. The dynamic nature of the Golgi complex. J Cell Biol 1989;108:277 – 97.

37. Kreitzer G, Schmoranzer J, Low SH, et al. Three-dimensional analysis of post-Golgi carrier exocytosis in epithelial cells. Nat Cell Biol 2003;5:126 – 36.

38. Saunders C, Limbird LE. Disruption of microtubules reveals two independent apical targeting mechanisms for G-protein-coupled receptors in polarized renal epithelial cells. J Biol Chem 1997;272:19035 – 45.

39. Ballangrud AM, Yang WH, Charlton DE, et al. Response of LNCaP spheroids after treatment with an α-particle emitter (213Bi)-labeled anti-prostate-specific membrane antigen antibody (J591). Cancer Res 2001;61:2008 – 14.

40. McDevitt MR, Barendswaard E, Ma D, et al. An α-particle emitting antibody ([213Bi]J591) for radioimmunotherapy of prostate cancer. Cancer Res 2000;60:6095 – 100.

41. Bander NH, Trabulsi EJ, Kostakoglu L, et al. Targeting metastatic prostate cancer with radiolabeled monoclonal antibody J591 to the extracellular domain of prostate specific membrane antigen. J Urol 2003;170:1717 – 21.

42. Countouriotis A, Moore TB, Sakamoto KM. Cell surface antigen and molecular targeting in the treatment of hematologic malignancies. Stem Cells 2002;20:215 – 29.

43. Khawli LA, Miller GK, Epstein AL. Effect of seven new vasoactive immunoconjugates on the enhancement of monoclonal antibody uptake in tumors. Cancer 1994;73:824 – 31.

44. Epenetos AA, Snook D, Durbin H, Johnson PM, Taylor-Papadimitriou J. Limitations of radiolabeled monoclonal antibodies for localization of human neoplasms. Cancer Res 1986;46:3183 – 91.

45. Au JL, Jang SH, Zheng J, et al. Determinants of drug delivery and transport to solid tumors. J Control Release 2001;74:31 – 46.

46. Jain RK. Vascular and interstitial barriers to delivery of therapeutic agents in tumors. Cancer Metastasis Rev 1990;9:253 – 66.

47. Ahnen DJ, Nakane PK, Brown WR. Ultrastructural localization of carcinoembryonic antigen in normal intestine and colon cancer: abnormal distribution of CEA on the surfaces of colon cancer cells. Cancer 1982;49:2077 – 90.

48. Tobioka H, Isomura H, Kokai Y, Sawada N. Polarized distribution of carcinoembryonic antigen is associated with a tight junction molecule in human colorectal adenocarcinoma. J Pathol 2002;198: 207 – 12.

49. Delaloye B, Bischof-Delaloye A, Buchegger F, et al. Detection of colorectal carcinoma by emission-computerized tomography after injection of 123I-labeled Fab or F(ab′)2 fragments from monoclonal anti-carcinoembryonic antigen antibodies. J Clin Invest 1986;77:301 – 11.

50. Mach JP, Buchegger F, Forni M, et al. Immunoscintigraphy for the detection of human carcinoma after injection of radiolabeled monoclonal anti-carcinoembryonic antigen antibodies. Curr Top Microbiol Immunol 1983;104:49 – 55.

51. McIntosh DP, Tan XY, Oh P, Schnitzer JE. Targeting endothelium and its dynamic caveolae for tissue-specific transcytosis *in vivo*: a pathway to overcome cell barriers to drug and gene delivery. Proc Natl Acad Sci U S A 2002;99:1996 – 2001.

52. Curnis F, Sacchi A, Corti A. Improving chemotherapeutic drug penetration in tumors by vascular targeting and barrier alteration. J Clin Invest 2002;110:475 – 82.

Is Prostate Specific Membrane Antigen A Multifunctional Protein?

Ayyappan K. Rajasekaran†, Gopalakrishnapillai Anilkumar, and Jason J. Christiansen

Department of Pathology and Laboratory Medicine, David Geffen School of Medicine,
University of California, Los Angeles, California 90095.

†Correspondence should be addressed to
Ayyappan K. Rajasekaran
Department of Pathology and Laboratory Medicine
Room 13-344 CHS
University of California, Los Angeles
Los Angeles, California 90095
Phone (310) 825-1199
Fax (310) 267-2410
Email: arajasekaran@mednet.ucla.edu

Running head: Is PSMA a multi-functional protein?

ABSTRACT

Prostate Specific Membrane Antigen (PSMA) is a metallopeptidase predominantly expressed in prostate cancer (PCa) cells. PSMA is considered as a biomarker for PCa and is under intense investigation for use as an imaging and therapeutic target. Although the clinical utility of PSMA in the detection and treatment of PCa is evident and is intensely pursued, very little is known about its basic biological function in PCa cells. The purpose of this review is to highlight the possibility that PSMA might be a multifunctional protein. We suggest that PSMA may have the function of a receptor internalizing a putative ligand, an enzyme playing a role in nutrient uptake, and a peptidase involved in signal transduction in prostate epithelial cells. Insights into possible functions of PSMA should improve the diagnostic and therapeutic values of this clinically important molecule.

prostate cancer; receptor; peptidase; endocytosis

OVERVIEW

Prostate specific membrane antigen (PSMA) was originally defined by the monoclonal antibody (mAb) 7E11 derived from immunization with a partially purified membrane preparation from the LNCaP prostatic adenocarcinoma cell line (26). Initial analysis demonstrated the widespread expression of PSMA within the cells of the prostatic secretory epithelium. Immunohistochemical staining demonstrated that PSMA was absent to moderate in hyperplastic and benign tissues, while malignant tissues stained with the greatest degree of intensity (26).

Subsequent investigations have recapitulated these results and evinced PSMA expression as a universal feature in practically every prostatic tissue examined to date. These reports further demonstrate that expression of PSMA increases precipitously in a manner proportional to tumor agressiveness (9, 13, 14, 30, 34, 50, 55, 64, 66, 71).

Consistent with the correlation between PSMA expression and tumor stage, increased levels of PSMA are associated with androgen-independent prostate cancer. Analysis of tissue samples from prostate cancer patients demonstrated elevated PSMA levels following physical castration or androgen-deprivation therapy. Unlike expression of PSA, which is downregulated following androgen ablation, PSMA expression is significantly increased in both primary and metastatic tumor specimens (30, 71). Consistent with the elevated expression in androgen-independent tumors, PSMA transcription is also known to be downregulated by steroids, and administration of testosterone mediates a dramatic reduction in PSMA protein and mRNA levels (27, 71). PSMA is also highly expressed in secondary prostatic tumors and occult metastatic disease. Immunohistochemical analysis revealed relatively intense and homogeneous expression

of PSMA within metastatic lesions localized to lymph nodes, bone, soft tissue and lungs, as compared to benign prostatic tissues (14, 40, 64).

Some reports have also indicated limited PSMA expression in extraprostatic tissues, including a subset of renal proximal tubules, some cells of the intestinal brush border, and rare cells in the colonic crypts (13, 26, 27, 36, 66). However, the levels of PSMA in these tissues are generally two to three orders of magnitude less than those observed in the prostate (58). PSMA is also expressed in the tumor-associated neovasculature of most solid cancers examined, yet is absent in the normal vascular endothelium (13, 34, 55). Although the significance of PSMA expression within the vasculature is unknown, the specificity for tumor-associated endothelium makes PSMA an intriguing potential target for the treatment of many forms of malignancy.

The highly restricted expression of PSMA and the upregulation in advanced carcinoma and metastatic disease portend a promising role for PSMA as a clinical biomarker for the diagnosis, detection, and management of prostate cancer. Furthermore, as an integral membrane protein, PSMA can be exploited as an antigenic target for a variety of clinical applications (19).

Immunoscintographic scanning using an ^{111}In labeled form of mAb 7E11 has shown promise for the detection and *in vivo* imaging of PSMA expressing tumor cells. This antibody has received FDA approval for the detection and imaging of metastatic prostate cancer in soft tissues and is currently marketed under the name of ProstaScint (Cytogen, Philadelphia, PA) (24, 36, 49). However, positive signals detected with this technology is likely ascribed to immunoreactivity of this antibody in dead or dying cells within a tumor mass, as the mAb 7E11 recognizes an intracellular epitope and is incapable of binding to viable cells (67). This observation provides a rationale to explain why ProstaScint is more effective at identifying metastases in well-vascularized soft tissues than in bone, in which metastatic lesions tend to be

relatively small and do not characteristically have a high percentage of necrotic or apoptotic cells. Development and application of antibodies that recognize epitopes encoded within the extracellular domain of PSMA substantially enhanced the sensitivity and should improve the usefulness of PSMA-based *in vivo* imaging techniques (24, 34).

In addition to *in vivo* imaging strategies, the use of PSMA specific antibodies is also being assessed for therapeutic purposes. PSMA specific mAbs have been conjugated to radionuclides and cytotoxic drugs (5, 6, 17, 38, 41). Such mAbs can be exploited as a vehicle with which to deliver concentrated doses of therapeutic agents directly to the site of prostate tumor cells, while sparing damage to normal tissues. These antibodies can induce cell death specifically in PSMA expressing cells and reduce the size of LNCaP spheroids, *in vitro* (57). Furthermore, administration of a single dose of radioactively labeled PSMA-specific mAbs was able to achieve a 15-90% reduction in mean tumor volume in xenograft bearing mice, concomitant with a 2 to 3 fold increase in the median survival time, relative to untreated control mice (69).

Despite the potential use of PSMA for immunotherapy of PCa, a paucity of information exists regarding the physiological functions of this protein. The purpose of this review is to highlight the possible functions of PSMA based upon its structural and enzymatic properties, cellular localization, trafficking route, interacting partners, and information gathered from related proteins.

STRUCTURE OF PSMA

The PSMA gene consists of 19 exons that span approximately 60 kb of genomic DNA. This gene encodes a type II transmembrane protein with a short, N-terminal cytoplasmic tail (19

amino acids), a single hydrophobic transmembrane domain (24 amino acids), and a large extracellular domain (707 amino acids) at the C-terminus (Figure 1) (28, 43).

The extracellular domain of PSMA is highly glycosylated, with N-linked oligosaccharides accounting for up to 25% of the molecular weight of the native protein (25). Regions within this domain share modest degrees of homology with the transferrin receptor (TfR) (28) and with members of the M28 family of co-catalytic aminopeptidases (47). Although the TfR has only a vestigial catalytic site, PSMA is known to possess both N-acetylated alpha-linked acidic dipeptidase (NAALADase) and folate hydrolase activities (11, 45). These two related peptidase activities hydrolyze gamma-peptide bonds between N-acetylaspartate and glutamate in the abundant neuropeptide N-acetylaspartylglutamate (NAAG) and the gamma-glutamyl linkages in pteroylpolyglutamate, respectively. The enzymatic activity of PSMA is largely inhibited phosphate, even at millimolar concentrations (56), and is dependent upon glycosylation and dimerization for proper function (18, 53). In contrast to the large extracellular domain, the cytoplasmic tail of PSMA consists of just 19 amino acids. In spite of its diminutive stature, the cytoplasmic domain interacts with a number of proteins and has a major impact on the localization and molecular properties of PSMA (2, 46).

Evidence using RT-PCR suggests the existence of alternative PSMA isoforms, including PSM' and recently described PSM-B and PSM-C. In contrast to the integral transmembrane orientation of full length PSMA, these variants are believed to exist within the cytosol and are thought to be the consequence of alternative splicing of the PSMA gene (52, 60). Although reports have suggested that the ratio of transmembrane to cytosolic PSMA transcript increases with cancer in a manner proportional to advancing disease grade, little is known regarding the significance of alternatively spliced PSMA mRNA.

A murine homologue to PSMA has also been identified. This protein is referred to as glutamate carboxypeptidase II (GCP-II) and shares over 80% amino acid identity within the extracellular domain and possesses the same enzymatic peptidase activities as human PSMA (3). Interestingly, while Tsai and colleagues reported that ablation of GCP-II resulted in embryonic lethality; Bacich and colleagues reported that GCP-II knockout mice experienced no detectable detriment (4, 68). The reasons for this discrepancy are not completely clear, highlighting the fact that caution must be taken when attempting to extrapolate data from mouse models to human PSMA. Additionally, these two homologues display disparate profiles of tissue expression (3) and deletion of GCP-II gene expression did not result in loss of NAALADase activity, suggesting the functional redundancy of this enzyme in murine cells (4). Furthermore, while PSMA and GCP-II share significant homology within their respective extracellular domains, these proteins have minimal conservation of sequence homology within their cytoplasmic domains, including domains involved in mediating PSMA endocytic traffic and binding of interacting partners, such as filamin a (FLNa) (2, 3, 46).

DIMERIZATION OF PSMA

Homodimerization is a fundamental feature of many transmembrane receptors. Induction of homodimer formation is often induced by ligand binding, which is in turn necessary for mediating the cellular response of the receptor (51). The TfR is an archetypal example of one such receptor. This type II transmembrane protein is involved in regulating cellular iron homeostasis through binding and internalization of iron-laden transferrin (1).

PSMA shares considerable homology with the TfR, both at the level of amino acid identity and at the level of domain organization (37). Like the TfR, PSMA is expressed as a non-

covalently linked homodimer on the cell surface (33, 53). This dimerization is apparently mediated by epitopes within the large extracellular domain, as truncated versions of PSMA lacking the cytoplasmic and transmembrane domains are still capable of interacting. PSMA dimerization is critical to maintain the conformation and enzymatic activity of PSMA (53). Although the possibility has yet to be fully addressed, the similarity between PSMA and TfR at the amino acid and structural level, combined with the common dimerization requirement, may suggest that these proteins share similar receptor and ligand transport functions.

RESEMBLANCE OF PSMA CELLULAR TRAFFICKING WITH MEMBRANE RECEPTORS

A variety of transmembrane receptors and membrane components are internalized from the plasma membrane and trafficked through the endocytic system. This endocytic trafficking allows cells to maintain homeostasis and internalize vital nutrients, lipids, and proteins. For example, binding of iron bound transferrin to the TfR results in an induction of receptor internalization and iron transport into the cell (31). Additionally, endocytosis of membrane receptors is also an established mechanism to down-regulate signal transduction cascades. One classical example is the regulation of epidermal growth factor receptor (EGFR) signaling. Binding of epidermal growth factor (EGF) induces EGFR endocytosis and signal attenuation (12).

Like the transferrin and EGF receptors, PSMA undergoes endocytosis from the plasma membrane. This endocytosis occurs through clathrin-coated pits and involves the first five N-terminal amino acids of the cytoplasmic tail. This motif of MWNLL appears to constitute a novel endocytic-targeting signal and likely interacts with the AP-2 adaptor protein complex (46).

Although PSMA is constitutively internalized from the cell surface, binding of antibodies or related antibody fragments to the extracellular domain increases the rate of PSMA internalization (35). These antibodies may be acting like a natural ligand, thus indicating that, like the TfR, PSMA may have a receptor function involved in endocytosis of a putative unknown ligand.

Interestingly, the NAALADase activity of PSMA is inhibited by the millimolar concentration of phosphate present in culture media (65). Therefore, since internalization assays are done under normal culture conditions, it appears that NAALADase activity is not required for the internalization function of PSMA. In addition, N-acetyl-aspartyl-glutamate (NAAG), a well-known substrate of PSMA did not increase the rate of PSMA internalization in PCa cells (our unpublished data).

Following endocytosis, a number of receptors are recycled back to the plasma membrane surface. While some proteins are recycled directly from early endosomes, other receptors are first targeted to a tubulovesicular membrane structure proximal to the centrosomes referred to as the recycling endosomal compartment (REC) (39, 48). The TfR is one of the best-studied markers of the REC. Following internalization, PSMA is targeted to the REC with similar kinetics to the TfR (2, 46).

The antibody induced, clathrin mediated internalization of PSMA and the accumulation in the REC supports the hypothesis that PSMA might function as a receptor internalizing a putative ligand. Whether PSMA acts in a manner analogous to the TfR in the transport or metabolism of specific elements, or like the EGFR in the regulation of signal transduction has yet to be addressed. However, future studies to identify the ligand of PSMA are crucial to answer this question.

ASSOCIATION OF PSMA WITH FILAMIN A (FLNa), AN ACTIN FILAMENT CROSS-LINKING PROTEIN

FLNa is a dimeric actin cross-linking phosphoprotein that plays a vital role in the stabilization of many receptors at the plasma membrane (59). It is known that many membrane receptors, like the metabotropic glutamate receptor, dopamine receptor, calcitonin receptor, tumor necrosis factor receptor and insulin receptor, interact with FLNa. The interaction between FLNa and these receptors plays a crucial role in modulating receptor function (16, 23, 54).

Using the N-terminal 19 amino acids as bait, the cytoplasmic domain was shown in to interact with the 23rd to 24th repeat of FLNa in a yeast two-hybrid assay. When expressed in a filamin-negative cell line, PSMA was rapidly internalized from the cell surface; however, ectopic expression of filamin A in these cells resulted in a 50% reduction in the rate of PSMA internalization. These data suggest that filamin A may stabilize PSMA at the cell surface by tethering it to the actin cytoskeleton, likely preventing AP-2 from binding. Interestingly, expression of FLNa also reduced the NAALADase activity of PSMA at the cell surface, perhaps by inducing a conformational change in the extracellular domain (2). These data suggest that competitive binding of AP-2 and FLNa to the PSMA cytoplasmic tail regulate endocytosis, recycling, and enzymatic activities of PSMA. Furthermore, the fact that glutamate receptor, a protein that transports glutamate, and PSMA, an enzyme that releases glutamate, both bind to FLNa raises the intriguing possibility that PSMA and glutamate receptor exist as a multi-protein complex on the plasma membrane. This interaction would potentially facilitate the generation and transport of glutamate into the cell.

FLNa is also known to play a role in cell adhesion and motility. Calderwood and colleagues have evinced an interaction between β integrin and FLNa, and further demonstrated

that this interaction is inhibitory to cell migration (10). Another binding partner for FLNa is RalA, a small GTP binding protein known to play a role in filopodia formation (42). We have seen an accumulation of PSMA in filopodial structures (our unpublished data) and it is not known whether this observation points towards a role for PSMA in cell migration.

RESEMBLANCE OF PSMA TO MULTIFUNCTIONAL PEPTIDASES

Numerous examples suggest a role for enzymatic peptidases in mediating cell migration by affecting signaling cascades. For example, the interaction of the neutral endopeptidase (NEP) cytoplasmic tail with Lyn kinases blocks the activation of PI3-kinase. This inhibition of PI3-kinase prevents FAK phosphorylation-mediated cell migration (62). NEP is also known to inhibit the proliferation of prostate epithelial cells by its direct association with PTEN (61). PTEN is a lipid and protein phosphatase, which inhibits PI3-kinase mediated activation of Akt, a kinase involved in cell survival. A catalytic mutant of NEP was also able to block the cell proliferation and migration, suggesting that the enzymatic activity of NEP was not necessarily required. Mutational analysis of the cytoplasmic tail of NEP identified a basic amino acid rich motif containing five lysine and arginine residues proximal to the transmembrane domain that mediates the interaction between NEP and PTEN (61). The cytoplasmic tail of PSMA also has a stretch of three basic arginine residues proximal to the membrane-spanning domain, thus raising a possibility that PSMA may also interact with PTEN.

CD26 is another interesting example of a multifunctional type II cell surface glycoprotein with important roles in cell signaling. This molecule is expressed on a wide variety of cells and possesses dipeptidyl peptidase IV (DPIV) activity (7, 8, 21). CD26 has been shown to regulate cell migration and proliferation independent of its enzymatic activity (20). CD26 is known to

bind adenosine deaminase, an enzyme involved in irreversible deamination of adenosine, and this association has been shown to be essential for the promotion of cell proliferation and cytokine production (29). CD26 has also been shown to affect the migratory behavior of T cells through interactions with extracellular matrix proteins such as collagen and fibronectin (22, 44). These examples clearly indicate that although PSMA is a peptidase, it could have multiple roles, not only as an enzyme but also as a protein with cell survival and migratory functions.

POTENTIAL ROLE OF PSMA ENZYME ACTIVITY IN PCa

Increased PSMA enzymatic peptidase activity is associated with metastatic PCa (32). However, the significance of these enzymatic activities in the context of benign and malignant prostatic cells remains to be elucidated.

The prostate gland is mainly composed of stromal, epithelial, and neuroendocrine cells. The dynamic balance of cell proliferation, differentiation, and apoptosis in general maintains the cellular and tissue homeostasis. This balance is generated by the continuous cross talk among these cell populations (63). For this purpose, epithelial and stromal cells secrete various types of growth factors, chemokines, and neuropeptides (70). Deregulation in this paracrine communication can result in derangement of the prostate gland such as benign prostate hyperplasia and prostate carcinoma (15). For example, the peptidase NEP normally acts to inhibit the migratory properties of prostate epithelial cells. NEP achieves the inhibition of prostatic epithelial cell migration by cleaving critical neuropeptides such as bombesin and endothelin and thereby prevents the relay of signal transduction mediated by G-protein coupled receptors (62). CD26 is also involved in regulation of paracrine signaling by promoting cleavage

of growth factors, chemokines, neuropeptides and hormones and thus contributes to the regulation of T-cell and monocyte migration (20).

Like NEP and CD26, PSMA is also a type II transmembrane glycoprotein with co-catalytic metallopeptidase activity. The increased expression of PSMA in prostatic adenocarcinoma may indicate a role in the cleavage of signaling molecules involved in maintaining prostate gland architecture and function. Although neuropeptide and growth factor substrates that influence signaling mechanisms have yet to be identified, the overexpression of PSMA could potentially disturb the growth balance of the prostate gland. Future investigation along these lines should provide important insights into the role of PSMA in prostate cancer.

CONCLUSION

In conclusion, we suggest that PSMA could be a multifunctional protein. We have summarized the potential multifunctional nature of PSMA in figure 2. Dimerization, structural similarity to TfR, and localization to REC indicate a potential receptor function for PSMA. NAALADase and folate hydrolase activities of PSMA are consistent with a role in enzyme activities involved in nutrient uptake. Interaction of PSMA with FLNa and its localization to filopodia indicates a possible role in cell migration. Finally, PSMA as a peptidase might also activate signaling cascades involved in cell survival, proliferation, and cell migration. Future investigations into these areas should provide valuable information regarding the possible functions of this clinically important molecule. Improved understanding of PSMA function should allow the fulfillment its therapeutic and diagnostic potential.

GRANTS

This work is supported by Department of Defense DAMD17-02-1-0661, W81XWH-04-1-0113, and NIH RO1-DK56216 grants to AKR. GA is supported by a Post Doctoral Traineeship award from Department of Defense W81XWH-04-1-0132.

ACKNOWLEDGEMENTS

We thank Sonali Barwe, Scott Raymond Maul and Sigrid Rajasekaran for the critical reading of the manuscript and Sonali Barwe for creating figure 2.

FOOTNOTES

Address for reprint requests and other correspondence: A. K. Rajasekaran, Room 13-344 CHS, University of California, Los Angeles, 10833 Le Conte Ave., Los Angeles, California, 90095. (E-mail: arajasekaran@mednet.ucla.edu)

FIGURE LEGENDS

Fig.1. Schematic diagram of PSMA structure. PSMA is a type II transmembrane protein with a short N-terminal cytoplasmic domain (CD), a hydrophobic transmembrane region (TM), and a large extracellular domain (ED). The CD contains an endocytic targeting motif and filamin A binding site (A). The large ED is highly glycosylated with 9 predicted N-glycosylation sites (Y). The ED contains 2 domains of unknown function that span amino acid residues 44-150 (B) and 151-274 (D), proline- and glycine-rich regions that span amino acid residues 145-172 and 249-273, respectively (C and E), a catalytic domain that spans amino acid residues 274-587 (F), and a final domain of unknown function (amino acids 587-750) to which a helical dimerization domain (amino acids 601-750) is localized (G).

Fig. 2 Representative diagram of the possible functions of PSMA. Evidence suggests that PSMA may perform multiple physiological functions within the cell. The peptidase activity and potential interaction with signaling molecules alludes to a role in signal transduction. Homodimerization of PSMA, homology to the transferrin receptor, and intracellular trafficking to the REC implies a role for PSMA as a receptor for an unidentified ligand. The peptidase activity of PSMA suggests a role in nutrient uptake, particularly related to glutamate absorption. The interaction of PSMA with FLNa and the localization to filapodial structures suggests a role in cell motility.

REFERENCES

1. **Aisen P.** Transferrin receptor 1. *Int J Biochem Cell Biol* 36: 2137-2143, 2004.
2. **Anilkumar G, Rajasekaran SA, Wang S, Hankinson O, Bander NH, and Rajasekaran AK.** Prostate-specific membrane antigen association with filamin A modulates its internalization and NAALADase activity. *Cancer Res* 63: 2645-2648, 2003.
3. **Bacich DJ, Pinto JT, Tong WP, and Heston WD.** Cloning, expression, genomic localization, and enzymatic activities of the mouse homolog of prostate-specific membrane antigen/NAALADase/folate hydrolase. *Mamm Genome* 12: 117-123, 2001.
4. **Bacich DJ, Ramadan E, O'Keefe DS, Bukhari N, Wegorzewska I, Ojeifo O, Olszewski R, Wrenn CC, Bzdega T, Wroblewska B, Heston WD, and Neale JH.** Deletion of the glutamate carboxypeptidase II gene in mice reveals a second enzyme activity that hydrolyzes N-acetylaspartylglutamate. *J Neurochem* 83: 20-29, 2002.
5. **Ballangrud AM, Yang WH, Charlton DE, McDevitt MR, Hamacher KA, Panageas KS, Ma D, Bander NH, Scheinberg DA, and Sgouros G.** Response of LNCaP spheroids after treatment with an alpha-particle emitter (213Bi)-labeled anti-prostate-specific membrane antigen antibody (J591). *Cancer Res* 61: 2008-2014, 2001.
6. **Bander NH, Trabulsi EJ, Kostakoglu L, Yao D, Vallabhajosula S, Smith-Jones P, Joyce MA, Milowsky M, Nanus DM, and Goldsmith SJ.** Targeting metastatic prostate cancer with radiolabeled monoclonal antibody J591 to the extracellular domain of prostate specific membrane antigen. *J Urol* 170: 1717-1721, 2003.
7. **Buhling F, Junker U, Reinhold D, Neubert K, Jager L, and Ansorge S.** Functional role of CD26 on human B lymphocytes. *Immunol Lett* 45: 47-51, 1995.
8. **Buhling F, Kunz D, Reinhold D, Ulmer AJ, Ernst M, Flad HD, and Ansorge S.** Expression and functional role of dipeptidyl peptidase IV (CD26) on human natural killer cells. *Nat Immun* 13: 270-279, 1994.
9. **Burger MJ, Tebay MA, Keith PA, Samaratunga HM, Clements J, Lavin MF, and Gardiner RA.** Expression analysis of delta-catenin and prostate-specific membrane antigen: their potential as diagnostic markers for prostate cancer. *Int J Cancer* 100: 228-237, 2002.
10. **Calderwood DA, Huttenlocher A, Kiosses WB, Rose DM, Woodside DG, Schwartz MA, and Ginsberg MH.** Increased filamin binding to beta-integrin cytoplasmic domains inhibits cell migration. *Nat Cell Biol* 3: 1060-1068, 2001.
11. **Carter RE, Feldman AR, and Coyle JT.** Prostate-specific membrane antigen is a hydrolase with substrate and pharmacologic characteristics of a neuropeptidase. *Proceedings of the National Academy of Sciences of the United States of America* 93: 749-753, 1996.
12. **Chang CP, Lazar CS, Walsh BJ, Komuro M, Collawn JF, Kuhn LA, Tainer JA, Trowbridge IS, Farquhar MG, Rosenfeld MG, and et al.** Ligand-induced internalization of the epidermal growth factor receptor is mediated by multiple endocytic codes analogous to the tyrosine motif found in constitutively internalized receptors. *J Biol Chem* 268: 19312-19320, 1993.
13. **Chang SS, Reuter VE, Heston WD, Bander NH, Grauer LS, and Gaudin PB.** Five different anti-prostate-specific membrane antigen (PSMA) antibodies confirm PSMA expression in tumor-associated neovasculature. *Cancer Res* 59: 3192-3198, 1999.
14. **Chang SS, Reuter VE, Heston WD, and Gaudin PB.** Comparison of anti-prostate-specific membrane antigen antibodies and other immunomarkers in metastatic prostate carcinoma. *Urology* 57: 1179-1183, 2001.

15. **Dawson LA, Maitland NJ, Turner AJ, and Usmani BA.** Stromal-epithelial interactions influence prostate cancer cell invasion by altering the balance of metallopeptidase expression. *Br J Cancer* 90: 1577-1582, 2004.
16. **Enz R.** The actin-binding protein Filamin-A interacts with the metabotropic glutamate receptor type 7. *FEBS Lett* 514: 184-188, 2002.
17. **Fracasso G, Bellisola G, Cingarlini S, Castelletti D, Prayer-Galetti T, Pagano F, Tridente G, and Colombatti M.** Anti-tumor effects of toxins targeted to the prostate specific membrane antigen. *Prostate* 53: 9-23, 2002.
18. **Ghosh A and Heston WD.** Effect of carbohydrate moieties on the folate hydrolysis activity of the prostate specific membrane antigen. *Prostate* 57: 140-151, 2003.
19. **Ghosh A and Heston WD.** Tumor target prostate specific membrane antigen (PSMA) and its regulation in prostate cancer. *J Cell Biochem* 91: 528-539, 2004.
20. **Gorrell MD, Gysbers V, and McCaughan GW.** CD26: a multifunctional integral membrane and secreted protein of activated lymphocytes. *Scand J Immunol* 54: 249-264, 2001.
21. **Gorrell MD, Wickson J, and McCaughan GW.** Expression of the rat CD26 antigen (dipeptidyl peptidase IV) on subpopulations of rat lymphocytes. *Cell Immunol* 134: 205-215, 1991.
22. **Hanski C, Huhle T, and Reutter W.** Involvement of plasma membrane dipeptidyl peptidase IV in fibronectin-mediated adhesion of cells on collagen. *Biol Chem Hoppe Seyler* 366: 1169-1176, 1985.
23. **He HJ, Kole S, Kwon YK, Crow MT, and Bernier M.** Interaction of filamin A with the insulin receptor alters insulin-dependent activation of the mitogen-activated protein kinase pathway. *J Biol Chem* 278: 27096-27104, 2003.
24. **Holmes EH.** PSMA specific antibodies and their diagnostic and therapeutic use. *Expert Opin Investig Drugs* 10: 511-519, 2001.
25. **Holmes EH, Greene TG, Tino WT, Boynton AL, Aldape HC, Misrock SL, and Murphy GP.** Analysis of glycosylation of prostate-specific membrane antigen derived from LNCaP cells, prostatic carcinoma tumors, and serum from prostate cancer patients. *Prostate Suppl* 7: 25-29, 1996.
26. **Horoszewicz JS, Kawinski E, and Murphy GP.** Monoclonal antibodies to a new antigenic marker in epithelial prostatic cells and serum of prostatic cancer patients. *Anticancer Res* 7: 927-935, 1987.
27. **Israeli RS, Powell CT, Corr JG, Fair WR, and Heston WD.** Expression of the prostate-specific membrane antigen. *Cancer Res* 54: 1807-1811, 1994.
28. **Israeli RS, Powell CT, Fair WR, and Heston WD.** Molecular cloning of a complementary DNA encoding a prostate-specific membrane antigen. *Cancer Res* 53: 227-230, 1993.
29. **Kameoka J, Tanaka T, Nojima Y, Schlossman SF, and Morimoto C.** Direct association of adenosine deaminase with a T cell activation antigen, CD26. *Science* 261: 466-469, 1993.
30. **Kawakami M and Nakayama J.** Enhanced expression of prostate-specific membrane antigen gene in prostate cancer as revealed by in situ hybridization. *Cancer Res* 57: 2321-2324, 1997.
31. **Klausner RD, Harford J, and van Renswoude J.** Rapid internalization of the transferrin receptor in K562 cells is triggered by ligand binding or treatment with a phorbol ester. *Proc Natl Acad Sci U S A* 81: 3005-3009, 1984.

32. **Lapidus RG, Tiffany CW, Isaacs JT, and Slusher BS.** Prostate-specific membrane antigen (PSMA) enzyme activity is elevated in prostate cancer cells. *Prostate* 45: 350-354, 2000.
33. **Lawrence CM, Ray S, Babyonyshev M, Galluser R, Borhani DW, and Harrison SC.** Crystal structure of the ectodomain of human transferrin receptor. *Science* 286: 779-782, 1999.
34. **Liu H, Moy P, Kim S, Xia Y, Rajasekaran A, Navarro V, Knudsen B, and Bander NH.** Monoclonal antibodies to the extracellular domain of prostate-specific membrane antigen also react with tumor vascular endothelium. *Cancer Res* 57: 3629-3634, 1997.
35. **Liu H, Rajasekaran AK, Moy P, Xia Y, Kim S, Navarro V, Rahmati R, and Bander NH.** Constitutive and antibody-induced internalization of prostate-specific membrane antigen. *Cancer Res* 58: 4055-4060, 1998.
36. **Lopes AD, Davis WL, Rosenstraus MJ, Uveges AJ, and Gilman SC.** Immunohistochemical and pharmacokinetic characterization of the site-specific immunoconjugate CYT-356 derived from antiprostate monoclonal antibody 7E11-C5. *Cancer Res* 50: 6423-6429, 1990.
37. **Mahadevan D and Saldanha JW.** The extracellular regions of PSMA and the transferrin receptor contain an aminopeptidase domain: implications for drug design. *Protein Sci* 8: 2546-2549, 1999.
38. **McDevitt MR, Barendswaard E, Ma D, Lai L, Curcio MJ, Sgouros G, Ballangrud AM, Yang WH, Finn RD, Pellegrini V, Geerlings MW, Jr., Lee M, Brechbiel MW, Bander NH, Cordon-Cardo C, and Scheinberg DA.** An alpha-particle emitting antibody ([213Bi]J591) for radioimmunotherapy of prostate cancer. *Cancer Res* 60: 6095-6100, 2000.
39. **Mukherjee S, Ghosh RN, and Maxfield FR.** Endocytosis. *Physiol Rev* 77: 759-803, 1997.
40. **Murphy GP, Barren RJ, Erickson SJ, Bowes VA, Wolfert RL, Bartsch G, Klocker H, Pointner J, Reissigl A, McLeod DG, Douglas T, Morgan T, Kenny GM, Ragde H, Boynton AL, and Holmes EH.** Evaluation and comparison of two new prostate carcinoma markers. Free-prostate specific antigen and prostate specific membrane antigen. *Cancer* 78: 809-818, 1996.
41. **Nanus DM, Milowsky MI, Kostakoglu L, Smith-Jones PM, Vallabahajosula S, Goldsmith SJ, and Bander NH.** Clinical use of monoclonal antibody HuJ591 therapy: targeting prostate specific membrane antigen. *J Urol* 170: S84-88; discussion S88-89, 2003.
42. **Ohta Y, Suzuki N, Nakamura S, Hartwig JH, and Stossel TP.** The small GTPase RalA targets filamin to induce filopodia. *Proc Natl Acad Sci U S A* 96: 2122-2128, 1999.
43. **O'Keefe DS, Su SL, Bacich DJ, Horiguchi Y, Luo Y, Powell CT, Zandvliet D, Russell PJ, Molloy PL, Nowak NJ, Shows TB, Mullins C, Vonder Haar RA, Fair WR, and Heston WD.** Mapping, genomic organization and promoter analysis of the human prostate-specific membrane antigen gene. *Biochim Biophys Acta* 1443: 113-127, 1998.
44. **Piazza GA, Callanan HM, Mowery J, and Hixson DC.** Evidence for a role of dipeptidyl peptidase IV in fibronectin-mediated interactions of hepatocytes with extracellular matrix. *Biochem J* 262: 327-334, 1989.
45. **Pinto JT, Suffoletto BP, Berzin TM, Qiao CH, Lin S, Tong WP, May F, Mukherjee B, and Heston WD.** Prostate-specific membrane antigen: a novel folate hydrolase in human prostatic carcinoma cells. *Clin Cancer Res* 2: 1445-1451, 1996.
46. **Rajasekaran SA, Anilkumar G, Oshima E, Bowie JU, Liu H, Heston W, Bander NH, and Rajasekaran AK.** A novel cytoplasmic tail MXXXL motif mediates the internalization of prostate-specific membrane antigen. *Mol Biol Cell* 14: 4835-4845, 2003.

47. **Rawlings ND and Barrett AJ.** Structure of membrane glutamate carboxypeptidase. *Biochim Biophys Acta* 1339: 247-252, 1997.
48. **Ren M, Xu G, Zeng J, De Lemos-Chiarandini C, Adesnik M, and Sabatini DD.** Hydrolysis of GTP on rab11 is required for the direct delivery of transferrin from the pericentriolar recycling compartment to the cell surface but not from sorting endosomes. *Proc Natl Acad Sci U S A* 95: 6187-6192, 1998.
49. **Rosenthal SA, Haseman MK, and Polascik TJ.** Utility of capromab pendetide (ProstaScint) imaging in the management of prostate cancer. *Tech Urol* 7: 27-37, 2001.
50. **Ross JS, Sheehan CE, Fisher HA, Kaufman RP, Jr., Kaur P, Gray K, Webb I, Gray GS, Mosher R, and Kallakury BV.** Correlation of primary tumor prostate-specific membrane antigen expression with disease recurrence in prostate cancer. *Clin Cancer Res* 9: 6357-6362, 2003.
51. **Schlessinger J.** Ligand-induced, receptor-mediated dimerization and activation of EGF receptor. *Cell* 110: 669-672, 2002.
52. **Schmittgen TD, Teske S, Vessella RL, True LD, and Zakrajsek BA.** Expression of prostate specific membrane antigen and three alternatively spliced variants of PSMA in prostate cancer patients. *Int J Cancer* 107: 323-329, 2003.
53. **Schulke N, Varlamova OA, Donovan GP, Ma D, Gardner JP, Morrissey DM, Arrigale RR, Zhan C, Chodera AJ, Surowitz KG, Maddon PJ, Heston WD, and Olson WC.** The homodimer of prostate-specific membrane antigen is a functional target for cancer therapy. *Proc Natl Acad Sci U S A* 100: 12590-12595, 2003.
54. **Seck T, Baron R, and Horne WC.** Binding of filamin to the C-terminal tail of the calcitonin receptor controls recycling. *J Biol Chem* 278: 10408-10416, 2003.
55. **Silver DA, Pellicer I, Fair WR, Heston WD, and Cordon-Cardo C.** Prostate-specific membrane antigen expression in normal and malignant human tissues. *Clin Cancer Res* 3: 81-85, 1997.
56. **Slusher BS, Vornov JJ, Thomas AG, Hurn PD, Harukuni I, Bhardwaj A, Traystman RJ, Robinson MB, Britton P, Lu XC, Tortella FC, Wozniak KM, Yudkoff M, Potter BM, and Jackson PF.** Selective inhibition of NAALADase, which converts NAAG to glutamate, reduces ischemic brain injury. *Nat Med* 5: 1396-1402, 1999.
57. **Smith-Jones PM, Vallabhajosula S, Navarro V, Bastidas D, Goldsmith SJ, and Bander NH.** Radiolabeled monoclonal antibodies specific to the extracellular domain of prostate-specific membrane antigen: preclinical studies in nude mice bearing LNCaP human prostate tumor. *J Nucl Med* 44: 610-617, 2003.
58. **Sokoloff RL, Norton KC, Gasior CL, Marker KM, and Grauer LS.** A dual-monoclonal sandwich assay for prostate-specific membrane antigen: levels in tissues, seminal fluid and urine. *Prostate* 43: 150-157, 2000.
59. **Stossel TP, Condeelis J, Cooley L, Hartwig JH, Noegel A, Schleicher M, and Shapiro SS.** Filamins as integrators of cell mechanics and signalling. *Nat Rev Mol Cell Biol* 2: 138-145, 2001.
60. **Su SL, Huang IP, Fair WR, Powell CT, and Heston WD.** Alternatively spliced variants of prostate-specific membrane antigen RNA: ratio of expression as a potential measurement of progression. *Cancer Res* 55: 1441-1443, 1995.
61. **Sumitomo M, Iwase A, Zheng R, Navarro D, Kaminetzky D, Shen R, Georgescu MM, and Nanus DM.** Synergy in tumor suppression by direct interaction of neutral endopeptidase with PTEN. *Cancer Cell* 5: 67-78, 2004.

62. **Sumitomo M, Shen R, Walburg M, Dai J, Geng Y, Navarro D, Boileau G, Papandreou CN, Giancotti FG, Knudsen B, and Nanus DM.** Neutral endopeptidase inhibits prostate cancer cell migration by blocking focal adhesion kinase signaling. *J Clin Invest* 106: 1399-1407, 2000.
63. **Sung SY and Chung LW.** Prostate tumor-stroma interaction: molecular mechanisms and opportunities for therapeutic targeting. *Differentiation* 70: 506-521, 2002.
64. **Sweat SD, Pacelli A, Murphy GP, and Bostwick DG.** Prostate-specific membrane antigen expression is greatest in prostate adenocarcinoma and lymph node metastases. *Urology* 52: 637-640, 1998.
65. **Tiffany CW, Cai NS, Rojas C, and Slusher BS.** Binding of the glutamate carboxypeptidase II (NAALADase) inhibitor 2-PMPA to rat brain membranes. *Eur J Pharmacol* 427: 91-96, 2001.
66. **Troyer JK, Beckett ML, and Wright GL, Jr.** Detection and characterization of the prostate-specific membrane antigen (PSMA) in tissue extracts and body fluids. *Int J Cancer* 62: 552-558, 1995.
67. **Troyer JK, Feng Q, Beckett ML, and Wright GL.** Biochemical characterization and mapping of the 7E11-C5.3 epitope of the prostate-specific membrane antigen. *Urol Oncol* 1: 29-37, 1995.
68. **Tsai G, Dunham KS, Drager U, Grier A, Anderson C, Collura J, and Coyle JT.** Early embryonic death of glutamate carboxypeptidase II (NAALADase) homozygous mutants. *Synapse* 50: 285-292, 2003.
69. **Vallabhajosula S, Smith-Jones PM, Navarro V, Goldsmith SJ, and Bander NH.** Radioimmunotherapy of prostate cancer in human xenografts using monoclonal antibodies specific to prostate specific membrane antigen (PSMA): Studies in nude mice. *Prostate* 58: 145-155, 2004.
70. **Wong YC and Wang YZ.** Growth factors and epithelial-stromal interactions in prostate cancer development. *Int Rev Cytol* 199: 65-116, 2000.
71. **Wright GL, Jr., Grob BM, Haley C, Grossman K, Newhall K, Petrylak D, Troyer J, Konchuba A, Schellhammer PF, and Moriarty R.** Upregulation of prostate-specific membrane antigen after androgen-deprivation therapy. *Urology* 48: 326-334, 1996.

Figure 1

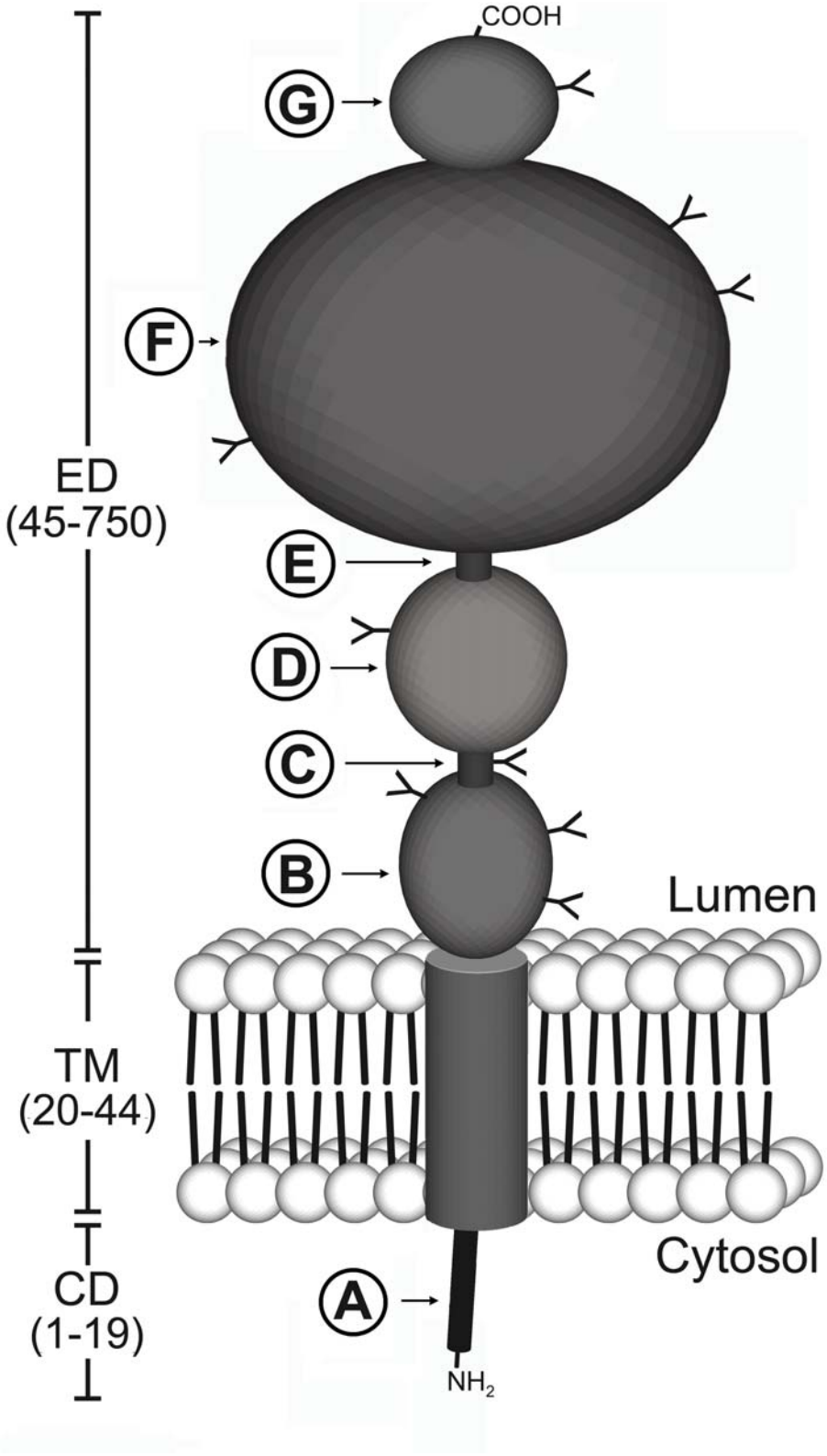

Figure 2

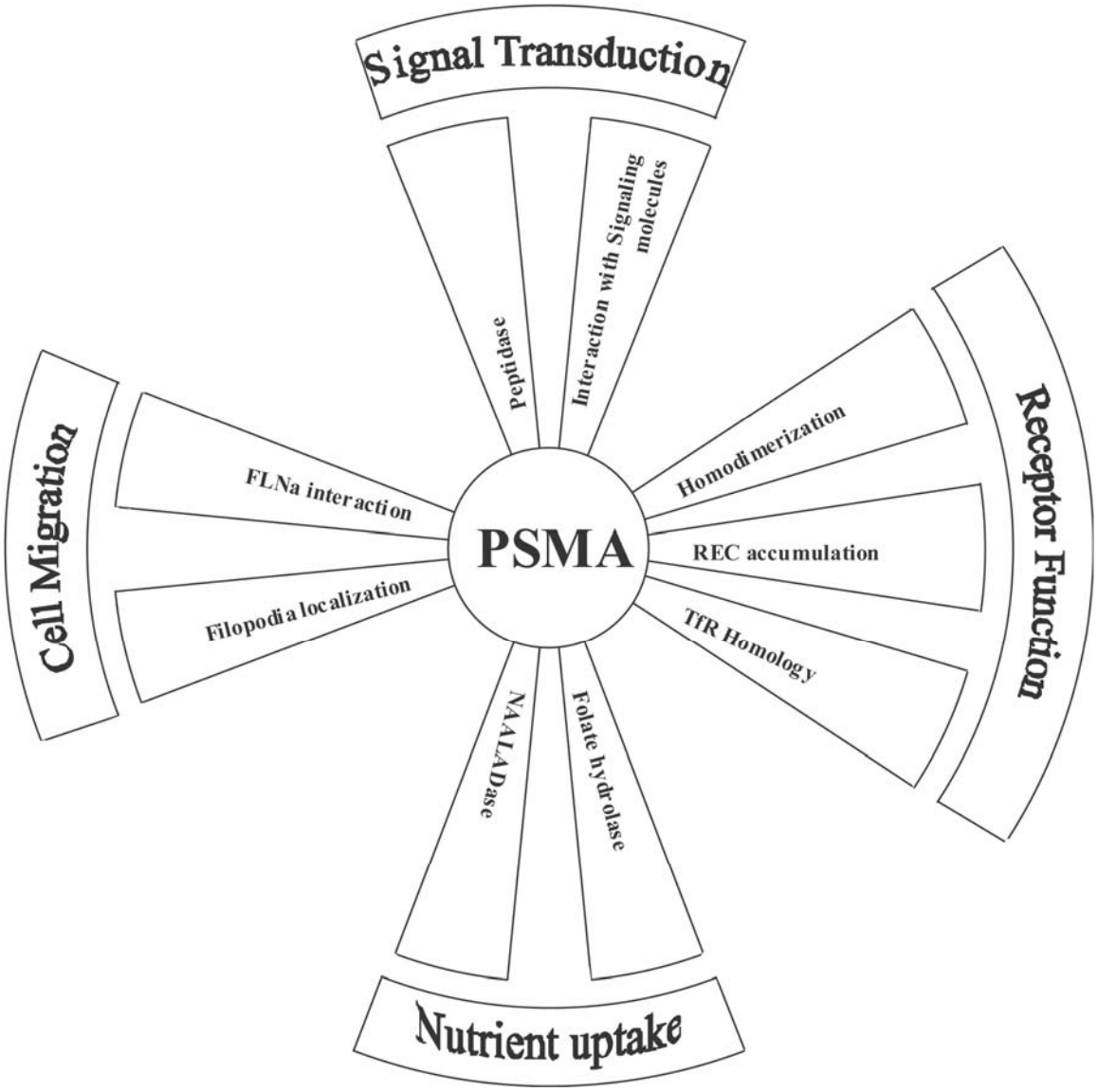
Signal Transduction
Peptidase
Interaction with Signaling molecules
Receptor Function
Homodimerization
REC accumulation
TfR Homology
Cell Migration
FLNa interaction
Filopodia localization
PSMA
NAALADase
Folate hydrolase
Nutrient uptake